

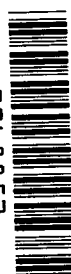
NASA
TT
F-434
c.1

K.A.Brusilovskii

MEASUREMENT OF PULSE DISTORTION IN DIGITAL INFORMATION TRANSMISSION

LOAN COPY: RETURN TO
AFWL (WLIL-2)
KIRTLAND AFB, N MEX

0068853



TECH LIBRARY KAFB, NM



TRANSLATED FROM RUSSIAN

Published for the National Aeronautics and Space Administration,
and the National Science Foundation, Washington, D.C.
by the Israel Program for Scientific Translations



0068853

AKADEMIYA NAUK SSSR. INSTITUT ELEKTROMEKHANIKI GOSPLANA SSSR
KOMITETA PO ELEKTROTEKHNIKE PRI GOSPLANE SSSR

Academy of Sciences of the USSR. Institute of Electromechanics of the
State Committee for Electrical Engineering, State Planning Committee of the USSR

K. A. Brusilovskii

MEASUREMENT OF PULSE DISTORTION IN DIGITAL INFORMATION TRANSMISSION

(Izmereniya iskazhenii impul'sov v sistemakh peredachi diskretnoi informatsii)

Izdatel'stvo Nauka
Moskva—Leningrad 1965

Translated from Russian

Israel Program for Scientific Translations
Jerusalem 1968

NASA TT F-434
TT 67-51370

Published Pursuant to an Agreement with
THE NATIONAL AERONAUTICS AND SPACE ADMINISTRATION, U.S.A.
and
THE NATIONAL SCIENCE FOUNDATION, WASHINGTON, D.C.

Copyright © 1968
Israel Program for Scientific Translations Ltd.
IPST Cat. No. 1819

Translated by Z. Lerman

Printed in Jerusalem by S. Monson
Binding: Wiener Bindery Ltd., Jerusalem

Available from the
U.S. DEPARTMENT OF COMMERCE
Clearinghouse for Federal Scientific and Technical Information
Springfield, Va. 22151

Table of Contents

INTRODUCTION	1
Chapter One. EVALUATION OF NOISEPROOF FEATURES OF DIGITAL DATA TRANSMISSION SYSTEMS	3
1. Channel rating criteria	3
2. Classification of pulse distortions and errors	5
3. Principles of distortion and error measurements.	9
Chapter Two. ELEMENTS OF THE STATISTICAL THEORY OF SIGNALS, DISTORTIONS, AND NOISE IN DIGITAL DATA TRANSMISSION SYSTEMS	12
1. Some peculiarities of signal statistics	12
2. Distribution of fortuitous distortions, bias distortions, and mutilations.	14
3. Distribution of characteristic distortions	16
4. Statistical model of noise	19
Chapter Three. ERRORS IN DIGITAL DATA TRANSMISSION	22
1. Distribution of errors in transmission of signals of various statistics	22
2. Statistical error models	26
Chapter Four. TEST SIGNALS AND THEIR GENERATORS	33
1. Principles of test signal generation	33
2. Regular code sequences and their application to test signal generation	34
3. Test signals based on code rings	35
4. Programmed test signal generators	38
5. Application of the theory of linear sequential circuits to the design of test signal generators and other components.	44
Chapter Five. DISTORTION AND MUTILATION METERS.	50
1. Evaluation of instrumental errors and their sources	50
2. Analog and digital electronic distortion meters for transmission rates of up to 300 baud	52
3. Digital distortion meter for high transmission rates	58

Chapter Six. DISTORTION AND ERROR DISTRIBUTION ANALYZERS	61
1. Brief survey of analyzers.	61
2. Electronic distortion analyzer for transmission rates of up to 75 baud	65
3. Analyzer for statistical channel tests at speeds of up to 2400 baud	68
4. Counting assembly for statistical reduction of data recorded on magnetic tape	72
5. Error-free interval analyzer	73
Chapter Seven. SOME COMPONENTS OF NONCONTACT TESTERS	75
1. Digital readout indicator	75
2. Transistor relay with reversible output signal	79
BIBLIOGRAPHY	84
SUBJECT INDEX	90



INTRODUCTION

Recent advances in digital data transmission and the rapid development of computer technology and information theory make it now possible to tap the potential of electrical communications much more efficiently than ever before. Communication systems, in a wide sense of the word, are no longer restricted to exchange of information; they gradually take on the function of control systems, as is the case, e.g., in the transmission of digital data to computer centers, where electronic digital computers automatically process the incoming data from various customers. The channel efficiency is considerably increased by setting up a single automated communication system with time sharing in which all forms of information are handled in a uniform binary code.

Unlike telegraph messages, digital data do not possess internal redundancy and error correction in the communication channel is therefore a more difficult undertaking. The reliability of digital data transmission consequently should be several orders of magnitude higher than the reliability of telegraph lines.

Efficient running of digital computers depends on input and output channels, which should be able to handle large quantities of data in a short time. Digital data are therefore transmitted at substantially higher speeds than telegraphic signals.

The high transmission speeds (thousands of bauds, as compared to 50—100 baud in telegraph transmission) and the exacting reliability requirements are unattainable without a thorough investigation of the characteristics of digital data transmission systems.

The selection of optimum transmission and coding techniques requires detailed knowledge of the statistics of real communication channels and, primarily, of error probability distributions. The error distribution can be obtained in a general form by investigating a mixed input, where a noise of known statistics is superimposed on the signal. The problem can be solved for each particular case with the aid of a computer. Having obtained the statistical channel characteristics in the form of an error probability distribution function, we can use the computer again to find the optimum coding technique for the given system.

This general approach, as well as the more primitive empirical approach of the engineer, require special equipment for measurement and statistical analysis of distortions and errors in digital data transmission. New high-quality measuring equipment is necessary not only for research purposes, but also for routine measurements in transmission engineering, since lacking the essential instrumentation one is unable to design new noiseproof transmission systems and to effectively utilize the existing equipment.

Development of adequate measuring instruments is a highly topical problem, since digital data are mostly transmitted over already existing telegraph and telephone lines, which have been built and designed without proper regard for the new speed and reliability requirements.

Many organizations in the USSR and elsewhere are currently devoting considerable efforts to the development of appropriate meters and testers for digital data channels and to the theoretical analysis of various problems connected with such measurements. However, the fairly extensive literature on the subject does not include specialized books which would offer a comprehensive treatment of the theory and the practical methods of measurement.

This book, which should be regarded as an introduction to the extensive field of digital data transmission quality measurements, is intended to partially fill this gap. It deals with a selection of topics pertaining, first, to some statistical features of distortion and error distributions in communication channels (mainly wires) and, second, to the design of appropriate measuring instruments and their components. It is an outgrowth of the original research in which I and my co-workers have been engaged since 1958.

The book is divided into seven chapters. The first three chapters briefly discuss the criteria for the evaluation of noiseproof features of communication channels and the elements of the statistical theory of signals, noises, distortions, and errors in digital data transmission. Some statistical error models encountered in the analysis of transmission over telephone lines are considered.

Chapter Four deals with the fundamental properties of test signals and the functional principles of test signal generators.

Chapters Five and Six discuss analog and digital distortion meters and various error and distortion distribution analyzers. Because of space limitations, only those instruments are described which have been developed under my direction or with my active participation. Analyzers constitute an exception to this rule, because of their great significance as the measuring instrument of the future in digital data transmission. In distinction from the conventional testing equipment, the instruments described in this book are all built on the contemporary principle of noncontact solid-state switching elements, using semiconductor triodes (transistors) and ferrites.

In the concluding chapter various questions related to the optimum design of a digital indicator register and a transistorized output relay are discussed. Again because of space limitations we had to omit descriptions of other component elements, discussion of the telegraph distortion terminology, instrumental errors, methods of reduction of experimental findings, and an analysis of the actual results obtained with the various testers described in the book. These topics, as well as descriptions of other similar instruments are covered by the references listed at the end of the book.

I would like to extend my sincere thanks to V. V. Sidel'nikov, who encouraged me in writing this book, for his untiring editorial efforts, and to V. I. Shlyapoberskii and S. M. Mandel'shtam for their advice and comments.

I am particularly grateful to V. S. Bleikhman and to all others who took part in the development of the instruments described in this book, especially A. A. Afanas'eva and S. Yu. El'kind.

Chapter One

EVALUATION OF NOISEPROOF FEATURES OF DIGITAL DATA TRANSMISSION SYSTEMS

1. CHANNEL RATING CRITERIA

A digital (telecoded) communication system consists of transmitting and receiving terminals which handle digital information and perform encoding and decoding operations (Figure 1). Modulation and demodulation (restitution) are employed to convert d.c. to a.c. signals and vice versa. The common modes of modulation are amplitude, frequency, and phase modulation.

An a.c. communication channel in conjunction with a modulator and a demodulator constitutes a d.c. channel. The signal at the input and the output of the d.c. channel is a train of binary pulses characterized by two states, which are designated 1 and 0.

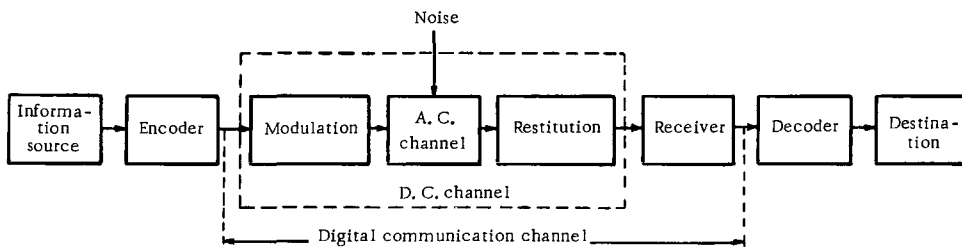


FIGURE 1.

Depending on the volume of information to be transmitted, we use low-speed transmission (at about 50—100 baud) through narrow-band (telegraph) channels or high-speed transmission (600—2400 baud and higher) through wide-band (telephone) channels.

In the communication channel the signal is distorted by additive and multiplicative noises. Additive noise, i.e., noise added to the signal, is divided into the following principal types /58, 63, 97/: fluctuation (smooth) noise, impulse noise, and sinusoidal noise. Multiplicative noise constitutes the brief interruptions of the line caused mainly by failure of contacts in switches and by overloading of amplifiers /22, 76/.

External noises and instrumental distortions may cause lack of correspondence between the transmitted and the received messages. Transmission reliability is a criterion which shows to what extent the received message is a faithful reproduction of the transmitted message. In properly designed and built equipment the instrumental distortion is low, so that noise is the main factor which lowers the transmission reliability.

The probability of incorrect reception of a symbol or a group of symbols characterizes to what extent the channel is noiseproof; in general this property is expressed as the signal-to-noise ratio of the channel /32, 33, 58/.

Evaluation of noiseproof features, or the signal-to-noise ratio, of digital data transmission systems generally calls for inspection of the distortion of square pulses in the d.c. channel of a system block-diagrammed in Figure 1. It should be remembered that noise of a certain kind, e.g., additive fluctuation noise, acting on the a.c. channel is not necessarily of the same kind in relation to the d.c. channel. To first approximation, however, we may assume that the kind of noise is conserved in the two channels /11/.

External noises and the real transient response of the communication channel (which is not square, as an ideal response should be) thus cause distortion of pulses transmitted through the d.c. channel.

Irrespective of the reasons which cause signal distortion, the distortion actually amounts to a certain displacement of the pulse edges. The length, or duration, of the received pulses is thus different from the original pulse length.

An important feature of receivers in digital data systems is their margin, i.e., ability to receive correctly pulses which have been distorted within certain limits. Without going into the specific aspects of signal correction /66/, we only mention that numerically the margin is equal to the maximum permissible distortion which does not cause a receiver error.

The effective margin of modern synchronous digital transmission systems employing solid-state devices without mechanical contacts is approximately 46%, that of electromechanical systems is between 28 and 35% (the lower figure corresponds to start-stop systems, the higher to synchronous systems).

The difference γ between the receiver margin μ and the total distortion δ_z of the received pulses gives the transmission stability margin

$$\gamma = \mu - \delta_z. \quad (1)$$

Stability of transmission is ensured only when $\gamma > 0$, so that the inequality $\delta_z < \mu$ must always be satisfied.

Telegraph systems utilize the start-stop phase correction principle, and their margin is therefore relatively low. In digital data transmission the synchronous correction technique is adopted, and their margin is correspondingly higher.

The evaluation of noiseproof features of telegraph systems and digital data transmission systems is based on fundamentally different criteria: telegraph systems are rated in terms of the permissible overall distortion $\delta_{z \text{ perm}}$ /30/, whereas the figure of merit of digital data transmission

systems is basically the probability of error. The error probability is the more general criterion, since δ_{perm} only shows how far the system is from the extreme operating conditions, when the error probability is particularly high. This criterion is valid only for additive-noise systems with prevalence of fluctuation noise. In systems with strong impulsive noise and frequent line interruptions, pulse distortion only partially characterizes the probability of error.

The use of the two criteria for the rating of digital data transmission systems is due in a certain degree to historical factors. Indeed, quality measurements of digital data transmission originated mainly in application to telegraphy, where only the magnitude and the distribution of pulse distortions were measured. In view of the comparatively low faithfulness standards of telegraph transmissions (error probability not exceeding $3 \cdot 10^{-5}$, i. e., up to three distorted characters in 10^5 transmitted words) and the high redundancy, knowledge of pulse distortion and its distribution is quite sufficient in most cases for estimating the noiseproof features of the communications system. Furthermore, δ_{perm} can be measured with comparatively simple telegraph distortion meters.

With the advent of new means of communication, namely digital data transmission systems [21, 45] with much stricter reliability standards (error probability not exceeding $10^{-5} - 10^{-8}$, depending on system destination), the magnitude of overall distortion lost some of its importance as a figure of merit. On the other hand, error probability measurements required more sophisticated equipment, the so-called error distribution analyzers.

2. CLASSIFICATION OF PULSE DISTORTIONS AND ERRORS

A classification of pulse distortions in digital data transmission is depicted in Figure 2.

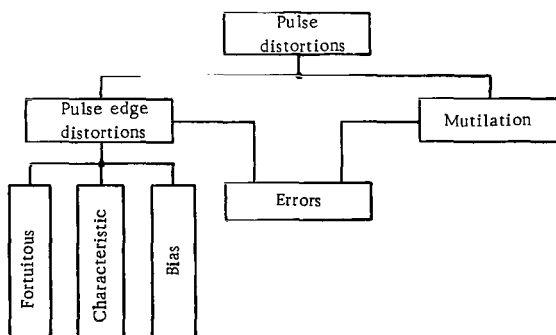


FIGURE 2.

Fortuitous distortions are caused by random noises. Characteristic distortions are due to transients in the communication channel and in the receiver, and they are thus dependent on the form of the channel transient response and the transmission speed [31]. Bias distortion is caused, e. g., by lack of symmetry between the receiver and the transmitter; the main reasons are relay bias and inequality of line battery voltages.

Mutilation refers to distortion due to impulse noise and short duration interruption of pulses (within the limits of faithful reproduction). Interruption due to fading is particularly critical in radio transmission, but it has been shown [22-24, 26, 60, 76, 77] that line interruptions also constitute one of the main sources of errors in signal transmission over wires.

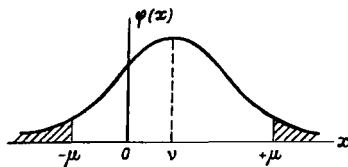


FIGURE 3.

We have already indicated that the permissible overall distortion δ_{perm} can be used as a figure of merit of data transmission systems with fluctuation noise, as well as systems with characteristic and bias distortion. The order of magnitude

of δ_{perm} is characterized by the previously cited values of the margin μ .

If the communication stability margin is nonpositive $\gamma \leq 0$, the signal is received incorrectly, i. e., an error occurs. Errors are thus regarded as a limiting case of pulse distortion.

If the distribution of distortions is known (i. e., the d -variate probability density function $\varphi_d(x_1, x_2, \dots, x_d)$ is given, where x_i is the displacement of the i -th edge in a d -element code combination), then, for a given μ , we can find the probability P_{err} of an error in the transmitted combination:

$$P_{\text{err}} = 1 - \int \int \dots \int_G \varphi_d(x_1, x_2, \dots, x_d) dx_1 dx_2 \dots dx_d, \quad (2)$$

where G is the domain of integration; this is a d -dimensional cube with faces distant μ from its center.

Consider the particular case of a single-unit combination. This corresponds to $d=1$; the cube degenerates to a straight line of length 2μ , and relation (2) takes the form

$$P_{\text{err}_0} = 1 - \int_{-\mu}^{\mu} \varphi(x) dx. \quad (2a)$$

Errors occur when the distortions lie in the cross-hatched regions in Figure 3, i. e., when signal distortion is greater than μ .

If the probability density $\varphi(x)$ is normally distributed, say, i. e.,

$$\varphi(x) = \frac{1}{\sigma \sqrt{2\pi}} e^{-\frac{(x-v)^2}{2\sigma^2}}, \quad (3)$$

where σ^2 is the variance of distortions, σ the rms (standard) deviation, v the expectation value or the arithmetic mean deviation, i. e., a parameter

which characterizes the displacement of the center of the probability density distribution relative to $x=0$, then

$$P_{\text{err}_0} = 1 - \left[\Phi\left(\frac{\mu + v}{\sigma}\right) + \Phi\left(\frac{\mu - v}{\sigma}\right) \right], \quad (4)$$

where Φ is the Laplace function.

For $v=0$, we have

$$P_{\text{err}_0} = 1 - 2\Phi\left(\frac{\mu}{\sigma}\right). \quad (5)$$

Expressions (4) and (5) give the error probability for the simplest case of single-unit combinations. The error probability for a d -unit combination is generally determined from the relation

$$P_{\text{err}} = dP_{\text{err}_0} = d \left[1 - 2\Phi\left(\frac{\mu}{\sigma}\right) \right]. \quad (5a)$$

This approach, however, ignores the possibility that the receiver margin may be greater than the overall displacement of several pulse edges within a multi-unit combination. In the general case equation (5a) is inapplicable and we thus return to relation (2), remembering that the pulse edge displacements within a single code combination are correlated (this is particularly true for start-stop codes).

The error probability P_{err_0} can be determined by an alternative technique. Let the unconditional probabilities of the symbols 1 and 0 be $P(1)$ and $P(0)$, respectively. The error probability in a binary communication system is thus

$$P_{\text{err}_0} = P(1)P(1 \rightarrow 0) + P(0)P(0 \rightarrow 1), \quad (6)$$

where $P(1 \rightarrow 0)$ and $P(0 \rightarrow 1)$ are the probabilities of errors of the type $1 \rightarrow 0$ and $0 \rightarrow 1$.

Let us now consider the reasons for the appearance of errors in transmission and the classification of transmission errors. If the errors introduced by the terminal equipment /2, 3/ are ignored, the remaining errors can be divided into three principal groups according to their origin.

(a) Errors which constitute the limiting case of signal distortion and are caused by fluctuation noise. Since the fluctuation noise level is generally fairly small, the errors of this group are relatively infrequent.

(b) Errors caused by impulse noise. Impulsive noise is an aperiodic train of isolated pulses produced by short-lived e.m.f. surges. The impulse noise amplitude may be fairly large, and errors of this kind are considerably more probable than fluctuation noise errors /75, 97/.

(c) Errors due to short duration interruptions in the communication channel. As we have already remarked, the resultant action of these brief line interruptions is equivalent to the action of impulsive noise: they distort the transmission of pulse trains and mutilate single pulses.

Reduction of error probability by improvement of channel quality is technically very difficult and economically inexpedient. Digital data are therefore generally transmitted over existing channels, and the reliability of transmission is raised by incorporating various redundancies in the message (e.g., error-detecting or error-correcting signals;

multiple transmission with a known number of repetitions; automatic repeat request systems, etc.).

Numerous tests with digital data transmission over telephone channels /70, 83, 93/ show that, excepting the relatively lengthy communication breakdowns, the errors produced by brief line interruptions and by impulsive and fluctuation noise are bunched in clusters or bursts separated by error-free intervals. The error bursts are independent of each other.

If the accurately received elementary pulses are designated by 1 and the pulses in error by 0, the sequence of "good" and "bad" pulses at the receiver output is representable as a sequence of zeros and ones, which simulate a random process with two states and a discrete argument. This random sequence is called an error stream with discrete time, or in short a discrete error stream. Detailed knowledge of error stream statistics is absolutely essential in any attempt to improve the transmission reliability by introduction of redundancy into the transmitted message.

Channel rating in terms of the average error frequency is thus insufficient for effective protection against transmission errors. For example, if error detection and correction is attempted for m -unit combinations, the probability $P_m(w)$ of w errors occurring in a block of m elements must be known before a block-type error-correcting code can be chosen.

If the errors are independent, $P_m(w)$ is readily computed from the probability P_{err} of a single error: in the case of uncorrelated errors channel reliability is entirely determined by P_{err} .

Before recurrent and other codes without block structure can be used, the error stream should be partitioned into bursts, the burst lengths determined, the duration of error-free intervals found, and the density of errors in each burst established.

The distance between any two errors in a burst is less than the correlation length l_c . The channel is described by the following parameters: the probability of an error burst l_{err} elements long (for a given l_c); the probability of an error-free interval l elements long between successive error bursts (for a given l_c); and finally the conditional probability of an error in a burst, which characterizes the error density in the burst. The last parameter is analogous to P_{err} for uncorrelated errors, assuming that the occurrence of an error burst is an independent event.

We see from the preceding that, structurally, the errors are of many different kinds; since no established terminology is available, we give here some basic definitions of errors of various kinds according to the procedure of statistical investigation of data transmission channels developed following the recommendations of the International Telegraph and Telephone Consultative Committee (CCITT).

Before proceeding with the actual definitions, note that here and in what follows a digit is a signal element corresponding to one bit, which is characterized by its form (1 or 0) and its position in the code combination.

Single error: a wrong digit situated between two correct digits.

Error burst (or cluster): a section of the pulse train in which at most l_c accurately received digits are interposed between wrong digits.

Persistent error α_{per} digits long ($\alpha_{\text{per}} \geq 2$): a section of the received pulse train containing a succession of α_{per} wrong digits one after another.

Multiple (α_m -tuple) error: an erroneous combination of a given length containing α_m incorrectly received digits.

Multiple (α_u -tuple) transposition, sometimes called translation: an erroneous combination of a given length, containing an equal number α_u of $1 \rightarrow 0$ and $0 \rightarrow 1$ errors.

3. PRINCIPLES OF DISTORTION AND ERROR MEASUREMENTS

A classification of methods of distortion and error measurements in digital data transmission systems is shown in Figure 4. We see from this classification that measurement of distortions and mutilations and analysis of their distribution require, first, special distortion and mutilation meters and, second, suitable distribution analyzers. The instruments should be adapted for measurements during synchronous and start-stop transmission. The error probability is determined with special error distribution analyzers.

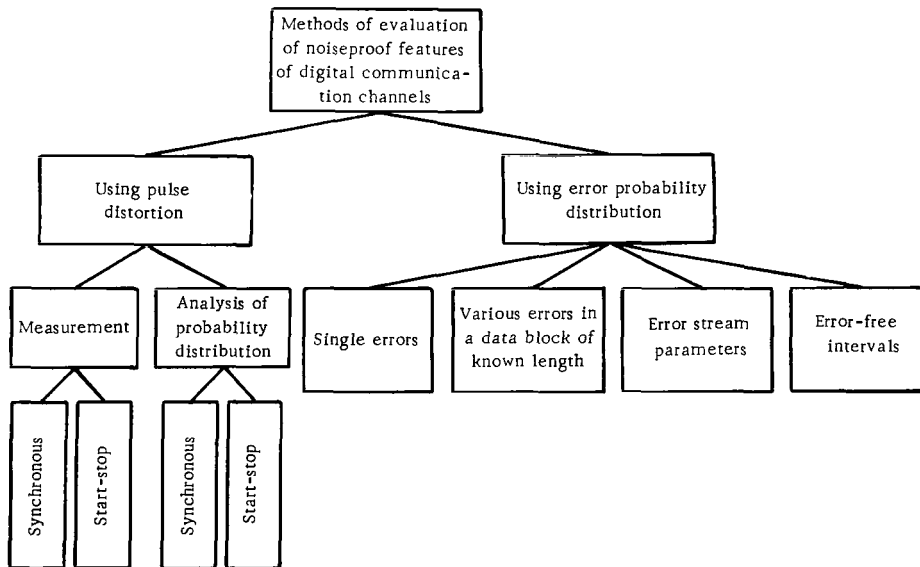


FIGURE 4.

The terminology pertaining to telegraph distortions, techniques of distortion measurement and addition, resolution of distortions into components, and other related topics are treated in sufficient detail in CCITT publications /51/ and in /24, 30, 39, 48, 82/. These problems are also discussed in textbooks /31, 43, 56/, and we do not intend to go into this subject here. It suffices to note that synchronous instruments

without phasing measure the isochronous distortion, i.e., the difference in length between the transmitted pulses and ideal standard pulses. Instruments with phasing, on the other hand, measure the edge displacement of each pulse. A clear distinction should therefore be made between edge displacement distribution and isochronous distortion distribution when discussing the distribution of synchronous distortions.

The design of distortion meters and analyzers of various kinds is described in subsequent chapters. Here we shall only consider the general procedure of evaluation of digital data transmission channels with the aid of error distribution analyzers.

The aim of these measurements is to determine the reliability of transmission. The tests provide us with either partial or complete information on the subject. By complete information we mean that the exact position of all the incorrectly received digits and the type of error ($1 \rightarrow 0$ or $0 \rightarrow 1$) are known. Complete information should preferably be obtained in a form suitable for subsequent computer processing, e.g., recorded on magnetic tape or punched on paper tape.

Partial information gives the frequency of errors, without specifying their time distribution during a test session of known length. Partial information is obtained if the total number of transmitted digits and the number of wrong digits are known. It is desirable to classify the errors according to different types ($1 \rightarrow 0$ and $0 \rightarrow 1$, persistent, groups of various lengths), and to determine the number of error blocks of various lengths, the number of combinations with α_m -tuple errors and α_n -tuple transpositions, the number of errors in bursts of different length, the number of error-free intervals and their length.

The number of communication breakdowns longer than 300 msec during the test should be recorded, and it is desirable to know the distribution of these breakdowns in time. Errors due to these breakdowns are omitted from reliability calculations.

The channel testing procedure is as follows. A test signal is sent from the transmitting end; in the receiver, the signal is compared digit by digit with an identical standard signal. Inequality of corresponding digits is registered as an error.

Two different testing techniques are used:

- (a) "loop" test, with the transmitting and the receiving equipment at the same end of the channel;
- (b) "end-to-end" test with the transmitting and the receiving equipment at the two different ends of the channel.

"End-to-end" tests should be preferred, but in some cases a "loop" technique can be applied conveniently with the same effect. Through testing can be carried out without using a transducer at the receiving end. In this case the test signal is compared to itself with the aid of a shift register where the number of bits is equal to the period of the test signal /89/.

By testing channels of different kinds (telegraph, radio telegraph, telephone), we may obtain the reliability as a function of channel type, secondary and primary multiplexing equipment, physical transmission line, channel length, number of telegraph links in tandem or number of repeaters, transmission speed, signal level, time of day, and preferably the season.

The main difference between tests of telegraph and telephone channels is that the former are tested in both the synchronous and the start-stop modes

at transmission rates $N = 50, 75, 150$, and 300 baud, whereas telephone channels are tested in the synchronous mode only at speeds $N = 150, 200, 300, 600, 1200, 2400$, and 4800 baud.

The secondary multiplexing equipment used in telephone channel tests is either the actual equipment of real digital data transmission systems or suitable testing equipment. Before the measurements, the channel and the multiplex equipment are appropriately tuned and adjusted.

The total number of test digits transmitted under each particular set of conditions should be at least 10^6 for telegraph channels and 10^7 for telephone channels. Readings of analyzer counters are taken at time intervals T satisfying the inequality

$$T \leq \frac{\theta}{6N\Delta D}, \quad (7)$$

where $\theta = 1$ for telegraph channels and $\theta = 5$ for telephone channels; ΔD is the expected loss of reliability. In either case, the distortion of the transmitted pulses is determined.

To sum up, correct choice of the operating algorithm for digital data transmission equipment, which is the ultimate goal of error statistics analysis, is possible only when all the measurements following the block diagram of Figure 4 have been completed.

Before going into a detailed discussion of the instruments, we will study the basic properties of the measured quantities, namely pulse distortions, errors, and their distributions. It should be remembered that the distribution of distortions and errors depends on the statistics of the transmitted signals, as well as such obvious physical factors as channel type, modulation technique, etc.

Chapter Two

ELEMENTS OF THE STATISTICAL THEORY OF SIGNALS, DISTORTIONS, AND NOISE IN DIGITAL DATA TRANSMISSION SYSTEMS

1. SOME PECULIARITIES OF SIGNAL STATISTICS

Error distribution in channels can be found by mixing a signal of known statistical structure with noise of a given type /58/. Signal statistics can be studied by analyzing real messages and communications.

The percentage frequency of various characters for start-stop telegraph transmission in five-unit code was established in /53/ by statistical reduction of 3000 telegrams. If z is the number of a character in an alphabet arranged in the order of decreasing frequency h , analysis of the data in /53/ gives the following approximate relation:

$$h = h_0 - v \log z, \quad (8)$$

where $v = \frac{h_0}{\log z_0}$, z_0 being the number of the last combination, i.e., the total number of code combinations of the given telegraph equipment. For example, for the ST-35 Soviet-made telegraph equipment, $h_0 \approx 0.1$ ("space"), $z_0 = 45$, and $v \approx 0.06$. Relation (8) for the ST-35 equipment is plotted in Figure 5, which also shows the experimental points.

Equation (8) is derived for all possible combinations, including letters, figures, and service codes. The same relation holds true for figures only, the numerals being arranged in the following sequence: 1, 0, 2, 3, 5, 4, 9, 7, 8, 6. In this case $h_0 \approx 0.27$, $z_0 = 10$, so that $v = 0.27$. For figures this approximate relation thus has the form $h = 0.27(1 - \log z)$.

Analysis of the same data shows that in a start-stop combination the probability of any of the six transitions is between 13.59 and 19.37%, i.e., they are all virtually equiprobable.

The signal statistics in digital data transmission systems can be determined from the following considerations /8, 10, 11/.

Statistical description of a digital message requires knowledge of the probability of m -digit groups in the message /65/, where $m = 0, 1, 2, 3, \dots$. To first approximation we may assume that a

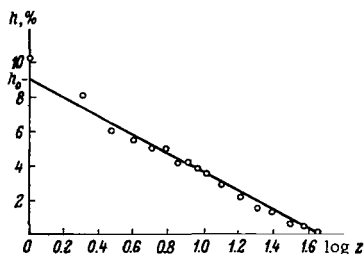


FIGURE 5.

message to be transmitted over a digital data channel is formed by successive selection of binary symbols from a certain pool of bits, all possible outcomes of this selection procedure being equiprobable and independent. If an m -unit code is used, the code pool is a set of 2^m different combinations of m elements each. In this case all combinations of equal length are equiprobable, i.e., the probability P_m of any m -unit combination is

$$P_m = \frac{1}{2^m}. \quad (9)$$

The message statistics is thus described by relation (9).

The forming of the message can be regarded as a succession of independent tests, the outcome of each being either 0 or 1; the probabilities of 0 and 1 are equal in each test, i.e., $P(0) = P(1) = 0.5$.

Let us consider a sequence of K digits (zeros and ones) formed in this way. The probability that there are K_0 zeros and $K - K_0$ ones in this sequence is given by a binomial distribution

$$P_K(K_0) = C_K^{K_0} P^{K_0}(0) P^{K-K_0}(1) = \frac{K!}{K_0! (K - K_0)!} \frac{1}{2^K}. \quad (10)$$

As K increases, the probability that nearly half of all the digits in the sequence are zeros becomes higher. Thus for $K = 20$, 74% of all the combinations have from 8 to 12 zeros, i.e., the number of zeros and ones in this case differs at most by 20% from the most probable value of 10.

If K is sufficiently large, the binomial distribution approaches the normal distribution, the center of the distribution and its variance remaining unchanged. In this case the probabilities $P_K(K_0)$ are approximately calculated from the normal distribution formula with the variance $\sigma^2 = KP(0)P(1) = 0.25K$. These calculations show that for $K = 150 - 200$, the number of zeros in 95% of all the combinations differs from $0.5K$ by no more than 15%. Moreover, the probability distribution of the random variable (the number of zeros in the sequence) departs by less than 1% from the normal distribution.

Analysis of noiseproof features of digital data transmission systems thus generally starts with the assumption of equal unconditional probabilities, $P(1) = P(0) = 0.5$, i.e., the relative frequencies of 1 and 0 are taken to be equal. In [58] the validity of this assumption is demonstrated in practice, but even if $P(1) \neq P(0)$, the results of the analysis are hardly affected.

Note that relation (9) corresponds to an approximate signal model; it describes the signal statistics at the encoder input. At the encoder output the signal may possess a certain redundancy, i.e., the probability of some combinations will be zero. However, if we take into consideration the probability of combinations formed by the adjoining parts of successive data blocks, we conclude that relation (9) is approximately satisfied by signals in real communication channels for all $m \leq m_{bl}$, where m_{bl} is the length of the data block at the encoder output.

For large m , equality (9) is not always satisfied in digital channels, and the probability P_m is computed for the particular coding technique used.

2. DISTRIBUTION OF FORTUITOUS DISTORTIONS, BIAS DISTORTIONS, AND MUTILATIONS

Let us consider the distribution of distortions and mutilations, ignoring for the start the characteristic distortions.

Fortuitous distortions and constant bias distortions in synchronous transmission. Numerous measurements have led to the conclusion [1, 24, 71] that the probability density $\varphi(x)$ of the fortuitous distortions of pulse edges relative to ideal (undistorted) marks follows the normal distribution (3). The parameter v characterizes the constant bias. For $v > 0$ the curve $\varphi(x)$ is displaced to the right of the vertical $x=v$ and for $v < 0$ it is displaced to the left.

In some cases (including the calculation of P_{err} from (2)) we are concerned not with the distribution of pulse edge displacements, but with the distribution of isochronous distortion, i.e., the algebraic difference between the maximum and the minimum displacement in a group of synchronously transmitted pulses. The isochronous distortion distribution is thus the distribution of a random variable which runs over all the possible algebraic differences of edge displacements in a given pulse train.

A.N. Zeliger [28] has shown that if the pulse edge displacements are normally distributed with a variance σ^2 , the isochronous distortion is also normally distributed with a variance $2\sigma^2$.

Fortuitous distortions and variable bias in synchronous transmission. Fortuitous distortions can be regarded as normally distributed with constant expectation value v and variance σ^2 only over comparatively short time intervals. In lengthy measurements over one channel the parameters σ and v are seen to vary, the variation of expectation value being caused by variation of bias.

If σ is assumed to be constant and the parameter v is regarded as normally distributed with zero expectation value, i.e.,

$$\varphi(v) = \frac{1}{\sigma_v \sqrt{2\pi}} e^{-\frac{v^2}{2\sigma_v^2}}, \quad (11)$$

where σ_v^2 is the variance of the random variable v , it is easily shown [29] that the distribution of pulse edge distortions remains normal with zero expectation value and variance $\sigma^2 + \sigma_v^2$.

The effect of random variations in σ and of simultaneous changes in v and σ on the distribution of pulse edge distortions can be estimated if v and σ are regarded as stationary random variables with known distributions. The generalized distribution $\varphi(x)$ for independent v and σ and stochastic relation between x and v and σ is given by the expression

$$\varphi(x) = \int_{-\infty}^{\infty} \int_{-\infty}^{\infty} \varphi(v, \sigma) \varphi\left(\frac{x}{v}, \sigma\right) dv d\sigma, \quad (12)$$

where $\varphi(v, \sigma)$ is the probability density distribution of the set of parameters v and σ ; $\varphi(x/v, \sigma)$ is the conditional distribution of x in the parameters v and σ .

It is easily seen that the generalized distribution is essentially different from the normal distribution. Even in the simple case considered in [29]

(uniformly distributed $\varphi(v)$ and $\varphi(\sigma)$) only an approximate expression could be derived for $\varphi(x)$ in the form of a slowly converging infinite series.

Mutilation. Experimental and theoretical studies show [23, 24] that mutilation of messages in telegraph and radiotelegraph channels follows a log-normal distribution:

$$\varphi(x) = \frac{1}{x\sigma\sqrt{2\pi}} e^{-\frac{(\ln x - v)^2}{2\sigma^2}}. \quad (13)$$

In voice-frequency telegraph channels mutilation essentially depends on the time of day and the day of the week. It is mostly caused by incorrect switching in telegraph working.

In digital data transmission over communication channels the signals are generally subjected to both edge distortion and mutilation. The distribution of pulse edges in synchronous transmission was investigated in [28], where it was shown to differ from the normal distribution. The difference becomes more pronounced as the probability of mutilation increases; it diminishes as the transmission speed is increased. In the absence of bias the distribution is nearly symmetric; as bias distortion increases, the distribution becomes progressively less symmetric.

Distortions in start-stop transmission. In transmission of start-stop codes the distortions of each pulse follow a normal distribution $\varphi(x_{sti})$ [55]. In calculations of P_{err} from (2) we first have to find the distortion distribution function $\varphi_d(x_1, x_2, \dots, x_d)$. To this end we consider the joint probability distribution of a system of d dependent normal variables $x_{st1}, x_{st2}, \dots, x_{std}$ [72].

Assuming equal variances and correlation coefficients r for all the component normal distributions $\varphi(x_{sti})$, we arrive at the following expression for the probability of start-stop distortion being less than μ [25, 72]:

$$\epsilon(\mu) = 1 - P(x^2 > x_q^2), \quad (14)$$

where $P(x^2 > x_q^2)$ is the distribution function of the Pearson correspondence criterion x^2 with d degrees of freedom, and

$$x_q^2 = \frac{\mu^2}{\sigma^2 [1 + (d-1)r]}.$$

$P(x^2 > x_q^2)$ is the upper limit of P_{err} , i.e.,

$$P_{err} < P(x^2 > x_q^2). \quad (15)$$

This inequality corresponds to the substitution of a d -dimensional sphere for the domain of integration in (2). It gives a very considerable error, which increases with the increase in the ratio μ/σ (i.e., with the improvement of the channel and the equipment) and with the increase in r . The large error is due to the omission of substantial portions of the exact d -dimensional integration domain when it is approximated with a sphere. Moreover, estimate (15) gives an incorrect dependence of P_{err} on r : according to this estimate the transmission reliability in the case of independent errors is less than in the case of correlated errors.

The exact formula for P_{err} with $d=2$ has the form

$$P_{\text{err}} = 1 - 4 \left[\Phi \left(\frac{\mu}{\sigma} \right) \Phi \left(a \frac{\mu}{\sigma} \right) + T \left(a \frac{\mu}{\sigma}, \frac{1}{a} \right) - T \left(\frac{\mu}{\sigma}, \frac{1}{a} \right) \right], \quad (15a)$$

where T is the Owen integral calculated from bivariate normal distribution tables, and $a = \sqrt{\frac{1+r}{1-r}}$.

For $d > 2$, equations (15) and (15a) with $r=1$ and $r=0$, respectively, are sufficiently accurate for the purpose of engineering calculations.

3 DISTRIBUTION OF CHARACTERISTIC DISTORTIONS

The input voltage $U_{\text{in}}(t)$ of the d.c. channel can be represented as a train of positive and negative elementary pulses of amplitude U_m and length t_0 . The j -th pulse starts at the time jt_0 , and the voltage of this pulse is given by the expressions

$$U_{\text{in}j}(t) = U_{mj} f(t - jt_0) \begin{cases} f(t - jt_0) = 0 & jt_0 > t > (j+1)t_0, \\ f(t - jt_0) = 1 & jt_0 \leq t \leq (j+1)t_0, \end{cases} \quad (16)$$

where $U_{mj} = \pm U_m$.

The voltage $U_{\text{in}}(t)$ is thus representable in the form

$$U_{\text{in}}(t) = \sum_{j=-\infty}^{\infty} U_{mj} f(t - jt_0). \quad (17)$$

The voltage $U_{\text{out}}(t)$ produced at the channel output by a square pulse input which began at the time t_1 and terminated at the time t_2 is determined by the transient response $H(t)$ of the channel, i.e.,

$$\frac{U_{\text{out}j}(t)}{U_m} = H(t - t_1) - H(t - t_2). \quad (18)$$

Input voltage (17) thus produces an output ($t_1 = jt_0$, $t_2 = (j+1)t_0$)

$$U_{\text{out}}(t) = \sum_{j=-\infty}^{\infty} U_{mj} \{H(t - jt_0) - H[t - (j+1)t_0]\}. \quad (19)$$

Since the frequency response of the communication channel is limited from above (the channel is in effect a low-frequency filter), the transient response $H(t)$ is not an ideal square function. The transmitted pulses are generally squared with the aid of some threshold device which is triggered with a time lag Δt_i relative to the successive input pulses. The time lag can be found from (19) by writing $t = it_0 + \Delta t_i$ and putting the response threshold equal to zero,

$$\sum_{j=-\infty}^{\infty} U_{mj} \{H(it_0 + \Delta t_i - jt_0) - H[it_0 + \Delta t_i + (j+1)t_0]\} = 0. \quad (20)$$

In real communication channels $H(t) = 0$ when $t < 0$, and relation (20) can be written in the form

$$U_{mj}H(\Delta t_i) + \sum_{j=-\infty}^{i-1} U_{mj} \{H[(i-j)t_0 + \Delta t_i] - H[(i-j-1)t_0 + \Delta t_i]\} = 0. \quad (21)$$

Let $i-j=k$; summation over k in (21) is taken from $k=1$ to $k=\infty$. For real transient responses, however, there is always a certain t' such that $H(t) \approx 1$ for $t > t'$; the sum may therefore be truncated at a finite $k=k_0$, where $k_0 = \frac{t'}{t_0} \approx 5-7$.

The random variable Δt_i is approximately representable as a sum of two terms

$$\Delta t_i = \Delta t_0 + \Delta_i, \quad (22)$$

where Δt_0 is the time lag when the i -th pulse was preceded by a "reversal" (it is thus independent of the preceding combination); Δ_i is the time lag dependent on the preceding k_0 -unit combination.

Equation (21) is now written in the form

$$U_{mi}H(\Delta t_0 + \Delta_i) + \sum_{k=1}^{k_0} U_{m(i-k)} \{H(kt_0 + \Delta t_0 + \Delta_i) - H[(k-1)t_0 + \Delta t_0 + \Delta_i]\} = 0. \quad (23)$$

The expression in braces in (23) determines the correlation between pulses due to characteristic distortions.

Expanding the left-hand side of equation (23) in a Taylor series and retaining the first two terms, we find (prime denotes differentiation)

$$\Delta_i = - \frac{U_{mi}H(\Delta t_0) + \sum_{k=1}^{k_0} U_{m(i-k)}H_1(t)}{U_{mi}H'(\Delta t_0) + \sum_{k=1}^{k_0} U_{m(i-k)}H'_1(t)}, \quad (24)$$

where

$$H_1(k) = H(kt_0 + \Delta t_0) - H[(k-1)t_0 + \Delta t_0], \quad (24a)$$

$$H'_1(k) = H'(kt_0 + \Delta t_0) - H'[(k-1)t_0 + \Delta t_0]. \quad (24b)$$

Since $H(0) = 0$ and consequently $H_1(0) = H(\Delta t_0)$, the working formula for Δ_i takes the form

$$\Delta_i = - \frac{\sum_{k=0}^{k_0} U_{m(i-k)}H_1(k)}{\sum_{k=0}^{k_0} U_{m(i-k)}H'_1(k)}. \quad (25)$$

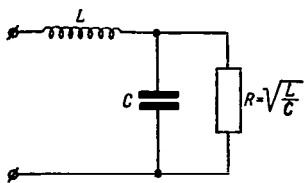


FIGURE 6.

This relation shows that the magnitude of characteristic distortion depends on the shape of the channel transient response and the code combination which preceded the given pulse, i. e., the statistics of the transmitted signals.

Let us consider the distribution of characteristic distortions in the case of a channel representable by a low-frequency L-filter (Figure 6). The signal transmitted over the channel is uniform, i. e., its statistics is given by expression (9). The transient response of the filter in Figure 6 is

$$H(t) = 1 - e^{-\frac{\omega_0}{2}t} \left(\cos \frac{\sqrt{3}}{2} \omega_0 t + \frac{1}{\sqrt{3}} \sin \frac{\sqrt{3}}{2} \omega_0 t \right), \quad (26)$$

where $\omega_0 = 1/\sqrt{LC}$.

It is easily seen that with this $H(t)$ all transients in the channel are virtually terminated when $\omega_0 t' = 3\pi$. Putting $\omega_0 t_0 = \pi$, we find $k_0 = t'/t_0 = 3$.

Note that Δt_0 is given by the equation

$$-1 + 2H(\Delta t_0) = 0, \quad (27)$$

i. e., $H(\Delta t_0) = 0.5$, whence $\Delta t_0 = 0.44t_0$.

Table 1 lists the relative characteristic distortion $x_i = \frac{\Delta_i}{t_0}$ of the i -th transition calculated for all the possible three-unit combinations preceding this transition.

TABLE 1.

$U_m(i-k)$				x_i
$k=3$	$k=2$	$k=1$	$k=0$	
1	1	1	-1	0
-1	1	1	-1	-0.01
-1	-1	1	-1	0.06
1	-1	1	-1	0.07
-1	-1	-1	1	0
1	-1	-1	1	-0.01
1	1	-1	1	0.06
-1	1	-1	1	0.07

In accordance with relation (9) all combinations are equiprobable in the signal, and the corresponding probability is $P_3 = 0.125$. We see from Table 1 that x_i takes on only one of the four values -0.01, 0, 0.06, and 0.07, the corresponding probability being twice as large as P_3 , i. e., 0.25. The distribution of the random variable x_i thus has the form shown in Figure 7 a.

Similarly to the preceding it can be shown that although the number of units in a combination increases with the increase in k_0 and the various possible values of x_i become correspondingly more numerous, the maxima of the probability density distribution $\varphi(x)$ of the characteristic distortions remain in the neighborhood of the above-cited x -values, i.e., $-0.01-0$ and $0.06-0.07$ (Figure 7b). These peaks correspond, as is seen from Table 1, to transmission of a single pulse after "reversals" and "dots".

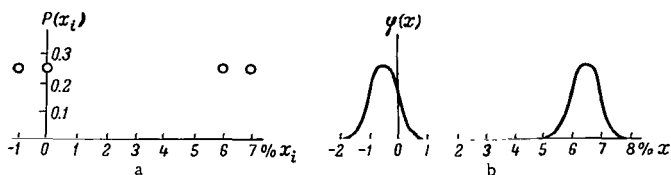


FIGURE 7.

The distribution function $\varphi(x)$ of the characteristic distortions retains its double-peak shape even if the probability distribution of combinations of various lengths in the transmitted signal is not uniform.

The approximate distribution of characteristic distortions may be written in the form

$$\varphi(x) = \frac{1}{2\sigma\sqrt{2\pi}} \left(e^{-\frac{(x+v_1)^2}{2\sigma^2}} + e^{-\frac{(x+v_2)^2}{2\sigma^2}} \right), \quad (28)$$

where $v_1 = -0.5\%$, $v_2 = +6.5\%$.

The distribution of pulse edge displacements due to the combined action of fortuitous and characteristic distortions is obtained to first approximation as a combination of the normal distribution (3) and the distribution (28). Strictly speaking, edge displacements due to fortuitous and characteristic distortions are dependent variables. However, since fortuitous distortions cause pulse elongation and shortening with equal probability, this dependence does not influence the sum of the random variables.

In the general case the overall distribution of transitions affected by the various distortions is essentially different from the normal distribution. It can be expressed, e.g., by means of the Pearson interpolation curves /37, 52/.

4. STATISTICAL MODEL OF NOISE

A statistical or stochastic model of noise is needed for the analysis of the relationship between signal statistics and error distribution in a communication channel. A model of this kind will enable us to consider the interaction of signals and noises, which in fact leads to errors /11/.

The analysis that follows refers to a simplified scheme of a communication system, shown in Figure 8. The transmitter input is a train of binary digits having the form

$$\dots a_{-i} \dots a_0 a_1 a_2 \dots a_i a_{i+1} \dots, \quad (29)$$

where $a_i = \pm U_m$ are the pulse voltage amplitudes at the channel input.

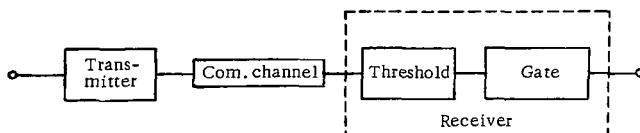


FIGURE 8.

Signal statistics is described by probability distribution functions and the probabilities $P(a_{i_1} \dots a_{i_q})$ of various q -unit combinations, where q is any positive integer and the elements a_i are selected from the sequence (29) in any order.

After modulation, transmission, and demodulation, the signal and the noise mixed with it in the channel are delivered to the receiver input.

Reception in the d.c. channel is generally made by the signal segment method, i.e., by taking a single reading of the modulator output voltage at the time corresponding to the keying midpoint. In this case the receiver has a threshold device which restores the square shape of the signal voltage and a gating stage.

If the sign of the input voltage delivered to the threshold device is reversed by noise interference, the pulse produced at the receiver output will be different from the original pulse and an error will be indicated.

Let the noise acting on the signal in the d.c. channel have an m -variate joint probability density-distribution of voltages $\varphi_m(x_1 \dots x_m)$, where m is the number of digits in the code group affected by noise.

Consider the case when the effect of characteristic distortions on the probability of faulty reception is negligible. From an arbitrary m -digit group we select w digits $i_1 \dots i_w$ and find the probability $P_m(i_1 \dots i_w)$ of error in these digits, the remaining digits being received without error. This is obviously equivalent to the following event: the noise in the crests of the pulses $i_1 \dots i_w$ is greater than U_m in magnitude and opposite in sign, while this is not so for the other digits $j_1 \dots j_{m-w}$.

In [11] the probability $P_m(i_1 \dots i_w)$ is given by

$$P_m(i_1 \dots i_w) = \underbrace{\int_{-U_m}^{-U_m} \dots \int_{-U_m}^{-U_m}}_{w \text{ times}} \underbrace{\int_{-U_m}^{\infty} \dots \int_{-U_m}^{\infty}}_{(m-w) \text{ times}} \varphi_m \left(\frac{x_{i_1}}{\text{sign } a_{i_1}} \dots \frac{x_{i_w}}{\text{sign } a_{i_w}} \times \right. \\ \left. \times \frac{x_{j_1}}{\text{sign } a_{j_1}} \dots \frac{x_{j_{(m-w)}}}{\text{sign } a_{j_{(m-w)}}} \right) dx_{i_1} \dots dx_{i_w} dx_{j_1} \dots dx_{j_{(m-w)}}, \quad (30)$$

where

$$\text{sign } x = \begin{cases} +1 & x > 0 \\ -1 & x < 0. \end{cases}$$

We are now in a position to describe the effect of noise on a transmitted signal by considering some discrete noise model. A convenient noise model is a train of three-unit pulses $b_i = +1, 0, -1$ which are synchronous with the signal pulses a_i .

The statistics of the equivalent noise model is described by a multivariate joint probability distribution $P(b_i \dots b_{i_m})$ of a certain pulse combination $b_i \dots b_{i_m}$. There is a digit-by-digit interaction between the binary signal and the equivalent noise model, the outcome of which is illustrated in Table 2. An error results when the noise has a nonzero value opposite in sign to the corresponding digit of the transmitted signal.

TABLE 2.

Noise	Received signal	
	when +1 is transmitted	when -1 is transmitted
0	+1	-1
+1	+1	+1
-1	-1	-1

The probability distribution $P(b_i \dots b_{i_m})$ is determined from the multivariate probability density distribution of the real noise voltages with the aid of the relation

$$P(b_{i_1} \dots b_{i_m}) = \int_{\psi_1(b_{i_1})}^{\psi_1(b_{i_1})} \dots \int_{\psi_m(b_{i_m})}^{\psi_m(b_{i_m})} \varphi_m(x_1 \dots x_m) dx_1 \dots dx_m, \quad (31)$$

where the functions $\psi_1(b_i)$ and $\psi_2(b_i)$ are defined as follows:

$$\psi_1(b_i) = \begin{cases} U_m & b_i = 0 \\ \infty & b_i = +1 \\ -U_m & b_i = -1 \end{cases} \quad \psi_2(b_i) = \begin{cases} -U_m & b_i = 0 \\ -\infty & b_i = -1 \\ U_m & b_i = +1 \end{cases}$$

Chapter Three

ERRORS IN DIGITAL DATA TRANSMISSION

1. DISTRIBUTION OF ERRORS IN TRANSMISSION OF SIGNALS OF VARIOUS STATISTICS

Bleikhman /9, 11/ derived the probability distribution $P_m(w)$ for the interaction of signals of various statistics with uncorrelated and correlated noises. Noise was represented by the equivalent discrete model of the preceding chapter, which is a random sequence of three-unit codes.

Uncorrelated noise. Let noise be a normal random process and let the instantaneous noise values at intervals equal to the duration of the unit pulse be independent. The noise probability density distribution is then written as

$$\varphi_m = \left(\frac{1}{\sigma \sqrt{2\pi}} e^{-\frac{(x-v)^2}{2\sigma^2}} \right)^m. \quad (32)$$

Let P_{n+} , P_{n-} , P_{n0} be the respective probabilities of the three kinds of noise, $b_i = +1$, $b_i = -1$ and $b_i = 0$. Making use of (31), we find the statistics of the equivalent noise model:

$$\left. \begin{aligned} P_{n+} &= \frac{1}{\sigma \sqrt{2\pi}} \int_{U_m}^{\infty} e^{-\frac{(x-v)^2}{2\sigma^2}} dx = 0.5 - \Phi\left(\frac{U_m - v}{\sigma}\right), \\ P_{n-} &= \frac{1}{\sigma \sqrt{2\pi}} \int_{-\infty}^{-U_m} e^{-\frac{(x-v)^2}{2\sigma^2}} dx = 0.5 - \Phi\left(\frac{U_m + v}{\sigma}\right), \\ P_{n0} &= \frac{1}{\sigma \sqrt{2\pi}} \int_{-U_m}^{U_m} e^{-\frac{(x-v)^2}{2\sigma^2}} dx = 1 - (P_{n+} + P_{n-}) = \\ &= \Phi\left(\frac{U_m - v}{\sigma}\right) + \Phi\left(\frac{U_m + v}{\sigma}\right). \end{aligned} \right\} \quad (33)$$

The probability P_{err_0} of faulty reception of a signal pulse is (Table 2)

$$P_{\text{err}_0} = P(0) P_{n+} + P(1) P_{n-}. \quad (34)$$

If the mean value of the random process is zero, i.e., $P_{n+} = P_{n-} = P_n$, we have $P_{\text{err}_0} = P_n$. The probability of a single error is thus constant and independent of the signal statistics. Two random events — errors in two arbitrarily chosen digits — are thus independent. The reception process

can be visualized as a succession of independent tests having as a positive outcome faulty reception of a single pulse. The probabilities $P_m(w)$ follow a binomial distribution for any signal:

$$P_m(w) = C_m^w P_n^w (1 - P_n)^{m-w}. \quad (35)$$

If $P_{n+} \neq P_{n-}$, but $P(1) = P(0)$, i.e., positive and negative pulses in the signal are equiprobable, we have

$$P_{\text{err}_0} = 0.5 (P_{n+} + P_{n-}). \quad (36)$$

$P_m(w)$ again has a binomial distribution:

$$P_m(w) = 0.5^w C_m^w (P_{n+} + P_{n-})^w [1 - 0.5 (P_{n+} + P_{n-})]^{m-w}. \quad (37)$$

In [9, 11] it is shown that in general, when $P_{n+} \neq P_{n-}$ and $P(1) \neq P(0)$, the distribution of $P_m(w)$ for various signals and noises is also close to binomial:

$$P_m(w) = C_m^w P_{\text{err}_0}^w (1 - P_{\text{err}_0})^{m-w}. \quad (38)$$

Thus, for a transmission channel with uncorrelated noise, $P_m(w)$ is a random variable which is independent of the test signal statistics. Error distribution can therefore be measured with an arbitrary test signal, provided that its $P(1)$ and $P(0)$ are equal to the corresponding probabilities of the real signal. In particular, if the transmitted signals have a nearly uniform statistics, i.e., $P(1) \approx P(0)$, dots can be used as test signals. In real channels, however, the noises are generally correlated.

Correlated noise. We now consider the case of noise with correlated elements, i.e., statistically the equivalent noise model is a simple Markov chain. Let b_{iq_1} , b_{iq_2} stand for the noise pulse in the i -th and the $(i+1)$ -th digits, respectively. Here

$$b_{iq_1} = \begin{cases} 0 & q_1 = 1 \\ +1 & q_1 = 2 \\ -1 & q_1 = 3 \end{cases} \quad b_{(i+1)q_2} = \begin{cases} 0 & q_2 = 1 \\ +1 & q_2 = 2 \\ -1 & q_2 = 3. \end{cases} \quad (39)$$

The noise can be described by the joint probability distribution $P_{q_1 q_2}$ of the noise values in the i -th and $(i+1)$ -th digits (Table 3). It is assumed that $P_{n+} = P_{n-} = P_n$.

TABLE 3.

q_1	q_2			$P_{q_1} = \sum_{q_2=1}^3 P_{q_1 q_2}$
	1	2	3	
1	$1 - 4P_n - 2rP_n$	$P_n - rP_n$	$P_n - rP_n$	$1 - 2P_n$
2	$P_n - rP_n$	rP_n	0	P_n
3	$P_n - rP_n$	0	rP_n	P_n
$P_{q_2} = \sum_{q_1=1}^3 P_{q_1 q_2}$	$1 - 2P_n$	P_n	P_n	

Correlation in our equivalent noise model means that the probability of the two-unit combinations $+1+1$ or $-1-1$ is rP_n , where the correlation coefficient of the random variables b_i and b_{i+1} satisfies the inequality $r \gg P_n$, while combinations $+1-1$ and $-1+1$ are not allowed. Note that if the noise pulses in the i -th and the $(i+1)$ -th digits were independent, noises of the form $+1-1$, $-1+1$, $-1-1$ would be equiprobable, i.e., $P(11) = P(-1-1) = P(+1-1) = P(-1+1) = P_n^2$.

For correlation coefficients close to unity, the probability of a nonzero element following a zero in the noise model is very low. The probability of $+1$ and -1 being followed by the same digit, on the other hand, is close to unity.

This correlated noise model corresponds to very rare clusters of pulses of one sign. The rarity of these clusters is explained by the fact that P_n is generally less than $10^{-4} - 10^{-5}$.

Let us find the distribution of $P_m(w)$ for the interaction of this correlated noise with uniform signals and with dots. The length of a noise burst, i.e., a succession of nonzero noise pulses, is l_n . Since P_n is small, an m -unit block apparently cannot accommodate more than a single noise burst even if m is large.

The probability of a zero being followed by a nonzero element, i.e., the probability of code groups $0+1$ and $0-1$, is

$$P(b_i = 0, b_{i+1} = \pm 1) = 2P_n(1-r). \quad (40)$$

The probability of a nonzero element following a nonzero element is

$$P(b_i = \pm 1, b_{i+1} = \pm 1) = r. \quad (41)$$

The probability of a zero following a nonzero element is

$$P(b_i = \pm 1, b_{i+1} = 0) = 1-r. \quad (42)$$

The probability P_l of a group of noise pulses of length l_n is

$$P_l = 2P_n(1-r)^2 r^{l_n-1}. \quad (43)$$

Let us determine the probability $P_l(w)$ that a group of l_n noise pulses produces w errors upon interacting with a signal which consists of equiprobable combinations. Since the noise burst is composed of elements of one sign, generation of w errors means that in an l_n -unit block of the signal w elements are of opposite sign relative to the sign of the noise pulses and $l_n - w$ elements have the same sign. There is a total of $C_{l_n}^w$ combinations of this kind, each with a probability of 0.5^{l_n} . Hence,

$$P_l(w) = \begin{cases} C_{l_n}^w \frac{1}{2^{l_n}} & w \leq l_n, \\ 0 & w > l_n. \end{cases} \quad (44)$$

We can now find $P_m(w)$ as the probability of the following random event: a group of noise pulses of arbitrary length l_n superimposed on an m -unit

block of a uniform signal causes w errors, i. e.,

$$P_m(w) = \sum_{l_n=1}^m P_l P_l(w) = 2P_n(1-r)^2 \sum_{l_n=w}^m r^{l_n-1} C_{l_n}^w \frac{1}{2^{l_n}}. \quad (45)$$

This formula is true for $w > 0$ only. For $w = 0$ the probability $P(l_n = 0)$ of no noise in an m -unit segment of the signal must be taken into consideration, whence

$$P_m(0) = \frac{(1 - 4P_n - 2P_n r)^{m-1}}{(1 - 2P_n)^{m-2}} + 2P_n(1-r)^2 \sum_{l_n=1}^m r^{l_n-1} \frac{1}{2^{l_n}}. \quad (46)$$

If dots are transmitted over the channel, $P_l(w)$ is defined by the following equalities:

$$P_l(w) = \begin{cases} 0 & w \neq 0.5l_n \\ 1 & w = 0.5l_n \end{cases} l_n = 2k \\ \begin{cases} 0.5 & w = 0.5(l_n - 1) \\ 0.5 & w = 0.5(l_n + 1) \end{cases} l_n = 2k + 1 \quad (k = 1, 2, \dots) \quad (47)$$

Thus, when noise interferes with dots, $P_l(w)$ does not vanish for three values of w only.

Making use of (46) we now obtain for $w \leq 0.5l_n$ and $l_n \leq m$

$$P_m(w) = \sum_{l_n=1}^m P_l P_l(w) = 0.5P_{2w-1} + P_{2w} + 0.5P_{2w+1} = P_n(1-r^2)^2 r^{2w-2}. \quad (48)$$

For $w > 0.5l_n$

$$P_m(w) = 0, \quad (48a)$$

and

$$P_m(0) = \frac{(1 - 4P_n - rP_n)^{m-1}}{(1 - 2P_n)^{m-2}} + 0.5P_n(1-r^2). \quad (49)$$

Relations (45)–(49) give a basis for comparison of the probability distributions $P_m(w)$ for the interaction of correlated noise with a uniform signal and with dots. The results are plotted in Figure 9. This figure also gives the binomial distribution corresponding to the interaction of any signal with uncorrelated noise. The curves in Figure 9 are plotted for $P_n = 10^{-3}$, $r = 0.8$. For dots $P_m(w)$ is taken equal to zero when $w > 0.5(m+1)$. Figure 9 shows that with correlated noise the probability distribution of $P_m(w)$ essentially depends on signal statistics.

It is clear from the preceding that the distribution of distortions and errors is dependent on signal and noise statistics. In the general case it is very difficult to pass analytically from the statistics of signals and noises to the distributions of distortions, mutilations, and even errors, but in particular cases the problem can be solved with the aid of a computer.

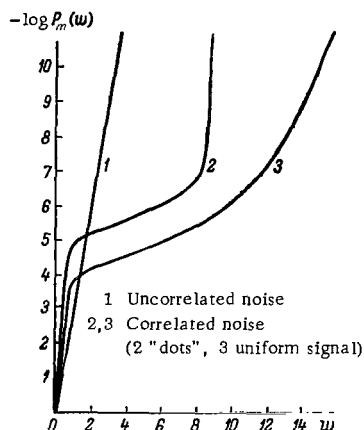


FIGURE 9.

In transmission and coding problems channel statistics are often specified by the parameters of the error stream [27]. The error stream is represented as some statistical model based on available experimental data.

2. STATISTICAL ERROR MODELS

Error models providing the best fit to experimental results for real channels are discussed in a number of publications [42, 73, 74, 85, 90-92]. The error model is largely determined by the type of the channel and its characteristic noises.

The simplest error stream model is a sequence of independent tests with two possible outcomes. This model is fully described by a single parameter which can be measured without difficulty. This is the probability P_{err_0} of faulty reception of a single elementary pulse. Given this parameter we can find the probability of incorrect reception of a block of digital data of arbitrary length, the probability of one, two, etc., errors in the block, and determine the effectiveness of various reliability improvement techniques.

Indeed, once P_{err_0} is known, we can assume that distortions of all the digits in the code group are equiprobable and, making use of the binomial distribution, we find the probability of an erroneous m -digit combination

$$P_{\text{err}_m} = \sum_{q=1}^m C_m^q P_{\text{err}_0}^q (1 - P_{\text{err}_0})^{m-q}. \quad (50)$$

However, this simple model generally does not correspond to the error stream characteristic of digital data transmission over real communication channels, where strong correlation normally exists between the individual errors. Error clusters or bursts consequently form at discrete times, and the error probability in such a cluster is considerably higher than the average error probability calculated for a lengthy transmission time. A proper statistical model should obviously allow for this peculiar feature of the real error stream.

The general approach to model development is to find a probabilistic scheme which formally corresponds to the principal error-causing factors and checks with the experimental findings to an extent which makes it adequate for practical engineering calculations. A one-to-one correspondence is generally assumed in digital data transmission systems between the occurrence of an error and the number of cases when the sum of signal and noise exceeds a certain threshold value. In real cases this threshold value, and hence the number of errors, depends on the modulation being used. In idealized statistical models, however, this dependence is ignored to first approximation.

E. Gilbert /85/ proposed a channel model in which the errors are bunched in clusters and the successive error bursts are dependent on one another. In this model the error stream is a stationary Markov random process. The channel is assumed to occupy one of the two states A and B: in state A the probability of an error burst in the channel is zero and in state B this probability has a sufficiently large finite value.

The probability of accurate or faulty transmission of a binary digit a_{i+1} depends on the state of the channel during the transmission of the previous digit a_i . Suppose that the channel was in state A during the transmission of a_i . The probability that it remains in the same state during the transmission of the next bit a_{i+1} is P_{AA} and the probability that it reverts to state B is $P_{AB} = 1 - P_{AA}$. Similarly, if the state of the channel during the transmission of a_i was B, there is a probability P_{BB} that it remains in the same state during the transmission of a_{i+1} and a probability $P_{BA} = 1 - P_{BB}$ that it reverts to state A.

The transition probabilities are thus given by a square matrix

$$Z = \begin{vmatrix} P_{AA} & P_{AB} \\ P_{BA} & P_{BB} \end{vmatrix}. \quad (51)$$

The parameters P_{AA} , P_{BB} , P_{AB} , P_{BA} are determined experimentally. The average error burst length is P_{BA}^{-1} and the average length of the error-free interval between successive error bursts is P_{AB}^{-1} .

The average probability of a single error is

$$P_{\text{err}_0} = \frac{P_{AB}}{P_{BA} + P_{AB}} P_0, \quad (52)$$

where P_0 is the probability of a "bad" digit in state B.

For example, if the average length of an error burst is 10 digits and the average length of error-free transmission is 10^3 digits, the matrix Z has the form

$$Z = \begin{vmatrix} 0.999 & 0.001 \\ 0.1 & 0.9 \end{vmatrix}.$$

P_0 can be taken equal to 0.5, which is borne out by experimental findings /83, 93/. The mean error probability then is $P_{\text{err}_0} = 5 \cdot 10^{-3}$.

A stationary, time-independent process is assumed and the probability of the states A and B during the transmission of a particular digit is

therefore constant (not dependent on the position of the digit in the combination). The corresponding probabilities are

$$P_{Bf} = \frac{P_{AB}}{1 - P_{BB} + P_{AB}}, \quad P_{Af} = 1 - P_{Bf} = \frac{1 - P_{BB}}{1 - P_{BB} + P_{AB}}. \quad (53)$$

The constancy of P_{Bf} and P_{Af} is not to be interpreted as pointing to independence of the successive digits. Accurate or faulty reception of a_{i+1} depends on whether a_i was received correctly or erroneously.

This error stream model is convenient in certain cases for qualitative and approximate quantitative analysis of transmission and coding techniques /80/. This model, however, is inherently approximate and it ignores some fundamental properties of the real error stream.

A different model based on the following three assumptions is described in /73/: (1) the errors are grouped in bursts, (2) the errors in each burst are correlated, (3) the bursts are independent of one another.

The assumption of burst independence is justified because error bursts are in fact independent channel disturbances. When digital data are transmitted over long-range communication channels these disturbances are caused by random voltage fluctuations, carrier frequency fading, overloading of line amplifiers, and other statistically independent phenomena. In transmission over switched channels, typical disturbances are caused, e.g., when selector contacts are disconnected by vibrations from neighboring selectors, etc. The independence assumption is generally true for most transmission channels, since otherwise two dependent disturbances can be traced to a common origin and consequently combined into one.

Since generation of disturbances is a series of independent events, the stream of errors is the simplest case of discrete Poisson stream.

It is further assumed that the time of disturbance is not related to the length of the disturbing pulse and that during the disturbance, i.e., in the error burst, the error stream is stationary in the first approximation and can be described with sufficient accuracy by the mean probability of error inside the burst. If the above conditions are satisfied, the discrete stream of correlated errors is representable as a model defined by the following three parameters.

(1) The probability of an error burst $P_{n_{err}}$, equal to the ratio of the number of independent sequences of correlated errors to the total number of transmitted symbols.

(2) The probability of an error burst of certain length, i.e., the conditional probability $P_{l_{err}}$ of an l_{err} -unit burst. This parameter is introduced to describe error correlation in the burst.

(3) The conditional probability of an error in a burst $P_{l_{err}}$; it is assumed that $P_{l_{err}} = \text{const}$.

This error model gives a fairly complete representation of errors in the relatively short switched channels of local telephone communications systems, where the main disturbances are caused by disconnected selector contacts. This model can be applied to calculate the probability of distortion of a data block of known length and the probability of distortion of several blocks in succession; in other words, this model allows for correlation between distorted blocks. This aspect is particularly important in evaluation of ARQ systems. In /73/ this model is used as a basis for a comparative effectiveness analysis of various recurrent codes.

These models are unfortunately not valid for the multisectional long-distance telephone lines.

A general statistical model corresponding to errors in digital data transmission over telephone channels can be apparently developed from A. A. Markov and S. N. Bernshtein's interpretation of the Pearson interpolation curves.

The probability density function $y = \varphi(x)$ for the Pearson curves is given by the differential equation

$$\frac{dy}{dx} = - \frac{x - M_0}{\beta_0 x^2 + \beta_1 x + \beta_2} y, \quad (54)$$

where M_0 is the curve mode, β_1 are constants.

The curves described by equation (54) are distribution curves if they meet the following three conditions: (1) y is a positive number between the distribution limits, (2) the area under the curve is equal to the distribution volume, (3) the distribution has finite moments.

The last requirement is satisfied in practice for any empirical distribution [52].

The general integral of (54) is

$$y = y_0 e^{-\psi x}, \quad (55)$$

where

$$\psi(x) = \int \frac{x - M_0}{\beta_0 x^2 + \beta_1 x + \beta_2} dx. \quad (56)$$

The value of this indefinite integral depends on the roots of the equation

$$\beta_0 x^2 + \beta_1 x + \beta_2 = 0. \quad (57)$$

Pearson curves corresponding to the real roots of this equation are motivated by the following testing procedure, due to Markov [52]. From a container holding a certain number of white and black spheres we draw one sphere n times. After each drawing the sphere is returned to the container and a certain number of spheres of the same color are added. According to Bernshtein [7], the drawing of a sphere of a certain color signifies that the conditions are favorable for the "multiplication" of spheres of the same color, and some spheres of the same kind are consequently added to the population. After many tests, the number of spheres in one of the two opposite classes will be distributed according to one of the Pearson curves.

To return to our case, let the drawing of a white sphere represent accurate reception of a transmitted digit, while a black sphere signifies a transmission error. In accordance with the multiplication scheme, the first error-free interval (or the first error in a burst) is followed by additional error-free digits (or additional errors). The length of error-free transmission and the length of error bursts are distributed according to one of the Pearson curves.

The coin-tossing game between two partners is a particular case of the above model. Analysis of individual gains and losses in this game (which is a case of the so-called random walk /61) shows that a gain scored by one of the participants is actually "conductive" to additional score by the same person. As the result the winning score seldom passes from one participant to the other, and the probability of this "change of luck" diminishes with time.

In a properly designed digital data transmission system errors are very rare and the total number of errors in relation to the total number of transmitted digits in a certain interval of time is very small. It is therefore a better policy to consider the distribution of error-free intervals than the distribution of error burst lengths.

Berger and Mandelbrot /74/ have shown that the distribution of intervals between successive errors in telephone channels has much in common with the behavior of the distances between the roots of the equation $G(v) = 0$, where $G(v)$ is a random process with independent increments of the type described for coin-tossing game.

Processes of this kind are encountered in various problems of economic statistics too. For example, this process corresponds to the distribution of annual incomes of persons whose annual income exceeds a certain limit x_0 set by taxation laws. This truncated distribution approximately coincides with the Pareto distribution /37/

$$P(\xi > x) = \left(\frac{x_0}{x}\right)^q, \quad x > x_0, \quad q > 0. \quad (58)$$

The density function of the Paretian distribution is

$$y = \begin{cases} \frac{q}{x_0} \left(\frac{x_0}{x}\right)^{q+1} & x > x_0 \\ 0 & x \leq x_0. \end{cases} \quad (59)$$

For $q > 1$ its mean is finite, being equal to $\frac{q}{q-1} x_0$.

Putting $q+1 = q_1$ and $qx_0^q = y_0$, we obtain a type XI Pearson curve /52/, specifically

$$y = y_0 x^{-q_1}, \quad a < x < \infty, \quad a > 0, \quad q_1 > 1. \quad (60)$$

In /74/ the Paretian distribution is applied to describe the behavior of error-free intervals in telephone channels. The distribution is defined by the following relations:

$$F(t) = P(l \geq t) = \begin{cases} t^{-\alpha} & t \geq 1, \\ 1 & t < 1, \end{cases} \quad (61)$$

where $P(l \geq t)$ is the probability that the interval between errors (or error bursts) is equal to or greater than some length of time t .

The corresponding probability density is

$$y(t) = \alpha t^{-\alpha-1}, \quad t \geq 1. \quad (62)$$

Taking the logarithm of the two sides in (61), we obtain

$$\log F(t) = -\alpha \log t. \quad (63)$$

The function $F(t) = t^{-\alpha}$ is thus a straight line in log-log coordinates, and its slope is determined by the parameter α .

When the Pareto distribution is used in the form (61) its moments are infinite for $0 < \alpha < 1$ and the analysis is of necessity confined to a certain sampling volume which is determined by the upper limit of the expected error-free interval. In this case the Pareto distribution takes the form /95/

$$F(t) = \begin{cases} 1 & t < 1, \\ t^{-\alpha} & 1 \leq t \leq L, \\ 0 & t > L. \end{cases} \quad (64)$$

$F(t)$ is thus a function of two parameters, α and L .

The behavior of the sum of n independent Paretian error-free intervals is also of some interest. For two error-free intervals the corresponding probability density function $y_2(t)$ of two identical components $y_1(t)$ is given by the convolution of the components, i. e.,

$$y_2(t) = \int_1^{t-1} y_1(\tau) y_1(t-\tau) d\tau. \quad (65)$$

Evaluation of this integral for large t gives the following approximate relation:

$$y_2(t) \simeq 2\alpha t^{-\alpha-1}. \quad (66)$$

In /66/ it is assumed that, in general,

$$y_n(t) \underset{t \rightarrow \infty}{\simeq} n\alpha t^{-\alpha-1}. \quad (67)$$

This model provides a fairly accurate approximation to the actual results obtained for various telephone channels. However, the parameter α , which is one of the fundamental quantities of the model, varies between fairly wide limits depending on the type of channel tested. Analysis of experimental data from /95/ shows that the mean α is 0.11—0.12 /70/ or 0.26—0.30 /83/. Figures 10a and 10b plot $F(t)$ vs. t in logarithmic coordinates. In Figure 10a the abscissa gives the length of an error-free interval in elementary keyings, and in Figure 10b this axis gives the intervals between incorrectly received code combinations. The unit of length on the abscissa axis is the number of code combinations.

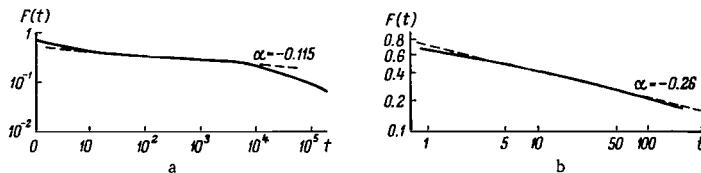


FIGURE 10.

The difference in the mean α is apparently due to differences in specific weight of short and long error-free intervals in various channels. According to Berger and Mandelbrot, α somewhat varies depending on the length of the intererror interval and its average value is about 0.25. For small error-free intervals (high error density) α increases to 0.33—0.5, and likewise for very long intervals, in excess of 10^5 digits (where α is as high as 1).

Prior to Berger and Mandelbrot /74/ and Sussman /95/, P. Mertz /90—92/ investigated the error burst model in telephone channels making use of a modified Pareto distribution. Mertz worked with a hyperbolic error distribution. Putting λ for the density of the error burst stream, we write for this distribution

$$(Ft) = 1 - \frac{A}{A + \lambda t}, \quad (68)$$

where A is a distribution parameter. The corresponding probability density is

$$y(t) = \frac{A\lambda}{(A + \lambda t)^2}. \quad (69)$$

Putting $y_0 = A\lambda$ and making a linear substitution $t_1 = A + \lambda t$, we find

$$y(t_1) = y_0 t_1^{-2}. \quad (70)$$

The last expression shows that Mertz' Paretian distribution is the same as that used by Mandelbrot for $\alpha = 1$.

The parameters λ and A of the hyperbolic distribution are related to the mean rate of error bursts and the length of the experiment. They are thus equivalent in a sense to L in the Pareto distribution (64).

The two models assume independence of the error-free intervals between error bursts and constitute alternative approaches to the conception of errors in digital data transmission over telephone channels. Mertz and Mandelbrot disagree in their estimates of α . Berger and Mandelbrot's model is obviously the more general of the two, since it allows for variable α , whereas Mertz assumes a constant α , $\alpha = 1$. We have previously noted that for a low error-burst density α increases, approaching unity. Mertz apparently had in mind this particular case of infrequent error bursts.

Application of these error models in selection of modulation modes, receiver algorithms, coding techniques, etc., falls beyond the scope of this book. In conclusion of this chapter it suffices to note that in /95/ Berger and Mandelbrot's model is applied to calculate the necessary characteristics for the selection of optimum codes, e.g., the probability of zero, single, and double errors in a data block of given length, the probability of error-free intervals for various error-correcting codes, etc.

Analysis of various coding techniques and codes can be very efficiently carried out with the aid of digital computers /78/ or simulated computer channels. Signals and noises of given statistics are simulated in the channel, or error distributions corresponding to the real state of channels of this kind are adopted from the start. In the latter case the transmission and coding techniques can be analyzed by the Monte Carlo method on a computer. Pseudorandom number representing the codes which are distorted by noise in transmission are generated by feeding the computer with adequate information on channel statistics. This information is best represented as a probability distribution of error-free intervals derived from the Paretian model.

Chapter Four

TEST SIGNALS AND THEIR GENERATORS

1. PRINCIPLES OF TEST SIGNAL GENERATION

We have previously shown that digital data transmission techniques, communication channels, and terminal equipment are tested by sending a special test signal which is compared digit by digit with an undistorted control signal in the receiver. The test signals are generated so that their statistics is as close as possible to that of real messages.

In accordance with the quite general considerations of Chapter Two, all combinations of equal length in a real signal are equiprobable. The test signal statistics must obviously satisfy this basic criterion. However, the number of different states in the oscillator circuit is finite and the test signal is of necessity periodic, so the requirement of equiprobable combinations cannot be exactly satisfied. A periodic signal cannot be made to simulate real signal statistics for any m ; adequate simulation is possible only for $m \leq M$, where M is a parameter determined by the period of the signal.

The choice of M is very important in the generation of test signals. If it is increased, the period becomes longer, but the complexity of the oscillator circuit increases simultaneously. The parameter M should be chosen with allowance for the statistical properties of the transmitted signal and channel noise. The coding technique and the characteristic distortions in the channel are also taken into consideration. With five-unit or seven-unit codes, M is generally in the range from 5 to 12, since increasing M above 10 does not introduce any substantial improvement in test signal statistics as far as its likeness to the real signal is concerned [11].

Telegraph networks and terminal equipment are tested by preprogrammed test signals. The analysis of the distribution of characteristic distortions for different signal statistics (Chapter Two) leads to the conclusion that these distortions are best evaluated by transmitting undistorted "reversals" and "dots". Bias distortions are also measured with the aid of "dots". Testing of telegraph channels and terminal equipment, however, requires transmission of an undistorted text which includes all possible combinations. In particular, voice-frequency telegraph channels with start-stop tape equipment are tested by transmitting the 8-combination Q9S recommended by CCITT.

2. REGULAR CODE SEQUENCES AND THEIR APPLICATION TO TEST SIGNAL GENERATION

Let us consider how test signals having the required properties are generated. A test signal is formed by periodic repetition of a certain sequence of binary digits, which is henceforth called a "word". We will now show that if the periodic repetition of the word ensures equiprobability of all combinations of length M in the generated signal, all combinations of length $m \leq M$ are also equiprobable.

The probability of any combination of length $m \leq M$ in the signal is the probability of a combination of length M in which the first m digits coincide with the m -unit combination the probability of which is being sought. The number of M -combinations meeting this requirement is 2^{M-m} . The probability P_m of any of these combinations is

$$P_m = \sum_1^{2^{M-m}} P_M = 2^{M-m} \frac{1}{2^M} = \frac{1}{2^m}, \quad (71)$$

which proves that all m -unit combinations ($m \leq M$) in the chosen word are equiprobable.

It thus suffices to consider words which satisfy the fundamental requirement for $m=M$, since, according to the proposition that we have just proved, this requirement will also be satisfied for all $m \leq M$. We start with words which are sequences of all the 2^M code combinations of length M , arranged in a certain order.

Not any order of combinations in a word ensures equiprobability of code groups of equal length, and a signal generated by periodic repetition of a word in which the order of combinations does not satisfy certain requirements is not a simulation of a real signal.

A word should constitute a regular code sequence, i. e., a sequence containing all the 2^M different M -unit code combinations, each combination occurring only once in the original sequence and in the $(M-1)$ sequences obtained by cyclic permutation of the digits of the original sequence. The probability P_M of any combination in a signal generated by periodic repetition of a regular word is determined by counting the number of times this combination appears in the test word and in the $M-1$ words obtained by cyclic permutations. This number, R , is then divided by the number of all possible combinations having different positions in the word. Since the original word is a regular sequence, we have $R=M$ and $P_M = M/M2^M = 1/2^M$.

Regular code sequences can be generated by a recursive technique, based on the following proposition.

If

$$a_1 \dots a_k a_{k+1} \dots a_M \mid a_{M+1} \dots a_{M+k+1} \dots a_{2M} \mid \dots \mid a_{(N-1)M+1} \dots a_{NM}, \quad (72)$$

where

$$a_i = \begin{cases} 0 \\ 1 \end{cases}, N = 2^M,$$

is a regular code sequence for an M -unit code set, the regular code sequence for an $(M+1)$ -unit code set is generated by writing the original sequence twice, adding at the end of each code combination either a zero or a one in any order, provided that the corresponding combinations of the first and the second sequence are augmented by different digits.

A number of corollaries follow from this proposition, which is proved in /10/. One of these corollaries states that reversing the enumeration of elements of a regular code sequence gives another regular sequence.

We are now in a position to form regular sequences for any M . Such sequences for $M=1, 2, 3, 4$ are given in /10/. A particular case of a regular sequence is provided by the natural numbers from 0 to 2^M-1 written in binary notation.

Note that a signal based on a regular code sequence contains all possible M -unit code combinations. It is thus adequate for testing the terminal equipment, as well as the communication channels.

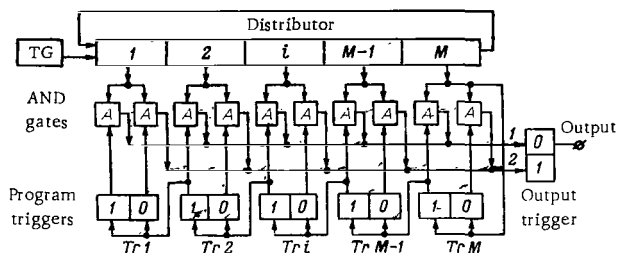


FIGURE 11.

The functional principle of a generator of regular code sequences can be understood by considering how a trigger works when pulses are delivered to its input at an appropriate rate. The trigger successively switches to states 0101..., i.e., its output is a regular one-unit binary code sequence.

If the first trigger is coupled to a second trigger, the states 0101... of the first correspond to the states 0011... in the second. Conversion of the parallel code combinations generated by the two triggers to serial codes gives a regular code sequence of the form 00 10 01 11 00..., which has been generated according to the preceding rule. The first trigger generates a regular one-unit code sequence, while the second trigger, which operates twice as slow, successively adds zeros or ones to the different code combinations of the first trigger.

A binary counter circuit using M triggers generates regular code sequences for a complete M -unit code set. Various sequences are possible depending on the correspondence between the trigger number and the bit position in the sequence, but all the $M!$ sequences are regular.

A block diagram of the corresponding test pulse generator is shown in Figure 11. The circuit includes a timing generator (TG), and M -bit distributor, coincidence gates A, program triggers Tr, and an output trigger.

3. TEST SIGNALS BASED ON CODE RINGS

A test signal can be based on a word in which not all, but only some of the code combinations are present. The missing combinations are generated by cyclic permutations of the digits of this word.

If the n last elements in one of the M -unit combinations are identical to the n first elements of some other combination, we shall say that these combinations intersect at a certain n -unit combination.

Ordering the code combinations according to their intersections, we can omit the common n units and thus obtain the required word, where the number of digits is less than the number of elements in the complete code set. The value of n is between the limits $0 \leq n \leq M-1$.

For $n=M-1$ we obtain a closed sequence where the number of elements is equal to the number of nonrepeating combinations that can be formed from sections of the given sequence. Since the complete code set contains 2^M M -unit combinations, the generated word, called a code ring /49/, contains 2^M elements, i.e., a factor of M less than a regular code sequence does.

A code ring thus has the form

$$a_1 a_2 a_3 \dots a_M a_{M+1} \dots a_N. \quad (73)$$

From (73) we can generate a complete code set where each combination appears only once:

$$| a_1 a_2 a_3 \dots a_M | a_2 a_3 \dots a_{M+1} | \dots | a_N a_1 a_2 \dots a_{M-1} |. \quad (74)$$

As the code ring contains 2^M elements, the probability of any of these elements when the ring is periodically repeated is 2^{-M} . To each element of the code ring corresponds its own nonrepeating M -unit code combinations, and the probability of any of these combinations in the signal is also 2^{-M} .

If the test signal is formed by periodic repetitions of the code ring, a simpler generator can be used, since the number of digits in a word is then $1/M$ of their number in a regular sequence.

Code rings containing 2^M elements are generated by M -bit shift registers with logic feedback /50/, which are called recurrent registers. Simple as well as fairly complex feedback configurations can be used. The total number of feedback paths necessary to generate code rings of a known length, $M=5$ say, is 2048.

A substantially simpler feedback configuration is required if a single element is subtracted from the code ring, leaving 2^M-1 elements in it. The missing element can be easily generated by providing an additional logic circuit.

Let us consider this interesting property for the particular case of a code ring with $M=3$. One of the regular code sequences arranged in the order of natural numbers is

$$000\ 001\ 010\ 011\ 100\ 101\ 110\ 111. \quad (75)$$

To form a code ring, we rewrite (75) in such a way that the adjoining 3-bit codes intersect, the last group intersecting with the first:

$$000\ 001\ 011\ 111\ 110\ 101\ 010\ 100. \quad (76)$$

The two possible code rings for 3-bit codes expressed by (76) are closed sequences of the following form:

$$00011101 \quad 10111000. \quad (77)$$

Code rings (77) can be generated by a 3-bit register. According to the procedure advanced in /50/, the feedback loop is synthesized as follows: the sequence of all 3-bit combinations corresponding to the code ring is written out and the feedback function ψ is expressed in symbols of Boolean algebra, remembering that the feedback should set the first bit of the register to 1 after certain combinations.

We designate by a, b, c the first, second, and third bits of the register; without a bar on top these symbols correspond to 1, while barred symbols signify that the corresponding bit in the register is 0. The feedback logic is to set the first bit of the register to 1 after the first, second, third, and fifth 3-bit combination of (76) (this is the sequence corresponding to the code rings (77)). Keeping this requirement in mind, we write the feedback loop function in the form

$$\psi = \bar{a}\bar{b}\bar{c} + a\bar{b}\bar{c} + ab\bar{c} + \bar{a}bc = \bar{b}\bar{c} + b(a\bar{c} + \bar{a}c). \quad (78)$$

For reduced code rings

$$0011101 \quad 1011100 \quad (79)$$

which correspond to the complete rings (77) the feedback loop functions are

$$\psi = \bar{a}c + a\bar{c}, \quad \psi = \bar{b}c + b\bar{c}. \quad (80)$$

The feedback logic described by function (78) obviously corresponds to a very complicated circuit, whereas the feedback function of a reduced code ring, obtained by omitting a single element from the complete ring, can be realized by a simple NAND logic (modulo-2 adder), symbolically denoted as $a \oplus c$ or $b \oplus c$, where \oplus is logical modulo-2 addition.

The adder has two inputs and one output. According to the fundamental rules of Boolean algebra, $0 \oplus 1 = 1$; $1 \oplus 0 = 1$; $1 \oplus 1 = 0$; $0 \oplus 0 = 0$. An output pulse is thus generated only when signals corresponding to two different bits are delivered to the inputs.

Similarly, for the complete code ring of the set of 5-bit codes, e.g.,

$$00000100101100111110001101110101, \quad (81)$$

the feedback logic function is

$$\psi = \bar{b}d(c\bar{e} + \bar{c}e) + \bar{a}\bar{b}\bar{d}\bar{e} + ac\bar{d}\bar{e} + bcd\bar{e} + b\bar{c}e + \bar{a}\bar{b}\bar{c}\bar{d}e + \bar{a}bcd\bar{e}, \quad (82)$$

whereas for the same ring without the first element this function takes the simple form $\psi = c \oplus e$ (compare (80)).

A block diagram of a test signal generator which realizes the code ring (81) is shown in Figure 12. This circuit, sometimes called a recurrent generator, consists of a timing generator (TG), a shift register 1—5 with logical feedback element 6 and inhibitors 7 and 8 which, jointly with element 9, generate the missing element that augments the reduced code ring to a complete ring.

The functional circuit of the generator block-diagrammed in Figure 12 is shown in Figure 13. This is a transistor-magnetic register with nine digits (1—9), five of which are controlled by timing pulses TP_1 and four

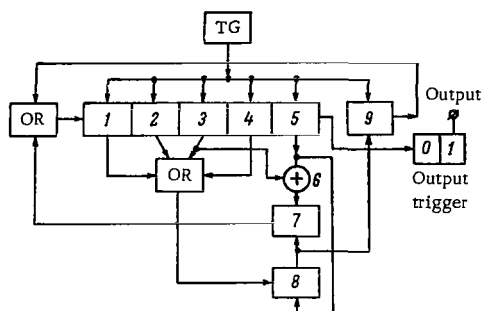


FIGURE 12.

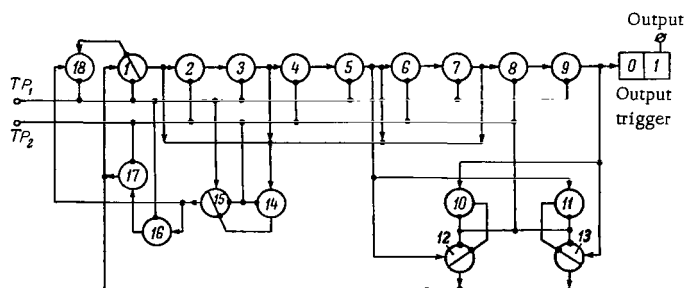


FIGURE 13.

by TP_2 . The feedback element is a four-bit modulo-2 adder (10, 11, 12, 13). A zero combination (i.e., a combination consisting of zeros only) is generated by the inverter circuits 14, 15 with the inhibitor 18. Elements 16 and 17 set the first bit of the register to 1 following the zero combination 00000. The code ring (81) is generated by reading from any of the locations 1, 3, 5, 7, 9.

4. PROGRAMMED TEST SIGNAL GENERATORS

An undistorted signal consisting of D unit pulses is generated by a pulse distributor and a programmed device in which a program describing the structure of the signal is stored. In addition to these fundamental components, the generator includes timing, memory or coincidence circuits, and an output device.

The generator block diagram is prepared with allowance for the particular pulse distributor used, while the choice of the latter is determined by the properties of the test signal. A shift register where the number of locations is equal to the number of pulses can be used as a

distributor only for relatively small D . It is easily seen that if two registers (coupled in series or in parallel) are used, the total number of elements in the distributor is substantially reduced. Indeed, when two registers are available, a signal consisting of d characters in m -bit uniform code is partitioned into d/q groups, each containing qm pulses (q is an integer). Clearly,

$$D = md > qm + \frac{d}{q}, \quad (83)$$

and $m = m_1 + m_2$, where m_1 is the number — system base of the code and m_2 is the number of check digits, i. e., for a quinary seven-digit uniform code $m_1 = 5$, $m_2 = 2$, $m = 7$. Each of the groups includes q characters of the text.

With two shift registers, one has qm and the other d/q locations; the total number of distributor inputs is D . Note that for parallel registers qm and d/q should be relatively prime numbers.

Let ρ be the ratio of the number D of switching elements in a single-register distributor to the sum of elements in two serial or parallel registers, i. e.,

$$\rho = \frac{D}{qm + \frac{d}{q}} = \frac{qmd}{q^2m + d}. \quad (84)$$

It is easily seen that the optimum relationship between the parameter q and the number of characters d in the signal is given by the inequality

$$(q-1)qm \leq d \leq (q+1)qm. \quad (85)$$

As d varies between the limits specified in (85), while q and m remain constant, the ratio ρ (the gain in the number of elements) is at its maximum. If register A has qm locations, the optimum number of locations for register B is between $(q-1)m$ and $(q+1)m$. In serial coupling, the optimum corresponding to the minimum of the sum $qm + d/q$ is attained when registers A and B each have the same number of locations, i. e., when $d/q = qm$.

The minimum and the maximum values of ρ , corresponding to the lower and the upper limits of d , are respectively given by

$$\rho_{\min} = \frac{q(q-1)}{2q-1} m, \quad \rho_{\max} = \frac{q(q+1)}{2q+1} m. \quad (86)$$

Table 4 lists the values of the various parameters for $m=7$ and $q=1, 2, 3, 4$. We see that for a test signal where the number of code combinations does not exceed $d_{\max} = 14$ ($D_{\max} = 98$), register A should have 7 locations and register B $D/7$ locations. For Q9S the number of locations in register B is 8, and the total gain achieved by using a two-register distributor instead of a single-register one is $\rho = 56/(7+8) = 3.7$.

The programmed device used with registers in series is a matrix. The generator has memory circuits whose pulses are delivered to the output. With parallel registers, on the other hand, the program is fixed by making proper connections between the outputs of the two registers and the coincidence gates.

Block diagrams of Q9S generators with a compound distributor consisting of two parallel and two serial registers are shown in Figures 14a and 14b.

The programmed device in Figure 14a is a matrix. The two-dimensional code combination generated by the matrix is converted to a time sequence with the aid of memory circuits M_1-M_6 and register A. The information is read from the output buses when pulses from the appropriate outputs of register B are delivered to the input buses.

TABLE 4.

Parameter	q			
	1	2	3	4
D_{\min}	—	98	294	588
D_{\max}	98	294	588	980
d_{\min}	—	14	42	84
d_{\max}	14	42	84	140
qm	7	14	21	28
d_{\min}/q	—	7	14	21
d_{\max}/q	14	21	28	35
p_{\min}	—	4.67	8.40	12.0
p_{\max}	4.67	8.40	12.0	15.56

In Figure 14b (pulse distributor with two parallel registers) the outputs of all the coincidence gates (there is one corresponding to each transition in the test signal) are connected with the output device.

The serial numbers k_1 and k_2 of the outputs of two parallel registers having qm and d/q locations, respectively, are related to the number k_c of the coincidence gate whose output pulse corresponds to the k -th transition of the D -unit signal by the following expressions:

$$k_1 = k_c - E \left\lfloor \frac{k_c}{qm} \right\rfloor qm, \quad (87)$$

$$k_2 = k_c - E \left\lfloor \frac{k_c}{d/q} \right\rfloor \frac{d}{q}, \quad (88)$$

where E indicates that the whole part of the expression in brackets is meant. Thus,

$$k_c = k_1 + E \left\lfloor \frac{k_c}{qm} \right\rfloor qm = k_2 + E \left\lfloor \frac{k_c}{d/q} \right\rfloor \frac{d}{q}. \quad (89)$$

If one of the ratios k_c/qm or $k_c q/d$ is an integrer, relations (87) and (88) are meaningless. It is easily seen that in this case

$$k_1 = qm, \quad k_2 = \frac{d}{q}. \quad (90)$$

Figures 14a and 14b are equivalent as far as the number of elements is concerned. However, the essential advantage of the circuit in Figure 14a

is that it can be adjusted conveniently: the unit pulses can be sensed successively, since the relevant information is stored in spatially distinct elements.

For D of over a hundred unit pulses (e.g., the test signal for page teletypes), two-register distributors do not provide the optimum solution. A better policy can be devised by further development of the principles outlined in this chapter: the distributor should include three (or more) registers in mixed serial-parallel coupling.

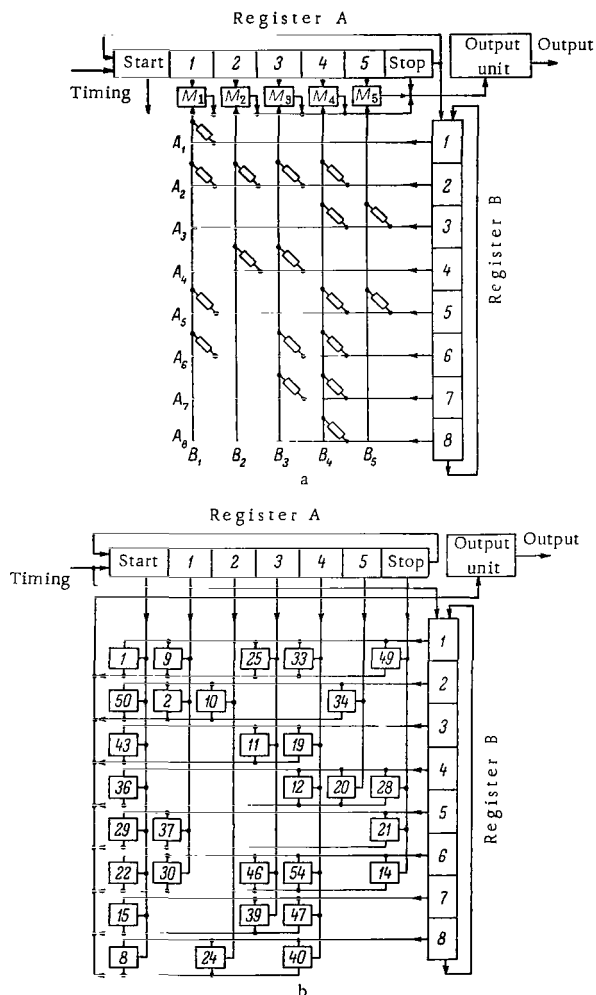


FIGURE 14.

Transistorized and ferrite components of test signal generators, such as the timing generator, distributor, memory or coincidence circuits, are in principle not different from the analogous components used in other pulsed devices [5, 57] and we do not discuss them here. The specific components of the test generator are the program matrix and the output device.

The output unit, comprising a trigger and a noncontact relay, converts the pulses produced at the output of the programmed device to square pulse trains. Calculations of noncontact relays are discussed in Chapter Seven.

The program matrix used with serially coupled registers in the distributor is a characteristic storage device containing detailed

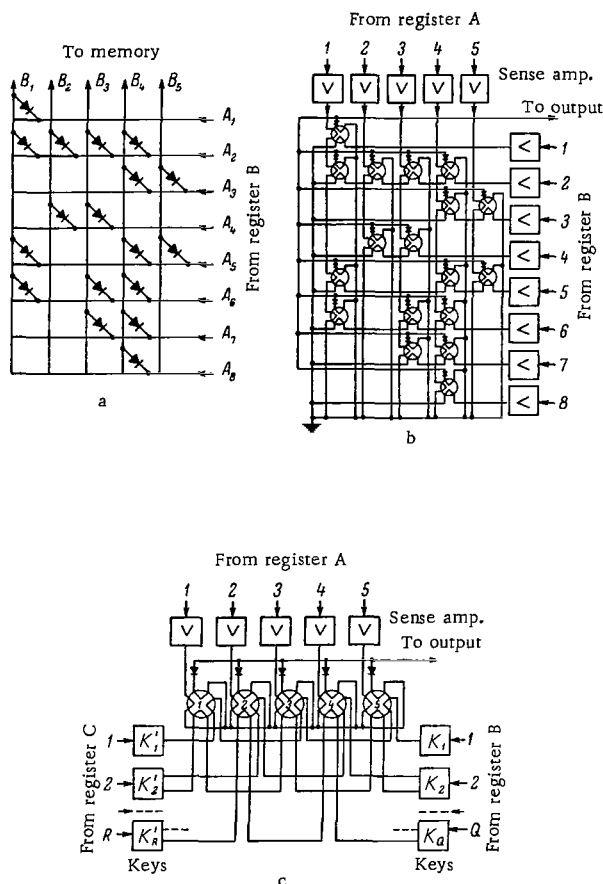


FIGURE 15.

information on the test text to be generated. The simplest matrix (Figure 15a) is that made of diode elements. Ferrite core matrices (Figure 15b) are a convenient substitute for diode matrices. When output pulses of register B are delivered to the write terminals, the ferrite cores of the corresponding bus in the matrix are set to 1.

Amplified output pulses of register A are delivered in succession to the read (sense) terminals of the cores. This matrix requires $qm + d/q$ read and write amplifiers, but it also acts as a storage circuit.

Since the outputs of all cores are combined and the read pulse obliterates the information previously stored in the core, the matrix need not contain more than m_1 cores (where m_1 is the number of code pulses in each combination) irrespective of the particular test signal to be generated.

A ferrite core matrix is used to considerable advantage in high- D generators, i. e., when three, and not two, registers are used. A block diagram of a generator with a ferrite matrix is shown in Figure 15c. Here register A is in series with parallel registers B and C. In addition to the distributor registers, the circuit contains five ferrite cores which act simultaneously as a program matrix and as coincidence gates, sense amplifiers, and keys setting the appropriate cores to 1. The information is successively read by pulses delivered from register A. The matrix output comprises pulses from ferrite cores which have been set to 1.

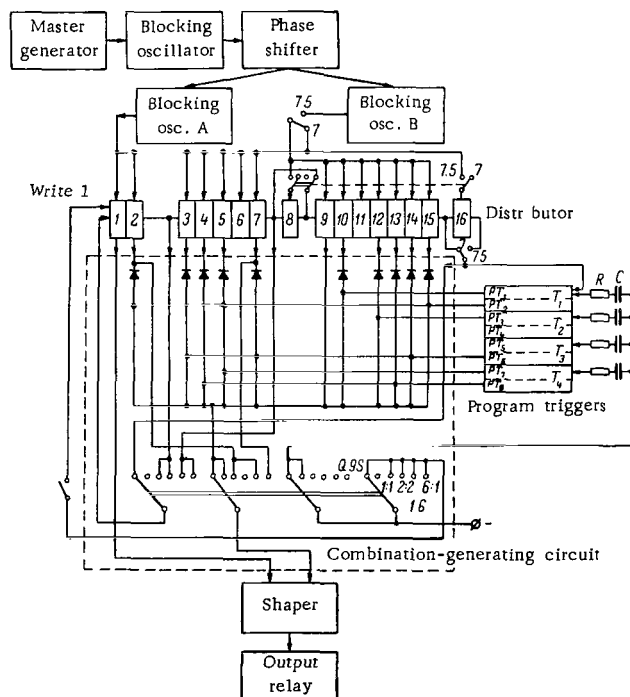


FIGURE 16.

Figure 16 shows a somewhat different block diagram of a generator of undistorted test signals using semiconductor devices and square-loop ferrites. It transmits 1:1, 2:2, 1:6, 6:1, and Q9S signals at up to 80 baud. A 16-bit distributor is used to generate the signal; its outputs are delivered through a switching network to a shaping device.

After each code combination the distributor outputs are switched by a programmed circuit consisting of five triggers. The circuitry and the operation of this generator are discussed in detail in /13/.

5. APPLICATION OF THE THEORY OF LINEAR SEQUENTIAL CIRCUITS TO THE DESIGN OF TEST SIGNAL GENERATORS AND OTHER COMPONENTS

Shift registers are one of the main components of test signal generators and other related equipment. The functional principles of these registers can be investigated with the aid of the theory of linear sequential modulo circuits /64, 67/.

Feedback shift registers successively assume different states which in autonomous operation constitute a periodic sequence with periods of certain length. The length of the periods is determined by the number of locations in the register and the kind of feedback used.

If the circuit logic is described by a modulo- p addition operator, the cyclic structure and the functional principle of the device can be investigated by analyzing the transition matrix and its characteristic polynomial.

Indeed, the state of a linear sequential modulo circuit equivalent to a shift register with k one-bit delay elements is described by a k -dimensional vector S_n with integral-number elements

$$S_n = \begin{bmatrix} s_{1n} \\ s_{2n} \\ \dots \\ s_{in} \\ s_{kn} \end{bmatrix}, \quad (91)$$

where s_{in} is the state of the i -th delay element at the time when the n -th input character is delivered.

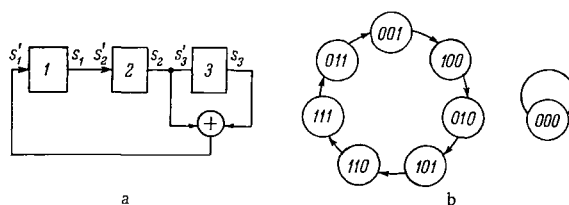


FIGURE 17.

Consider, e.g., the autonomous circuit shown in Figure 17a. It is described by the states s_1, s_2, s_3 of its three delay elements. The states s'_1, s'_2, s'_3 of these elements after a unit delay can be expressed as sums (modulo 2) of the states at the starting time, before the delay. The

relationship between the current and the future states of the circuit is thus described by a set of linear equations (modulo-2 addition is assumed throughout)

$$\begin{aligned} s'_1 &= s_2 + s_3, \\ s'_2 &= s_1, \\ s'_3 &= s_2. \end{aligned} \quad (92)$$

In matrix form these equations are written as

$$\begin{bmatrix} s'_1 \\ s'_2 \\ s'_3 \end{bmatrix} = \begin{bmatrix} 0 & 1 & 1 \\ 1 & 0 & 0 \\ 0 & 1 & 0 \end{bmatrix} \cdot \begin{bmatrix} s_1 \\ s_2 \\ s_3 \end{bmatrix}. \quad (93)$$

Putting

$$\begin{bmatrix} s_1 \\ s_2 \\ s_3 \end{bmatrix} = S, \quad \begin{bmatrix} s'_1 \\ s'_2 \\ s'_3 \end{bmatrix} = S', \quad \begin{bmatrix} 0 & 1 & 1 \\ 1 & 0 & 0 \\ 0 & 1 & 0 \end{bmatrix} = A, \quad (94)$$

we find $S' = AS$.

In general, the state of an autonomous linear sequential circuit is described by the equation

$$S_{n+1} = AS_n, \quad (95)$$

whence

$$S_n = A^n S_0, \quad (96)$$

where S_0 , S_n , S_{n+1} are column vectors which describe the initial, the current, and the future states of the circuit; A is a k -th order square matrix (the characteristic matrix of the set).

The characteristic matrix (transition matrix) thus interrelates the various states of the autonomous circuit, and the sequential behavior of the circuit is completely determined by the algebraic properties of the matrix.

Matrices defined over the modulo field of whole numbers have the same properties as the matrices over the field of real numbers. In particular, the matrix A may have an inverse A^{-1} , so that $AA^{-1} = \varepsilon$, where ε is the identity matrix. The inverse defines an operation by which the circuit reverts from the current to the preceding state, i.e.,

$$S_n = A^{-1}S_{n+1}. \quad (97)$$

The existence of the inverse for a linear sequential circuit implies that each state has a single forerunner. These are determinate circuits. Since the number of states of a linear sequential circuit with k delay elements is finite, being equal to p^k , any sequence of states of this determinate circuit is of necessity periodic, with a period of less than p^k .

The successive states of a linear circuit can be described by a state diagram /67/ where nodes correspond to the various states of the circuit and arrows represent transitions. In the state diagram of a determinate circuit, there is only one arrow entering each node and one arrow leaving the node.

State diagrams can be constructed by applying the matrix A to all possible states of the circuit. Let the circuit in Figure 17a be in the state 001, i.e.,

$$S_0 = \begin{bmatrix} s_1 \\ s_2 \\ s_3 \end{bmatrix} = \begin{bmatrix} 0 \\ 0 \\ 1 \end{bmatrix}, \quad (98)$$

then

$$\begin{aligned} S_1 &= AS_0 = \begin{bmatrix} 0 & 1 & 1 \\ 1 & 0 & 0 \\ 0 & 1 & 0 \end{bmatrix} \cdot \begin{bmatrix} 0 \\ 0 \\ 1 \end{bmatrix} = \begin{bmatrix} 1 \\ 0 \\ 0 \end{bmatrix}, \\ S_2 &= AS_1 = \begin{bmatrix} 0 & 1 & 1 \\ 1 & 0 & 0 \\ 0 & 1 & 0 \end{bmatrix} \cdot \begin{bmatrix} 1 \\ 0 \\ 0 \end{bmatrix} = \begin{bmatrix} 0 \\ 1 \\ 0 \end{bmatrix}, \end{aligned} \quad (99)$$

etc.

Iterating, we obtain the state diagram shown in Figure 17b. The diagram consists of a unit cycle representing the equilibrium 000 and another 7-element cycle. The fact that all the remaining $2^3 - 1$ states form a single closed cycle indicates that the circuit is a so-called maximum-period network.

In applications one is often interested not in the sequence of states of the linear circuit but in the length of the cycles (the period of the matrix). It is also desirable to know whether the given circuit is a maximum-period network or not.

The period l of the matrix A is the least integer such that $A^l = I$, the maximum period being $l_{\max} = p^k - 1$ /67/. In general, the period l can be found from the characteristic polynomial $F(X)$ of A . The characteristic polynomial is the determinant formed by subtracting X from the diagonal elements of A , thus:

$$F(X) = |A - X\epsilon|. \quad (100)$$

For the circuit in Figure 17a,

$$F(X) = \left| \begin{bmatrix} 0 & 1 & 1 \\ 1 & 0 & 0 \\ 0 & 1 & 0 \end{bmatrix} - X \begin{bmatrix} 1 & 0 & 0 \\ 0 & 1 & 0 \\ 0 & 0 & 1 \end{bmatrix} \right| = \begin{vmatrix} -X & 1 & 1 \\ 1 & -X & 0 \\ 0 & 1 & -X \end{vmatrix} = X^3 + X + 1. \quad (101)$$

The period l of A is equal to the degree of the root of the characteristic polynomial $F(X)$, while the structure of the cycles generated by the matrix A corresponds to the sets obtained when the multiplication group over the

field $G\varphi(2^n)$ is decomposed by the subgroup of the powers of the root of the characteristic polynomial.

A definite relationship is observed between the form of the characteristic polynomial and the structure of logical connections. The synthesis of these devices thus reduces to finding the corresponding maximum-period polynomial $F(X)$, which is known to enter the factorization of the binomial $X^{l_{\max}} - 1$ in factors irreducible over the field $G\varphi(2)$.

The above propositions and results of the theory of linear sequential modulo circuits essentially simplify the synthesis of optimum circuits for certain noncontact components of digital data transmission equipment, such as frequency dividers, distributors, quasirandom periodic sequence generators, etc.

In frequency dividers using a shift register the main problem is to design a circuit which divides in a given ratio K and has a minimum number of feedback elements. The feedback loops should be made technically as simple as possible, and the addresses of the register locations linked by the feedback paths should be determined. It is of course desirable to use the simplest feedback circuit available, namely the modulo-2 adder.

The synthesis of a linear sequential circuit from a given sequence of states in general constitutes an unsolvable problem. However, the problem is substantially simplified if we are to synthesize a maximum-period network for $p=2$, i.e., a divide-by- (2^n-1) element.

For any n we can construct one or several maximum-period irreducible polynomials. These polynomials have been investigated and appropriately tabulated [46, 59]. An irreducible polynomial of degree n corresponding to the given divide element is chosen from the tables, and the feedback register is then realized without difficulty.

In the general case, the polynomial has the form

$$F(X) = X^n + a_{n-1}X^{n-1} + \dots + a_2X^2 + a_1X + 1. \quad (102)$$

The degree n of the polynomial is equal to the total number of register bits, and the coefficients a_i are either 1 or 0. The polynomial coefficients, and hence the number of terms in the polynomial, depend on the structure of the register, i.e., the actual connections of the feedback paths.

In the limiting case of no feedback, the characteristic polynomial has the form

$$F(X) = X^n + 1, \quad (103)$$

which corresponds to a n -bit ring register which generates sequences of n combinations.

The number of feedback modulo-2 adders is equal to the number of terms in the polynomial (102) minus two. To find the addresses of the register locations which are coupled to the adder inputs, a conjugate polynomial is formed, which has the form

$$F(X) = X^n + a_1X^{n-1} + a_2X^{n-2} + \dots + a_{n-1}X + 1. \quad (104)$$

The powers of the terms in (104) give the addresses of the locations coupled to adder inputs. The inputs of the first adder are connected to the outputs of the last location and the location whose address is the power of the term following X^n in the conjugate polynomial. The output of this adder is in its turn coupled to one of the inputs of the second adder, and so on. The output of the last adder is delivered to the input of the first register location.

For example, suppose that we intend to synthesize a maximum-period linear circuit with a cycle $2^9 - 1 = 511$ digits long, which can be used to divide by 511. From tables /46, 59/ we choose the polynomial $X^9 + X^6 + 1$ and find the conjugate polynomial $X^9 + X^4 + 1$. The register should thus have nine locations and one feedback adder. The adder inputs are coupled to the 9th and the 4th register locations.

Note that for all n from 2 to 10 (with the exception of $n = 8$) the maximum division (by $2^n - 1$) is obtained with a single adder in the feedback loop, while for $n = 8$ three feedback adders are required /57, 66/.

The register can be made to divide by less than $2^n - 1$ in two ways. We may use only part of the combinations generated by the register, but unfortunately the circuit will then divide in steps that encompass a limited range of numbers, which is normally insufficient for practical purposes. A more general technique is therefore the following. In addition to feedback, a direct-action element is introduced, which acts on some register locations at the moment when a certain selected combination is generated and advances these locations $2^n - K$ steps.

As an example let us consider the 4-bit register shown in Figure 18. Its characteristic polynomial is $X^4 + X^3 + 1$. The polynomial is irreducible; it is furthermore a maximum-period polynomial with a period of 15.

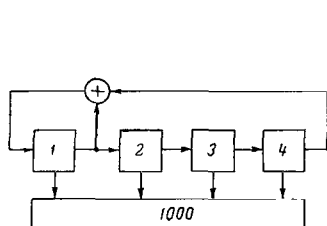


FIGURE 18.

If we introduce a coincidence gate which isolates one of the 15 possible states, say 1000, the gate produces output pulses at $1/15$ th the timing frequency, i. e., a division by 15 is achieved.

If this register is to be used in a divide-by-11 circuit, the direct-action element should switch the register to the state 1001 immediately after the 8th selected state (1010), i. e., four combinations are skipped. The direct-action circuit is

very simple in this case: at the time corresponding to the state 1010, it writes 1 in location 4 and inhibits the writing of 1 in location 3.

The results of this section suggest the following procedure for building a frequency divider with a given ratio K and a minimum number of elements:

(a) the number of register locations is determined from the relation

$$n = E \lfloor \log_2 K + 1 \rfloor; \quad (105)$$

(b) an irreducible polynomial of degree n is selected from tables and the conjugate polynomial is formed, which gives the essential data for the register circuit;

(c) the state diagram of the register is found (if $F(X)$ is known, the diagram is easily drawn with a template);

(d) the selected and the additional combinations are chosen from the state diagram, so that the distance between them is $2^n - K$, and the direct-action element is constructed.

Feedback shift registers are sometimes used also in distributors with numerous "contacts". The above procedure is fully applicable to these distributors as well.

Generators of quasirandom binary nonperiodic sequences which constitute a code ring are built remembering that a code ring corresponds to a maximum-period linear sequential circuit. The register for a recurrent generator is therefore chosen following the same procedure as in the case of frequency dividers, i.e., by inspecting the maximum-period irreducible polynomial.

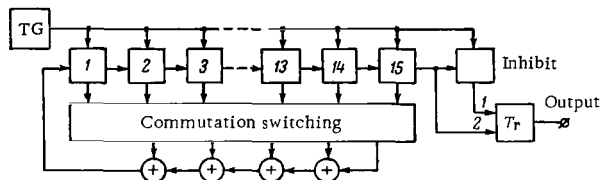


FIGURE 19

As an example, Figure 19 shows a block diagram of a generator producing quasirandom sequences $2^n - 1$ units long, where $n = 5, 6, \dots, 12$. The circuit comprises a timing generator (TG), a 15-bit shift register, a switching device, logical feedback elements, and an output trigger Tr . The timing frequency is equal to the transmission speed in bauds. The switching device connects the register outputs to different logical feedback adders, so that variable-period sequences are generated in the register.



Chapter Five

DISTORTION AND MUTILATION METERS

1. EVALUATION OF INSTRUMENTAL ERRORS AND THEIR SOURCES

Modern pulse distortion meters and analyzers fall in two broad categories: analog and digital. In analog instruments the distortion is determined by comparing the edges of transmitted keyings with voltages that vary in a known manner (linear, circular, helical sweep). In digital instruments, the distortion is represented as a number sequence. The elements of the sequence are pulses which follow one another at certain intervals. If the number of pulses and the standard interval are known, the distortion can be found. The accuracy of the measurements is determined by the ratio of the standard interval to the undistorted pulse length. By taking a sufficiently small standard interval and suitably increasing the number of discrete indicator elements corresponding to these intervals, we improve the accuracy of the digital techniques: digital instruments, being much more convenient in operation than analog ones, can thus also be made more accurate.

Analog instruments include pointer indicators /56/, stroboscopes /68/, and cathode-ray oscilloscopes /16, 20/. In the following we only describe the various digital instruments and analyzers.

The fundamental criteria that characterize the measuring capacity of instruments used in digital data transmission include accuracy, threshold response, and upper limit of measurements.

Accuracy is of course the main criterion; besides the functional principle of the instrument (whether analog or digital), the accuracy is determined by a number of constructional and operational factors, which are mostly of probabilistic, statistical character.

The accuracy of the various instruments is estimated by the same methods as those used in connection with similar general-purpose instrumentation, e.g., timing devices described in /41/. The sources of errors in digital distortion and mutilation meters, however, have certain characteristic and peculiar features inherent to digital communication systems, e.g., phase correctors /54/.

Determination of accuracy of these instruments is a complicated problem which falls beyond the scope of this book. We shall therefore only sketch the range of problems that are of fundamental importance for quality improvement of the instruments.

The apparatus of the probability theory and the related tools of the theory of information are very promising in this respect. They point the way to the design of qualitatively new devices in which the achievements of computer technology are applied to automation of the measuring process /38, 40, 44/.

The information-theoretical approach is particularly profitable for measuring instruments used in communications engineering, where many a problem has been solved by these methods /62/. If the statistical properties of the measured quantities and the instruments are known, good statistical matching can be attained between the instrumentation and the object of measurements, the accuracy and reliability of results correspondingly increasing.

However, despite these attractive features of information-theoretical methods, very little has been done on the subject of application of the theory of information to evaluation of optimum design techniques and assessment of the true potentials of instruments used in measurements in digital data transmission systems. No attempt has been made to generalize for these specialized instruments the results previously obtained for similar conventional equipment, while some of the results already available are of fundamental importance and can be directly extended to cover the problem at hand.

For example, the following conclusion /38, 40/ is highly significant for the institution of automatic quality control in digital data transmission systems: irrespective of the method of amplitude quantization, the best policy is to sample the process at random time intervals determined by the particular process being measured; the next best policy is to sample the process at equal intervals, while random sampling at intervals chosen by the observer is the worst of the three possibilities.

Application of information-theoretical methods requires, first, extension of the information-theoretical criteria /40/ to the instrument being considered and, second, study of signal-level and time quantization with allowance for the previously discussed statistical features of the measured quantities and instrumental error distributions.

One of the fundamental problems facing us at this stage is therefore a study of sources of errors and error distributions. A.N. Zeliger /27-29/ made some headway in this direction. He showed that in analog instruments

with cathode-ray indicators the main sources of errors (besides instability of timing frequency) are the finite dimensions of the indicator, the start-stop and output equipment, nonlinearity of the sweep voltage, and periodic changes in the comparator speed. The first three of the five factors above follow the law of equal probability, the fourth has a normal probability distribution, and the probability density of the fifth factor has an almost parabolic distribution.

Assuming the errors to be independent, we find the total instrumental error distribution as a combination of the probability distributions of the individual error components, making use of Lyapunov's characteristic functions. Fourier-transforming the given error distribution densities $\varphi(e_k)$, we obtain the

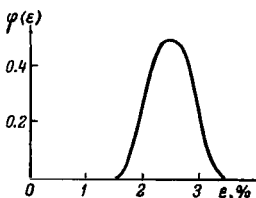


FIGURE 20.

corresponding characteristic functions $g_k(t)$, i. e.,

$$g_k(t) = \int_{-\infty}^{\infty} e^{j t \epsilon_k} \varphi(\epsilon_k) d\epsilon_k. \quad (106)$$

Then we form the product of these characteristic functions

$$g(t) = \prod_{k=1}^n g_k(t), \quad (107)$$

and inverting obtain the sought distribution density

$$\varphi(\epsilon) = \frac{1}{2\pi} \int_{-\infty}^{\infty} e^{-j t \epsilon} g(t) dt. \quad (108)$$

Figure 20 is a specimen curve $\varphi(\epsilon)$ calculated by this method for a start-stop distortion meter /20/ with a cathode-ray indicator and linear sweep voltage.

2. ANALOG AND DIGITAL ELECTRONIC DISTORTION METERS FOR TRANSMISSION RATES OF UP TO 300 BAUD

We now consider the principal technical specifications of a compact analog distortion meter with a cathode-ray tube and a digital distortion meter with a neon lamp register /14, 16, 47/.

In distinction from other conventional equipment, these instruments employ noncontact switching using transistors and ferrites. The instruments thus combine the advantage of small size, low power supply, and simple maintenance requirements with a very substantial technical potential.

The compact analog device (which is built in an oscillograph chassis) and the digital distortion meter are photographed in Figures 21 and 22. The principal specifications are listed in Table 5. Either instrument comprises a distortion meter and a test signal generator in a single chassis. Pulse edge distortions can be measured in both synchronous and start-stop modes of operation. The instruments also measure mutilation, transmit + and - signals to the channel or the telegraph set, and generate various test combinations listed in Table 5.

The instruments can be connected in series and in parallel to the circuit being tested. The noncontact input device will receive both square and rounded pulse trains of different polarities in single-current working, as well as double-current telegraph signals.

The assembly includes a telegraph relay tester, which measures the neutrality and transit time of a relay under typical operating conditions by employing square pulses.

The distortion is displayed on a cathode-ray screen 8 cm in dia. in the analog instrument and on a lamp register in the digital instrument. The display register is built from small neon lamps (MN-6) on the face panel of the instrument; they are covered by a transparent scale with



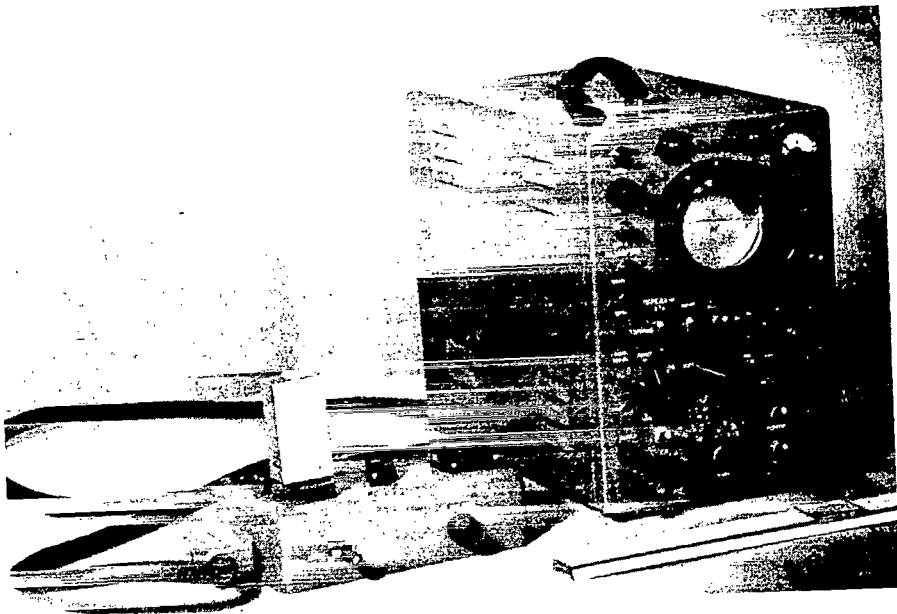


FIGURE 21.

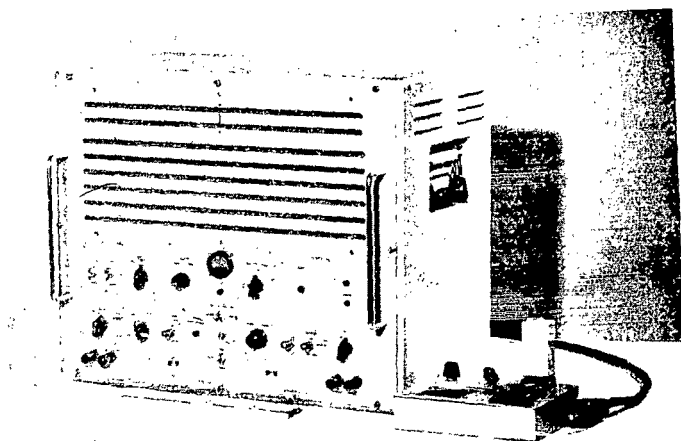


FIGURE 22.

numerals marked on it. When a lamp lights, the figure corresponding to the percentage distortion of the pulse train is illuminated on the panel.

Either instrument will perform the entire sequence of telegraph maintenance tests: channel control, transmitter tests and tuneup, relay tests. Comparison of the specifications in Table 5 shows that the cathode-ray instrument has approximately the same technical potential as the digital instrument; its accuracy, however, is lower and the start-stop combinations being measured cannot be scanned pulse by pulse. The small size and the relatively small weight of the analog device are obviously to its advantage. In the second tester, the digital approach and the visual display in the form of a lamp register ensure high accuracy of measurements, which is independent of operator mistakes arising whenever subjective evaluation of data is called upon.

TABLE 5.

	Cathode-ray instrument	Digital instrument
Percentage accuracy, synchronous mode	± 2	1% at 50—150 baud 2% at 200 and 300 baud
Ditto, start-stop mode	± 4	2
Range of transmission rates in synchronous mode, baud	40—300	(50, 75, 150, 200 300) $\pm 5\%$
Fixed transmission rates in start-stop mode, baud	45, 50, 75, 100	44.7; 47; 50; 75
Relays tested	RP-3, RP-4, RPS-11, TRM	RP-4, RPS-11, TRL, TRM
Test signal generator	undistorted test combinations	1:1; 2:2; 6:1; 1:6
	undistorted test signal with 7 and 7.5-contact division (according to International Code No. 2)	[Russian] RY
	fixed percentage distortion of start-stop working	[International] Q9S
Weight, kg	18	35
Power, watt	30	60

We now consider the characteristic features of the two testers.

The cathode-ray instrument employs a triangular sweep voltage which provides a linear time base. The cathode ray during each elementary keying moves from the center of the screen to its right-most edge, then from right to left, finally returning to the center. Pulse distortion registers as a brief spike, which is directed upward in the first and the fourth quarters of the sweep and downward in the second and third quarters.

A transparent scale with zero at its center, calibrated in 2% per division, is mounted in front of the screen. Late arrivals register as spikes right of the zero point (+), and early arrivals as spikes left of zero (-).

If the pulses are undistorted, two bright coincident spikes are seen on the screen. When the "Phase" button is pressed, the equipment is briefly switched to start-stop operation and the spikes shift to the zero mark of the scale (Figure 23a). If, however, the pulses are distorted, the spikes are separated by a time lag which is proportional to the amount

of distortion. If the distortion is between 0 and 25%, both spikes point upward (Figure 23b). For distortions from 25 to 50%, one spike points upward and the other downward (Figure 23c).

If the frequency of the signals is not a multiple of the generator frequency, the spikes travel across the screen. They can be arrested by adjusting the smooth tuning knob of the instrument.

Measurements during start-stop operation are analogous to the preceding. The various distortions of the pulses in a start-stop combination produce a number of spikes left or right of the origin (or simultaneously on both sides of the zero). The distance between the zero spike and the rightmost or leftmost spike gives the maximum start-stop distortion.

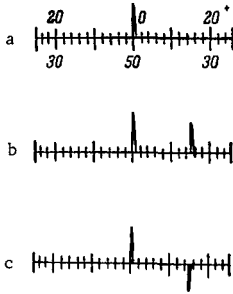


FIGURE 23.

The functional principle of the tester is illustrated by the block diagram in Figure 24, where TG is the timing generator.

The timing frequency can be adjusted smoothly by means of a variable-capacitance condenser. Frequency division is thus varied between such limits as ensure adequate transmission speeds. The output pulses of the divider are delivered to the sweep voltage shaper, and the voltage is then applied to the horizontal-deflection plates of

the cathode-ray tube providing the time base.

The rounded pulses to be tested are squared by the electronic input device; the square pulses trigger the start-stop device and are also delivered to the differentiating unit. The latter is intended to generate brief spikes marking the pulse edges. These spikes are fed into a gate whence they continue to a stepup transformer and then to the vertical-deflection plates of the tube. In parallel the spikes are delivered to the tube modulator providing pulse brightup.

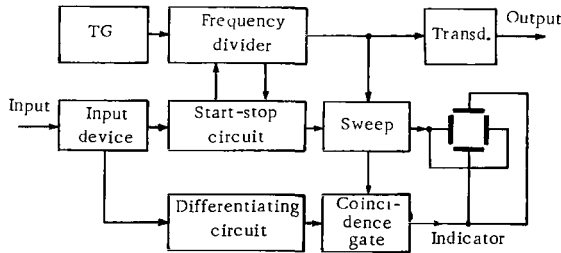


FIGURE 24.

In the digital tester, the readout register has eight horizontal rows of neon lamps. In the synchronous mode the readings are provided by the two upper rows, where the lamps are set at 1%-intervals. The distortion is determined from the distance between two glowing lamps. If the distortion does not exceed 1%, only one lamp glows. If the frequency of the pulses is not a multiple of the timing frequency, the glowing dots

travel along the row from one lamp to another. The motion can be arrested by turning the smooth adjustment knob; by pressing the "Phase" button the glowing lamp is shifted to the origin, i. e., to the rightmost neon lamp with the 1% mark. At 200 and 300 baud, the synchronous readout register displays two pulses.

In the start-stop mode, the instrument will measure the distortion of each individual pulse in the start-stop combination. The distortion reading is taken from the six lower rows of the register, where the neon lamps are spaced at 2% intervals. The topmost of these six rows corresponds to the first pulse of the code group, the next row to the second pulse, etc.; the sixth row corresponds to a stop transition.

The instrument can be adjusted to give maximum start-stop distortion readings. In this option the start-stop distortion readings are taken from the synchronous register or only from the one top row of the start-stop register.

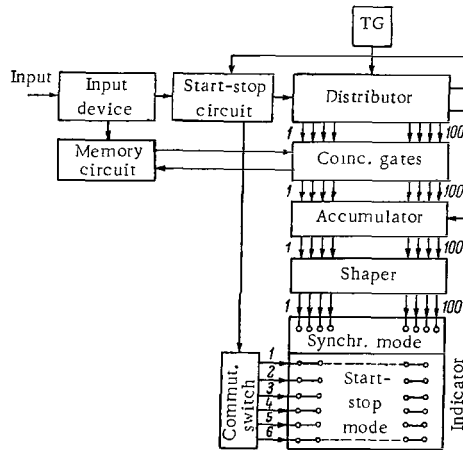


FIGURE 25.

At low speeds the accuracy of measurements in the synchronous mode can be made higher than the rated accuracy. Indeed, by turning the selector knob to 150 baud say, we measure distortions to within 1% at 150 baud, to within 0.5% at 75 baud, and to within 0.33% at 50 baud. This improvement is understandable since the register does not scan the entire pulse but only a certain section thereof, the length of which is equal to the ratio of the actual low speed to the selected high speed.

A block diagram of the digital tester is shown in Figure 25.

When the instrument is on, each of the transitions following the start transition is registered by the memory circuit. If there is a coincidence between a pulse from the memory circuit and a pulse from one of the distributor outputs, a pulse is sent to the corresponding accumulator. When distortion is recorded by a distributor element whose address is determined by the number of timing pulses received, the memory circuit is cleared to the initial state and the accumulated data are read out.

A triggering pulse is sent to the shaping circuit which controls the appropriate neon lamp. Since the distributor and the accumulator each have 100 elements, and the time interval between the output pulses produced by the distributor is therefore equal to 1% distortion, the address of the accumulator element and the corresponding indicator lamp give a direct pulse distortion reading.

In start-stop measurements, the distributor is triggered by a start-stop device when a start transition is received at the input. The distributor is stopped after 6.5 unit pulses.

The start-stop indicator is based on the matrix principle: the readout register has 50 vertical and 6 horizontal inputs, the vertical inputs receiving pulses from odd accumulator outputs, i.e., at 2% distortion intervals. Neon lamps are provided at intersections of horizontal and vertical buses. When a signal is delivered to one of the vertical and one of the horizontal inputs, a neon lamp at their intersection is lighted.

The six horizontal rows are switched by a 6-input—6-output commutating switch. The inputs receive start-stop output pulses corresponding to the position of the tested pulse in the start-stop combination.

In the synchronous mode, the start-stop unit and the 6 lower rows of the readout register are turned off, and the distributor operates continuously.

The accumulator in this tester is essential in order to permit scanning of each start-stop combination over the 6 horizontal rows of the display register. The accumulator sends input pulses to the register at strictly constant intervals, regardless of the measured distortion. Measurement and readout are thus separated in time, which is essential for synchronizing the switching of indicator lines with the midpoints of unit pulses. All the lamps in the register thus glow precisely the same time, irrespective of the magnitude of pulse distortion.

Test signal generator in both testers has a noncontact output device — a transistorized relay described in Chapter Seven. The generator transmits at any speed 120 V single-current pulses and ± 60 V double-current pulses of up to 100 mA.

The block diagram of the test pulse generator of the digital tester is shown in Figure 26. The generator comprises two shift registers in series and a ferrite core program matrix. Register A has 15 locations, which is due to the requirement of 7.5-contact division, and register B has 8 locations (the number of characters in the text). The timing frequency controlling register A is double the transmission frequency.

The first write amplifier writes 1 in the corresponding cores of the program matrix, in accordance with the code combination of the first character. Register A and a sense amplifier read the data from the matrix cores and convert the two-dimensional code combination into a time sequence. The output pulses from cores set to 1 are delivered to the output device.

When the first code combination has been read, the write pulse is generated in the second bit of register B, the second character is written, etc. The outputs of the 2nd and 14th cores of register A, corresponding to start and stop transitions, are delivered directly to the output trigger, bypassing the amplifier and the program matrix.

The test pulse generator of the cathode-ray instrument has a simpler circuitry. It consists of a 15-bit distributor, a program trigger, an output trigger, and a trigger which selects the constant distortion of the starting pulse. Switching of outputs enables the distributor to generate 1:1, 1:6, and 6:1 signals. When the RY test signal is being generated, the distributor outputs are switched by the program trigger, as well as by the ordinary switching circuit.

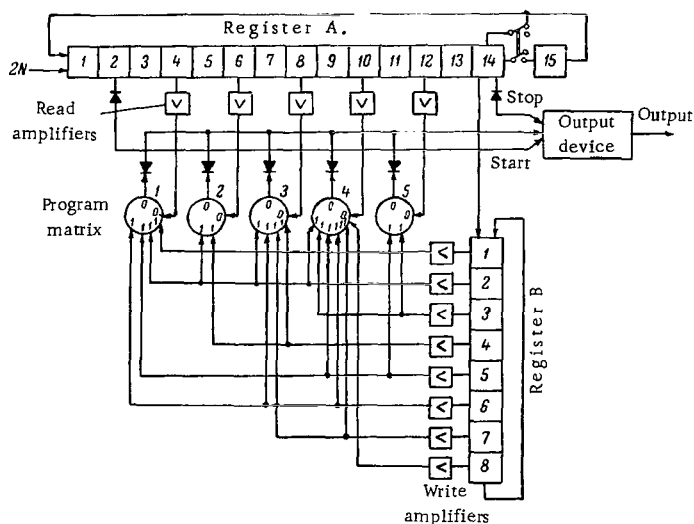


FIGURE 26.

The characteristic features of the two testers are described in greater detail in the previous publications of the author /14, 16/.

3. DIGITAL DISTORTION METER FOR HIGH TRANSMISSION RATES

Distortion meters for high transmission speeds are built on the same principles as the previously described digital tester for speeds of up to 300 baud. The fundamental components of the high-speed distortion meter are therefore a high-frequency master generator, a distributor, a coincidence gate, and indicator lamps with shaping circuits.

The master pulses and timing are provided by the digital data transmission system with which the meter is used, and no independent generator is required. The corresponding block diagram is shown in Figure 27.

The master pulses and timing are delivered to the instrument through shaper circuits. The master frequencies f_1 and f_2 are a factor of $2n$ higher than the transmission frequency (n is the number of time scale divisions, equal to the number of readout indicators) and show a relative phase difference of 180° ; the timing frequency is equal to transmission frequency.

The pulses to be measured, before arriving at the coincidence gate, are synchronized with f_1 , and the timing pulses are synchronized with f_2 .

The distortion is measured as the displacement of the pulse edges relative to timing pulses. A discrete time scale is provided by the distributor, which uses an n -bit transistor-magnetic shift register.

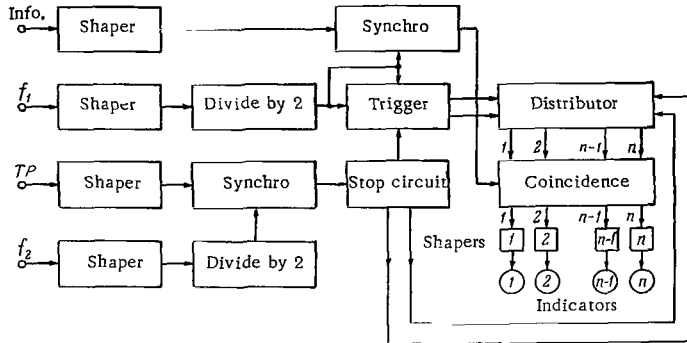


FIGURE 27.

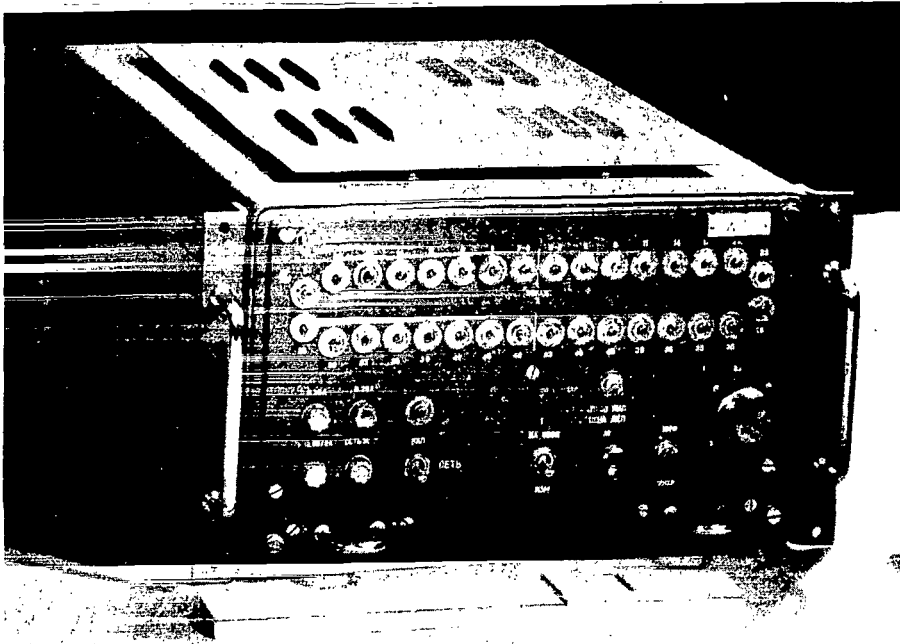


FIGURE 28.

The distributor is controlled by a high-frequency trigger energized by the f_1 impulses. The distributor is started and stopped by timing pulses. A timing pulse writes 1 in the first register location and reads 1 from all the other locations. The high-frequency trigger is simultaneously returned to the initial state, and the next f_1 pulse sets the trigger to read 1 from the first location, so the bit starts traveling along the register as required. The distributor is stopped, 1 is written, and the trigger is set in the spacing between the f_1 pulses. This is the reason why the timing pulses actuating the stop mechanism are synchronized with f_2 pulses, which are phase-shifted 180° relative to f_1 .

When the frequency dividers are on, the accuracy of measurements is $100/n\%$ in the $\pm 50\%$ distortion range; with frequency dividers off the accuracy is $100/2n\%$ in the $\pm 25\%$ range.

Figure 28 is a photograph of the distortion meter for transmission speeds of up to 2400 baud with $n = 32$.

Chapter Six

DISTORTION AND ERROR DISTRIBUTION ANALYZERS

1. BRIEF SURVEY OF ANALYZERS

Distortion analyzers can be divided into three groups /12/.

1. Analog devices which register the distortion of each pulse in a code combination. This group includes the start-stop analyzers with electric spark recording on paper tape /88/ and with electrothermal recording on a circular diagram /81/.

2. Digital instruments with counters, which count the distorted pulses in various specified distortion intervals. This group includes start-stop and synchronous electronic analyzers /1, 84, 87, 96/, synchronous electromechanical analyzers /94/, and simplified counting devices which give the proportion of pulses with distortion exceeding a predetermined value /87/.

3. Combined analyzers using recording and counting devices. This group includes the synchronous electromechanical recording instrument developed in 1953 under the direction of Prof. P. A. Kotov. In principle, the same recorder can be built using noncontact circuitry /35/.

All the above analyzers operate at transmission speeds of up to 50 baud. The most promising is the counting analyzer, since the counter readings can be readily converted to pulse distortion distribution curves. Comparison of experimental curves with standard curves corresponding to distortions of a known kind or their combinations sheds light on the reasons for the appearance of various transmission distortions.

These data are very difficult to obtain from readings of analyzers that record the distortion of every individual pulse. Combination of counting and continuous recording techniques, however, gives valuable information on the character and origin of distortion.

The functional principle of a counting analyzer will be described for the particular case of the electronic start-stop analyzer /96/. The simplified block diagram of the analyzer is shown in Figure 29. This is a noncontact device with 20 counters which automatically count distortions. The distortion is determined from the position of the pulse edge in relation to a time scale divided into 100 equal divisions. Full scale length corresponds to a single unit pulse, and each division is thus equal to 1% of code pulse length.

The time scale, which is repeated for each pulse, is generated by a noncontact distributor which is triggered by a start-stop device actuated by a start transition. The distributor outputs are coupled to counter circuits which comprise a scaler and an electromechanical

counter. The counters are actuated by coincident pulses from the distributor and the memory circuit. The memory circuit produces an output pulse when the edge of each keying is sensed.

When one of the counters is actuated and the time position of pulse edges relative to the start transition is recorded, the memory circuit is cleared, i. e., restored to the initial state.

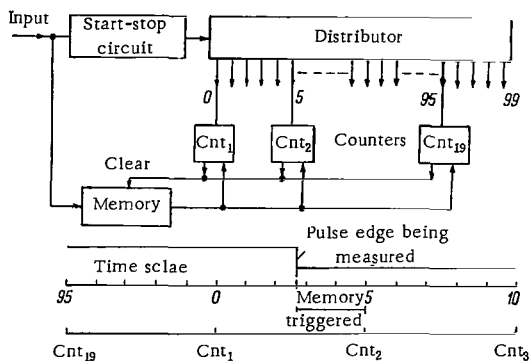


FIGURE 29.

The time cycle of the distributor is repeated 6.5 times during the length of the corresponding code combinations.

Two counter setting options are provided: 5% and 1% intervals. In the latter case the measured distortions are within $\pm 10\%$.

The telegraph distortion "spectrometer" /84/ is essentially analogous to the counter analyzer just described. This is a transistorized instrument with 40 rather than 20 counters. The distortions are thus recorded either between $\pm 50\%$ at 2.5% intervals or between $\pm 20\%$ at 1% intervals. The greater counter spacing is used in channel tests, and the smaller spacing option is used in start-stop transmitter tests.

A block diagram of an electronic start-stop analyzer with 16 counters is described in /34/.

The analyzer described in /19/ measures the relative start-stop distortion; the magnitude of the maximum distortion of each start-stop combination is determined in relation to the start pulse and then divided by the length of an undistorted pulse.

In the next section we shall consider the technical potential and the functional principle of transistor—ferrite counting analyzer for synchronous and start-stop measurements at transmission rates of up to 75 baud.

Error distribution analyzers are digital instruments with the general block diagram shown in Figure 30. The transmitter has a master generator and a test signal generator. The test signals are transmitted over the channel and picked up by the receiver, where they are regenerated and compared with control signals produced by precisely the same generator as in the transmitter.

The result of this comparison is delivered to a counter. The synchronizing circuit ensures cycle-by-cycle and unit-by-unit synchronization of the test and control combinations. Unit-by-unit synchronization is achieved

with the aid of a phase corrector which adds and subtracts pulses as required, or a controlled frequency divider /54, 57, 66/. Cycle synchronization is achieved by sending a special phasing combination from the transmitting to the receiving end. Unit-by-unit synchronizing signals are delivered to the regenerating circuit, and the cycle synchronization pulses are fed to the control signal generator.

The analyzer can have four different counter arrangements. According to the first variant, the instrument counts the total number of errors during the session, according to the second variant errors of different kinds in a data block of a certain length are counted. The third counting arrangement gives the parameters P_{nerr} , P_{lerr} , and P_{terr} of the error stream regardless of the transmitted block length, and finally the fourth arrangement measures the distribution of error-free intervals.

In the first case the statistical treatment of the results is based on a simple error stream model with a single parameter, the probability of error in one character. In real channels, however, the errors cannot be regarded as independent, and the simple method measuring the average error probability gives results which do not check with the actual situation.

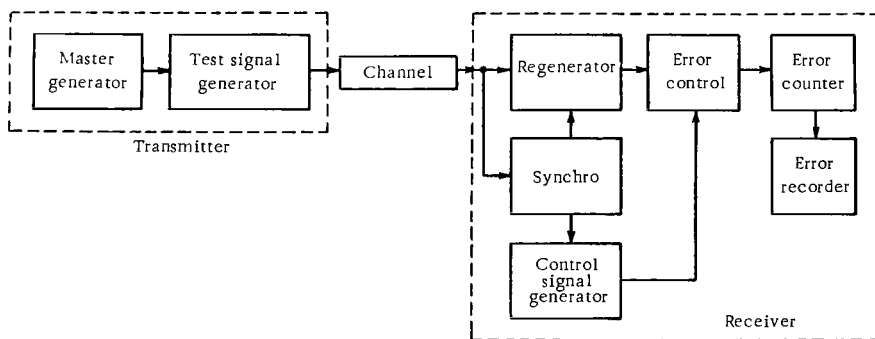


FIGURE 30.

The actual distribution of errors is determined by separately counting the errors of the various kinds for code combinations of constant length (second variant above). Application of these analyzers gives starting data for calculations of the expected probability of faultless transmission of digital data blocks and estimates of error rates in distorted blocks.

However, despite the considerable popularity of the second method of measurement, the results are valid only for the particular block length used in tests. They are therefore not fully applicable to general evaluation of transmission and coding techniques. Analyzers of the third and fourth types are more promising in this respect.

We now consider some characteristic features of the different error analyzers available.

Among the most remarkable average-error analyzers (the first variant) is the instrument /6/ which measures the probability of a single error in high-speed digital data transmission systems (36,000 to 60,000 baud) using wide-band channels.

The test generator of this analyzer produces a pseudorandom sequence of 160 characters and combinations of the form 1:1, 1:6, and 6:1. The distinctive feature of the analyzer is its unit-by-unit synchronization circuit: this is a phase automatic frequency control unit with a discrete phase discriminator and a continuous integrator driven by the master generator frequency /48/. Cycle synchronization does not require a special starting keying: the control signal is shifted until the received and the generated signal are in phase.

Analyzers with a counting arrangement of second kind are described in Soviet /18, 35/ and Western /79, 86, 89/ literature. One of these instruments will be described in the next section.

In Prof. P. A. Kotov's statistical analyzer of binary communication channels /36/ errors are counted according to different kinds and recorded on magnetic tape. Additional processing of the taped information using a special counting setup (see Sec. 4 of this chapter) provides data for the evaluation of arbitrary-length codes.

In the modified version of this analyzer, designed and built by P. A. Kotov, L. P. Purtov, A. S. Zamrii, I. P. Voitenko, and N. F. Shapovalov, the magnetic tape is automatically started when an error is indicated and stopped if no additional errors are sensed for some time. Elimination of continuous tape transport minimizes used tape space and facilitates the conduction of lengthy experiments for the accumulation of statistical data sufficient for the determination of error distributions and distribution of error-free intervals. The error-actuated analyzer is intended for measurements at speeds of from 50 to 2400 baud. It comprises a transceiver and a three-channel tape recorder. The analyzer compares the transmitted signals with control signals which constitute a 511-character pseudorandom code-ring sequence. The results are distributed between three outputs: $0 \rightarrow 1$ errors, $1 \rightarrow 0$ errors, and accurately transmitted characters. The analyzer outputs are coupled to counting circuits using Soviet-made OG-3 dekatrons and MES-54 electromechanical counters.

The error pulses ($0 \rightarrow 1$ and $1 \rightarrow 0$) are recorded in two channels, after a certain delay in which the magnetic tape transport attains normal uniform speed. The third channel records the synchronizing pulses for the counting device.

Cycle phasing of the recurrent generators is done by a phase counter which is triggered by a special start combination. Unit-by-unit synchronization is done by a correcting system using a reversible counter.

If the transmission is interrupted for more than 300 msec, the tape recorder is turned off, the number and length of interruptions being registered by a special counter.

A third-type analyzer for measurements of error stream parameters at speeds of up to 300 baud was designed by V. L. Morev and P. A. Yunakov /42/. The analyzer carries out the following operation: parceling of the error stream into discrete bursts, calculation of the average error burst rate, determination of burst length distribution, and calculation of the average error frequency in bursts.

A block diagram of the analyzer is shown in Figure 31. Error bursts are isolated by a memory circuit. This is a condenser which is charged almost instantaneously to a certain fixed potential by input error pulses; when no error is sensed, the condenser is discharged through a large

resistance. The state of the memory circuit (whether cleared or set) is indicated by a Schmitt trigger, which thus serves as an error burst indicator. The trigger is flipped as long as an error burst is in transit, plus a certain additional length of time determined by the condenser time constant.

The error bursts received during the test run are counted by Cnt_2 ; the input gate G_1 is open at this stage. The total length of bursts is determined by Cnt_3 , which counts the timing pulses passing through the gate G_2 . This gate is controlled by the output voltage of the error burst indicator.

Cnt_1 counts the total number of errors. Dividing the readings of Cnt_1 by the readings of Cnt_3 we find the average probability of error in a burst.

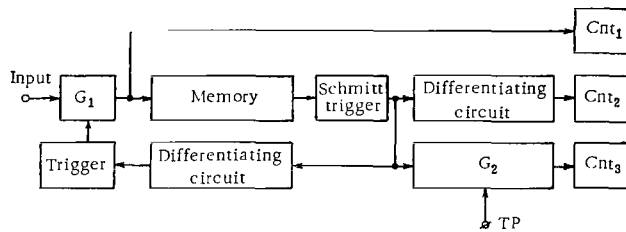


FIGURE 31.

The burst length distribution is determined by a sampling method, closing the input gate G_1 . The subsequent error bursts do not affect the analyzer, so the counters Cnt_3 and Cnt_1 respectively display the length of the analyzed burst and the number of errors in the burst.

An analyzer of the fourth kind is described in Sec. 5 of this chapter.

2. ELECTRONIC DISTORTION ANALYZER FOR TRANSMISSION RATES OF UP TO 75 BAUD

A start-stop/synchronous distortion analyzer /1/ photographed in Figure 32 automatically measures and counts the distorted pulses using 20 electromechanical counters corresponding to 20 distortion ratings. The capacity of each counter is 10^4 pulses.

The distortion is measured in this analyzer along the same lines as above (see Figure 29). The discrete time scale divided into 100 divisions is generated by a noncontact distributor, which is controlled by a stable tuning-fork generator. The generator ensures transmission rates of 40, 44.7, 47, 50, and 75 baud.

The analyzer block diagram is shown in Figure 33. The pulses to be analyzed are delivered to the input device using ferrites and a transistor trigger. The noncontact input device permits series and parallel connection of the analyzer to a functioning communication channel without interfering with the channel's normal operation.

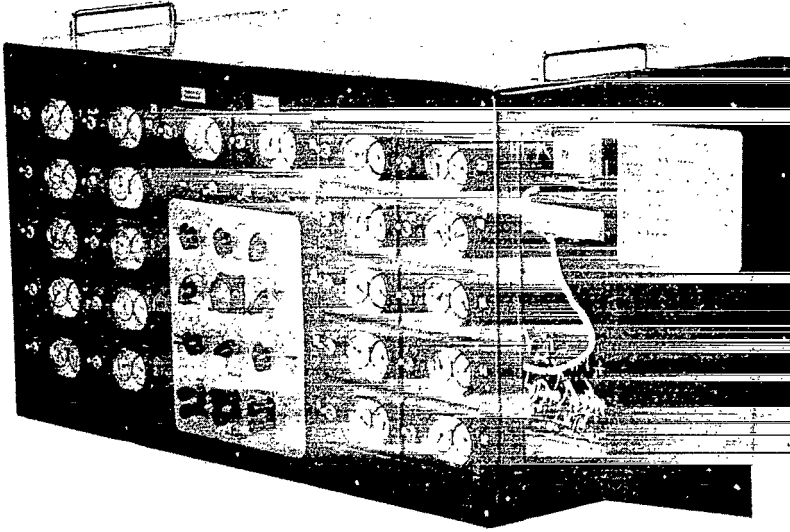


FIGURE 32.

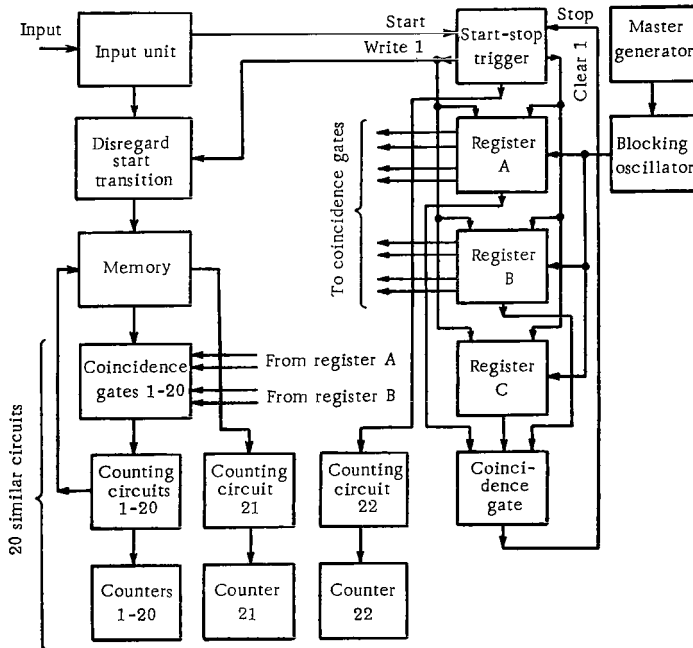


FIGURE 33.

In the start-stop mode, the start transition triggers both the input and the start-stop unit, which actuates three parallel ferrite shift registers. Two registers associated with coincidence gates constitute a distributor which generates a time scale with 1% divisions.

To permit measuring 50% distortion of the stop impulse, the distributor cycle corresponding to each pulse of a code combination is repeated 6.5 times during the analysis of the entire combination. The start-stop device and the third seven-digit register stop the distributor for the duration of the period between the midpoint of the rest pulse and the beginning of the start pulse.

The bit 1 is written simultaneously in the first location of the three registers; the timing pulses delivered to the shift terminals are generated by a delayed blocking oscillator which is actuated by the tuning-fork generator through an emitter follower.

The start-stop unit comprises a trigger and a transistor amplifier. A coincidence gate controlled by pulses from the corresponding cores of the three registers produces the master pulse which resets the start-stop device to the initial state after 6.5 distributor cycles. The pulses corresponding to the edges of the test keying are compared with time scale divisions by a memory circuit comprising a trigger and an amplifier. The trigger applies negative potential to all the coincidence gates of the distributor connected with counter circuits.

Connecting the outputs of various cores of the first and second register to each coincidence gate we obtain various distortion ratings, i. e., the counters can be set at an arbitrary interval within the limits of a whole number of time scale divisions. Each of the counting circuits comprises a univibrator, an amplifier, and a counter. The counting circuits are so linked to the memory circuit that the latter is returned to the initial state when a distortion is recorded by a counter. This eliminates omissions and prevents multiple counting of distortion of the same pulse.

The start transition must not be counted, and the memory circuit is therefore connected to the input trigger through a switch circuit controlled by the start-stop trigger.

In the synchronous mode the start-stop device is disconnected and the time scale is generated continuously by the distributor.

Distortions of single-current and double-current keyings can be measured with this instrument; there is an option for analyzing the distortions of all transitions, as well as only of start-rest transitions and vice versa. This is essential for the separation of bias and characteristic distortions and for the analysis of the start-stop distortion of each transition in a code combination.

In loop tests, test combinations (e. g., 1:1, 2:2, 1:6, 6:1 and the Q9S) are generated by a transducer synchronized with the analyzer generator. The phase of the synchronizing pulses is adjusted manually.

Five different counter arrangements are possible, and the particular counting mode is chosen so as to ensure the most effective analysis of the distribution of distortions. The first counting mode brings out the general character of the distribution between $\pm 50\%$ at 5% intervals. The second mode is used to analyze small distortions ($\pm 9\%$) at 1% intervals, which is essential, e. g., in transmitter tests. The other modes or their combinations are applied to the analysis of large distortion distributions, e. g., in tests of noisy channels, in checking the error-correcting features of equipment, etc.

The total number of input pulses is determined with counter 21 (see Figure 33), which registers how many times the memory circuit has been set. Counter 22 indicates how many times the start-stop trigger has been actuated, i. e., the number of code combinations received. Real-time fault indication is obtained by comparing the sum of readings of counters 1 through 20 with the readings of counter 21.

Detailed description of analyzer circuitry, procedure for the reduction of experimental data, and some actual findings obtained with this analyzer are given in /1/.

3. ANALYZER FOR STATISTICAL CHANNEL TESTS AT SPEEDS OF UP TO 2400 BAUD

Functional principle. The analyzer counts the number of accurately transmitted m -bit code combinations analyzing the errors into the following groups: (a) single and α_m -tuple errors for $\alpha_m = 0, 1, 2, 3, 4, 5, 6-10, 11-15, 16-25$; (b) persistent errors α_p units long, for $\alpha_p = 2, 3, 4, 5$, and over 5; (c) α_u -tuple transpositions for $\alpha_u = 1, 2, 3, 4, 5$, and over 5.

The tests can be made at speeds of from 40 to 2400 baud with combinations of $m = 6, 8, 10, 12, 14, 16, 18, 20, 25$ digits. The analyzer can be used in loop tests and in end-to-end tests; in the latter case two analyzers are required, or at least an analyzer and a test signal generator identical to that used in the analyzer.

In distinction from other instruments, this analyzer phases the keying in the two operating modes by means of phased-in timing signals which control the speed of the analyzer and the transmission rate. Phase correctors are thus unnecessary in this setup. After all, in channel tests the analyzer is always used in conjunction with channel-forming equipment which includes its own phase correctors, and it is clearly superfluous to duplicate them in the measuring instrument. A photograph of the analyzer is shown in Figure 34, and a simplified block diagram is given in Figure 35.

The instrument comprises a receiver and a transmitter terminal, each with two test signal generators TG_s and TG_r . Sequential or parallel combinations of d. c. pulses are delivered from the analyzer output to the transmitter terminal; the receiver terminal delivers demodulated pulses to the input.

An output pulse is produced by the comparator (a modulo-2 adder) when only one of the two inputs receives a signal. The output pulses corresponding to distortions are delivered to three counting circuits, one of which counts single and multiple errors, the other persistent errors, and the third transpositions.

TG_s generator produces m -unit static test combinations selected by toggle switches on the control panel of the equipment. These static combinations are used to test the transmission of m -bit codes over communication channels, to sequentially check the transmission of each bit, and to repair possible malfunctions that are detected by these tests.

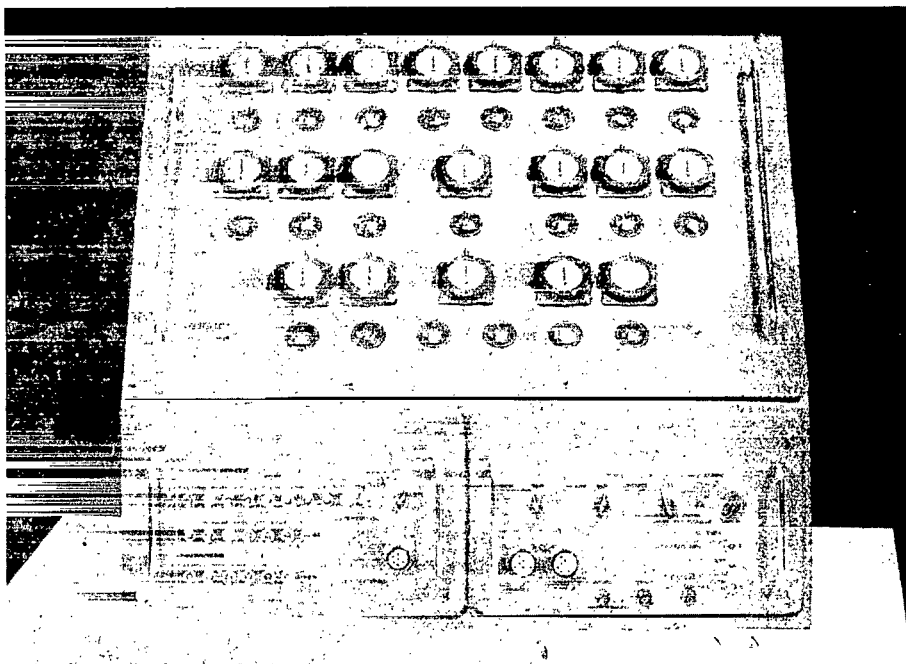


FIGURE 34.

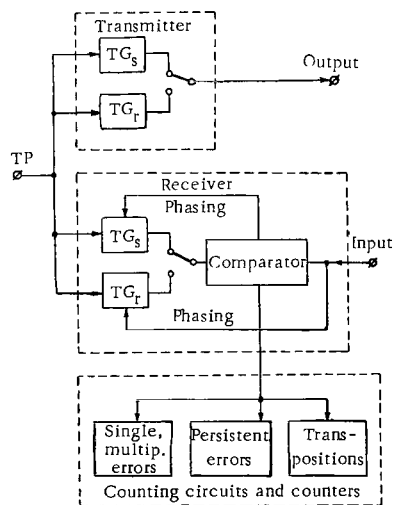


FIGURE 35.

The second (recurrent) generator TG_r produces dynamic test signals, i.e., quasirandom sequences.

The test signals from the two generators are formed as parallel or sequential code combinations. The analyzer thus has four operating modes. The distinction between these modes is only the method by which the combinations received from the channel are phased with the corresponding undistorted combinations of the receiver terminal.

Main components. The static code generator is a single-timing m -bit ferrite-core shift register. The receiver generator differs from the transmitter generator in having a cancel circuit which is actuated if phasing-in has failed.

The number of bits in the transmitted combination is determined by the number of cores in the shift register, which is varied by a pie switch.

The recurrent generator is a single-timing shift register with nine ferrite cores and logical feedback in the form of a modulo-2 adder. The adder input pulses are delivered from the 4th and the 9th register cores, and its output pulse writes 1 in the first core. This generator produces a reduced code ring of $2^9 - 1 = 511$ bits.

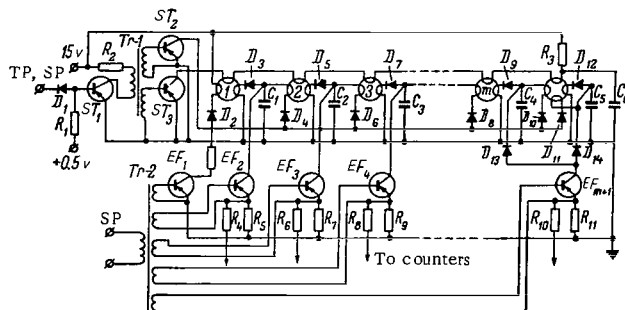


FIGURE 36.

The counting circuit for single and multiple errors (Figure 36) is an $(m+1)$ -unit single shift register, with emitter followers EF connected to its outputs. The emitter followers act as coincidence gates and register clear circuits. The timing pulses TP for the register are provided by the output of the device which performs unit-by-unit comparison of the transmitted code groups with undistorted combinations.

Initially, 1 is written in the first core of the register. If the combination is without errors, the register receives no timing pulse. When a code combination has been received, a sense pulse SP is delivered to the timing terminals of the register cores and to the outputs of all EF. If no error is indicated, the first core is cleared from 1 to 0, since its read terminal is shorted in the process by the small EF load resistance. If, on the other hand, there are α_m errors in the combination, the $(\alpha_m + 1)$ -th core is set to 1 and the sense pulse produces an output pulse across the $(\alpha_m + 1)$ -th EF load.

The output of each EF is coupled through a shaper to a counter. The counter of the first EF records the number of correct code combinations,

and the counter of the α_m -th follower gives the number of combinations with $\alpha_m - 1$ errors.

The counting of persistent errors is done by a similar circuit. The only difference is that the shift register input is provided by an anti-coincidence gate, one of its inputs receiving the shift pulses and the other error pulses. The anticoincidence gate "interrogates" the register upon receiving the first correct pulse after a group of error pulses. The sense pulse discovers the α_p -th core in the state 1, which corresponds to a persistent error $\alpha_p - 1$ pulses long.

The transposition counting circuit consists of two identical $(0.5m + 1)$ -unit shift registers, the corresponding cores being linked by diode coincidence gates. The shift terminals of one of the registers receive pulses corresponding to $0 \rightarrow 1$ errors, and those of the other register pulses of $1 \rightarrow 0$ errors. At the end of the code group, a sense pulse is delivered to the registers and the gates. If 1 is written in the corresponding cores of the registers, the code group contained transpositions and one of the gates produces an output pulse which is counted. A pulse at the output of the α_r -th gate associated with the α_r -th cores of the two registers corresponds to $\alpha_r - 1$ transposition errors in the analyzed combination.

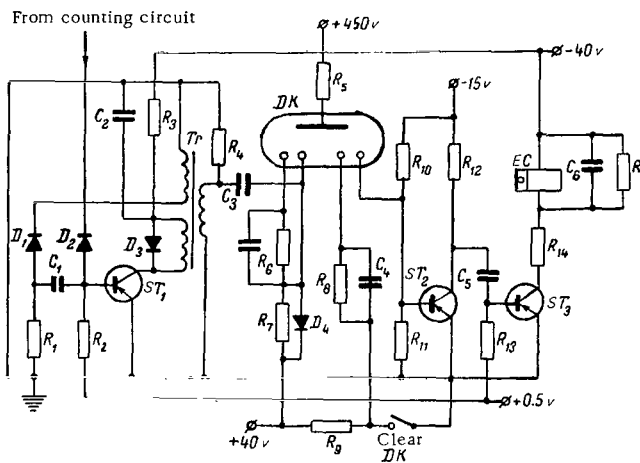


FIGURE 37.

The counters are a Soviet-made OG-3 dekatron (DK in Figure 37) with MES-54 electromechanical counter coupled to its output (EC in Figure 37). The dekatron scaler adapts the analyzer to high-speed transmissions (2400 baud) and increases the counter capacity from 10^3 to 10^4 pulses.

The dekatron is triggered by a solid-state blocking oscillator using a semiconductor triode ST_1 which forms a negative pulse no less than $20 \mu\text{sec}$ long with an amplitude of no less than 150 V. The positive output pulses of dekatrons control the d.c. amplifiers ST_2 , ST_3 which actuate the electro-mechanical counters.

4. COUNTING ASSEMBLY FOR STATISTICAL REDUCTION OF DATA RECORDED ON MAGNETIC TAPE

The errors and the parameters in this case are as for the previous analyzer. The setup is used to process information recorded on a three-channel magnetic tape by a tape recorder associated with the analyzer /36/.

Figure 38 is a photograph of the counting assembly (the tape recorder is shown on the left). The block diagram is given in Figure 39.

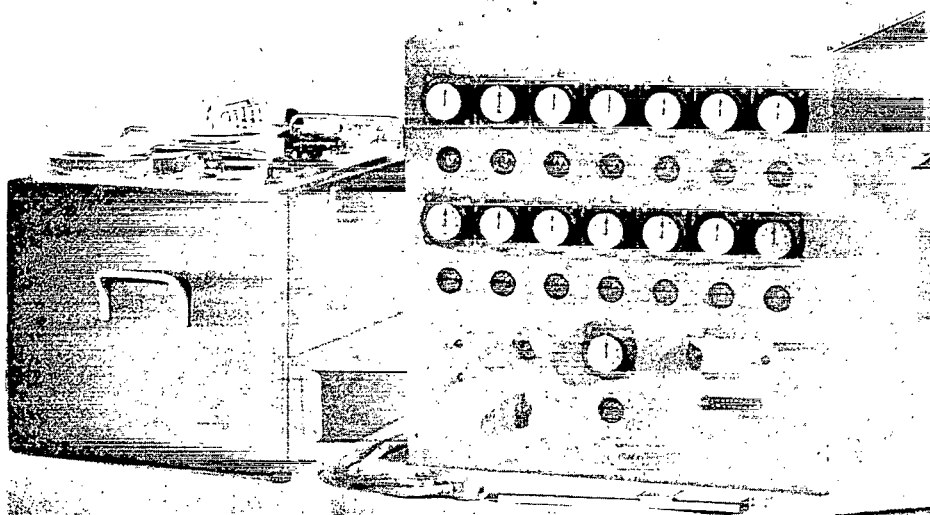


FIGURE 38.

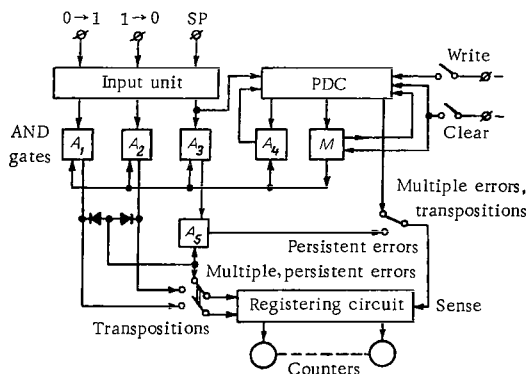


FIGURE 39.

The data recorded in the three channels of the magnetic tape are delivered to the input through the replay amplifiers /36/ and matching stages. These are bell-shaped pulses of about 10 V amplitude and 150 msec duration, corresponding to synchronizing signals (SP) and $1 \rightarrow 0$ and $0 \rightarrow 1$ errors.

Before the counting is initiated, the gates G_1 , G_2 , G_3 are closed by a memory trigger (MT) and no data flow from the input device to the counting circuits. When SP corresponding to the given starting phase is received, the trigger MT is flipped by a pulse delivered from the phase and digit counter (PDC). The latter uses transistor-magnetic triggers which act as variable frequency dividers. The gates are prepared for the reception of the short pulses shaped by the input unit, which are the data to be analyzed. Thanks to PDC, the counting can be initiated starting with any digit of the code group. This feature is highly significant for correct analysis.

An MT output pulse also clears the PDC and writes in information pertaining to the number of digits of the code group to be analyzed, which is known beforehand.

The assembly has a single registering circuit, and suitable switching is provided to permit the multiple and persistent errors and transpositions to be analyzed in three reruns of the tape. After each rerun the registering circuit is cleared and the analyzer is switched to measure errors of the next kind.

The components of this assembly are in many respects similar to the corresponding components of the analyzer described in the previous section. The registering circuit is assembled of ferrite-core single-shift registers with transistor coincidence gates. OG-3 dekatrons and MES-54 counters are used as indicators.

The readings of the analyzer described in Sec. 3 of this chapter or the readings of the counting assembly can be readily converted to give the total volume of transmitted information with breakdown according to accurate and faulty ($1 \rightarrow 0$ and $0 \rightarrow 1$) pulses. If these quantities are known, and the number of code groups of certain length with errors of each of the three kinds is also given, we can easily compute the probability of error in a single digit and in a code group for simple and error-correcting codes. These results have definite bearing on channel quality and code effectiveness.

5. ERROR-FREE INTERVAL ANALYZER

The analyzer of the distribution of error-free intervals in telephone channels utilizes Berger and Mandelbrot's error model.

According to measurements, the maximum error-free interval in real telephone channels is not greater than 10^6 pulses. The upper limit of the test interval is therefore taken as $2^{20} = 1,048,576$ pulses. The $2^0 - 2^{20}$ interval is divided into ten parts, each 3.2^q pulses long, where $q = 0, 1, \dots, 9$.

There are 12 counters in the analyzer, 10 corresponding to the various intervals, the 11th intended for counting successive errors in individual intervals, and the 12th for accumulating the total error count per session.

Such components as the timing generator, the input unit, the phase corrector, the control signal generator, and the bit-by-bit comparator of the received and the control signals are the same as in other analyzers. The only difference is the design of the counting circuit (Figure 40), which is a divider using 20 serially connected dynamic triggers.

The ten test intervals are generated by connecting memory circuits M to each pair of adjoining triggers and coupling the outputs of the M to half-adders (i.e., circuits producing an output of 1 only when 1 and 0 are delivered to certain inputs). The counters are connected to the half-adder outputs.

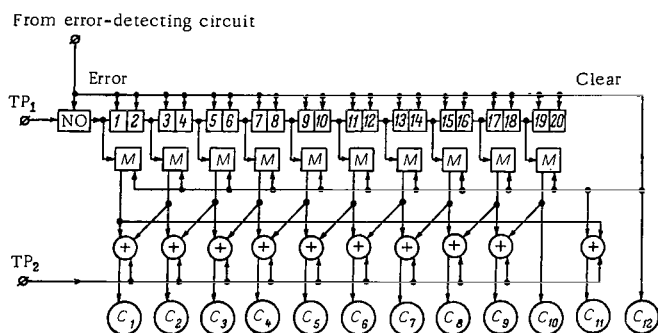


FIGURE 40.

An error pulse is delivered to counter 12, to memory circuits, and to the first input of the half-adder associated with counter 11. Simultaneously, this pulse sets the first trigger of the counting circuit to 1 and clears the other triggers. If errors are indicated, the counting circuit does not receive the timing, and vice versa.

The length of the error-free interval is determined by the number of timing pulses delivered to the divider input after the last error. This count is registered by the memory circuits. When a pulse corresponding to the first error after an error-free interval is received, the train of timing pulses is interrupted and the count stops. The dynamic triggers are cleared and the data recorded by the memory circuits is read out.

The counter connected to the output of the half-adder whose input is a single 1 is actuated. The other half-adders also receive ones from the higher-digit memory circuits, and the associated counters are therefore not tripped.

High digits thus inhibit counting of low digits, and the circuit only registers the leading digit stored in the M, i.e., the sought interval between successive errors.

The analyzer gives the distribution function of error-free intervals in logarithmic scale. The Pareto distribution parameter α is readily obtained from this function as the slope factor of the straight line approximating to the middle section of the distribution curve.

Chapter Seven

SOME COMPONENTS OF NONCONTACT TESTERS

1. DIGITAL READOUT INDICATOR

Choice of indicator elements. Researches in the field of industrial psychology, which studies among other things various means and ways for facilitating the operator's job, show that the operator responds faster to the visual display of data provided by digital readout devices and the number of reading errors in this case is substantially less than the average for various pointer instruments, stroboscopes, cathode-ray oscillographs, and other analog indicators.

The design of digital readout indicators is therefore a problem of some importance not only for the testers described in Chapter Five of this book but also for a great many other instruments used in digital measurement techniques. The readout is presented by illuminated or glowing digits in the indicator, i.e., the data are displayed visually and digitally in the decimal number system /17/.

The main requirements in this case are distinct readout and high reliability. The indicator elements should therefore have a long-life durability and be controlled by simple circuitry. Since the indicator consists of a few hundreds of identical elements, they should be small, cheap, and have low power consumption. The indicator elements should be inertialess; e.g., the glow time θ of an indicator element of the instrument described in Chapter Five, Sec.2 is determined from the following condition: there should be no overlapping between the elements of two adjoining indicator lines in distortion measurements of individual pulses in each code group in the start-stop mode at the maximum keying speed $N_{st, max}$, i.e.,

$$\theta < \frac{1}{N_{st, max}}. \quad (109)$$

For $N_{st, max} = 75$ baud, we have, e.g., $\theta < 1.3$ msec.

Ordinary filament lamps clearly do not meet the various requirements enumerated above. Cold-cathode thyratrons are also inapplicable in practice, because their parameters show substantial scatter and are variable in time. Furthermore, a thyatron cannot be reliably extinguished without complex noncontact switch controlling the anode voltage; false thyatron firings may occur when this voltage is relieved or restored.

Application of small-sized neon lamps associated with semiconductor triodes makes it possible to do away with high-voltage switching and creates a more reliable indicator circuit than that using thyratrons.

Neon lamps give a sufficiently bright light and can be used in an indicator of a fairly small size.

Figure 41 plots the cumulative distribution functions of the firing potential U_f and the glow potential U_g of Soviet-made MN-6 neon lamps. The curves are plotted from measurements of U_f and U_g of 1000 lamps which have functioned for 10 to 100 hrs (the step curves).

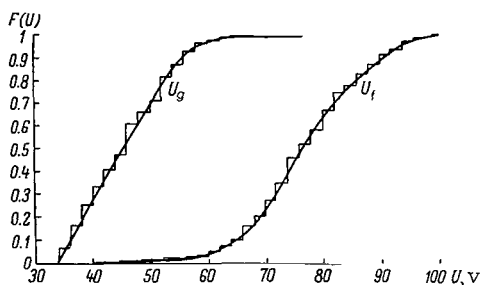


FIGURE 41.

The curves in Figure 41 show that some 90% of the lamps have the following parameters:

$$60\text{ v} \leq U_f \leq 95\text{ v}, \quad 35\text{ v} \leq U_g \leq 60\text{ v}. \quad (110)$$

The indicator provides clear readout if the neon lamps glow for no less than 3 msec with a normal working current of 0.8–1 mA. This glow time is sufficient to ensure accurate visual response.

According to inequality (109), MN-6 neon lamp indicators can be used in distortion measurements of individual pulses in start-stop code combinations at keying rates of approximately up to 300 baud. In synchronous measurements and in start-stop measurements using a single row the speed restriction is not valid, since simultaneous glowing of several indicator elements is permissible.

Indicator control circuits. The neon lamps should be controlled by a circuit which lights the appropriate lamp, and only that lamp, when a brief pulse is produced at one of the distributor outputs (by generating the required U_f and U_g from the range indicated in (110)) and maintains that lamp lit for a given time θ .

The control circuit should protect the indicator against the possibility of false firing of any of its elements due to noise pulses, malfunction of any of the subcircuits, time variation of the lamp parameters, and parasitic coupling through lamps and their control circuits.

If the output terminal of a square-loop core is connected directly to a neon lamp, the control pulses (which have a duration of not more than a few msec) must have a greater amplitude (about a hundred volts). Although a ferrite core can generate pulses of this amplitude, the power of the pulse will be insufficient for lighting the neon lamp. Neon lamps thus cannot be controlled directly by the core output pulses.

Alternatively, the initial ionization can be produced by a control pulse, while steady glow is maintained by a d.c. voltage source. However, in view of the scatter of the parameters of MN-6 lamps, reliable operation of these circuits requires a very careful selection of lamps, and even then the circuits function erratically due to time variation of the lamp parameters.

The difficulties involved in direct control of neon lamps by core output pulses can be overcome by means of intermediate switching elements ISE, which are triggered by the core pulses and control the neon lamps.

The block diagram of an indicator for start-stop measurements is shown in Figure 42b. The circuit is a two-dimensional matrix; at any time only one of the neon lamps is lighted, that which occupies the intersection of the vertical line with open ISE and the horizontal line with a made commutating switch CS. The remaining ISE are closed and CS are open.

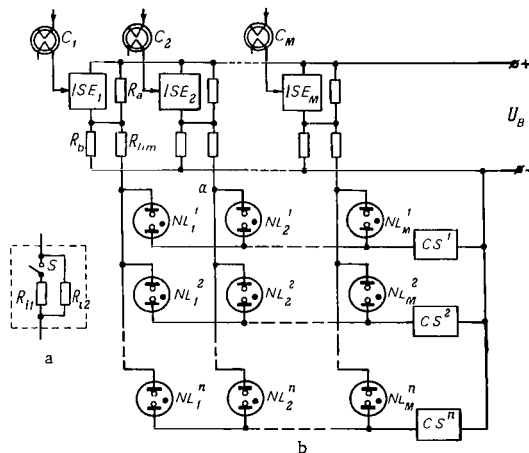


FIGURE 42.

The ISE equivalent circuit is shown in Figure 42a. It comprises a switch S in series with a resistor R_{i1} , shunted by a resistor R_{i2} . ISE control amounts to making and breaking the switch S ; here $R_{i2} \gg R_{i1}$, and R_{i1} and R_{i2} can be regarded as the internal resistance of the ISE with made and broken S , respectively.

In Figure 42b, R_{lim} is a resistance which limits the current in the neon lamps NL ; the divider $R_a - R_b$ lowers the voltage across the ISE when the switch S is open and the commutating switch is cut off. The divider facilitates the operation of the ISE, since when the voltage U_B is switched a voltage $U_{s0} < U_B$ is applied to the ISE.

Putting U_{sp} for the permissible voltage across ISE, we have

$$U_{s0} < U_{sp} < U_B, \quad (111)$$

where

$$U_{s0} = \frac{U_B}{1 + R_b \left(\frac{1}{R_a} + \frac{1}{R_{i2}} \right)}. \quad (112)$$

For reliable operation of the indicator it is necessary that all the vertical rows of neon lamps, with the exception of the row with the currently lighted lamp, are maintained at a constant potential which is insufficient for lighting any of the neon lamps. This minimum potential is determined by the resistance R_b . The voltage across this resistor when the switch S is broken is $U_B - U_{s0}$ and no false firing of the indicators occurs if

$$U_B - U_{s0} < U_g. \quad (113)$$

When any of the ISE is triggered and the commutating switch is made, a voltage $U_B - U_s$ is applied to the corresponding neon lamp (U_s is the voltage across ISE when the switch S is made). Faultless indicator conditions are thus given by

$$U_B - U_s > U_f. \quad (114)$$

Making use of (111) and (113), we find

$$U_f + U_s < U_B < U_{sp} + U_g. \quad (115)$$

The parameters U_B , R_a , and R_b for a given ISE and for given neon lamps can be selected from inequalities (115). The maximum U_f and the minimum U_g should be substituted in (115) from (110). With MN-6 neon lamps, $U_B = 100 - 105$ V, $R_a = 200$ kohm, $R_b = 100$ kohm, $R_{lim} = 20$ kohm.

ISE should provide the necessary time delay when a short triggering pulse is delivered and simultaneously generate a voltage greater than the lamps' U_f . It is desirable to separate between these functions, using low-voltage triodes for time delay and low-gain high-voltage triodes for firing the neon lamps. Time delay can be ensured by using a blocking oscillator, a trigger, or a univibrator. The most reliable circuit (Figure 43a) is that using a univibrator with low-voltage triodes ST_1 and ST_2 controlling the high-voltage triode ST_3 which starts the neon lamp. A negative pulse of length θ from the univibrator output (the resistor R_4) is delivered to the base of a normally cutoff high-voltage transistor ST_3 . The transistor is opened by this pulse and the neon lamp is lighted. When the time θ has elapsed, ST_3 is cut off and the lamp is extinguished.

The following equality should be satisfied for the univibrator to return to the initial state by the time the next starting pulse arrives:

$$5R_3C_2 < \frac{1}{N_{st, max}} - \theta. \quad (116)$$

The sequential switching of the horizontal rows in the indicator is performed by a noncontact commutating switch with transistor elements. The transistor switches are controlled by high-frequency pulse trains. A voltage of appropriate frequency is modulated by low-frequency master pulses coming from the measuring part of the equipment, which control the on and off states of the transistors and the entire switching circuit.

The high-frequency generator is common for the entire switching circuit. One of the switching "channels" is shown in Figure 43b.

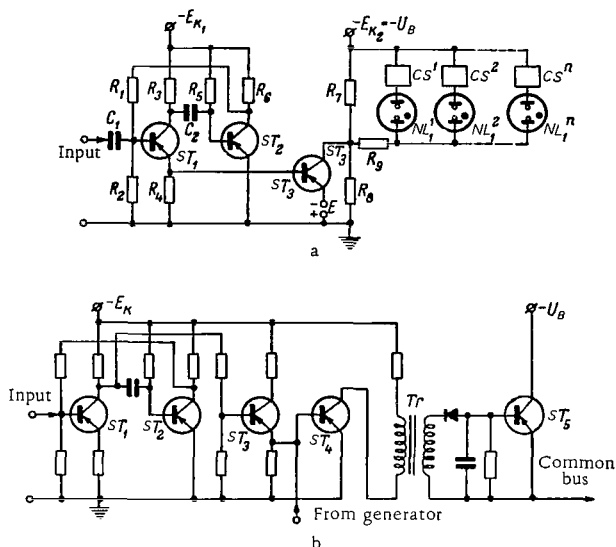


FIGURE 43.

2. TRANSISTOR RELAY WITH REVERSIBLE OUTPUT SIGNAL

Functional principle. Electromagnetic polarized relays widely used in automation and communications have certain distinct shortcomings which are characteristic of all contact devices (periodic adjustment, limited service life, low speed, high radio-frequency noise level). The applicability of these relays in telegraph and other binary transmission systems is limited to transmission speeds not exceeding 75–100 baud.

A need was thus felt for a noncontact device operationally equivalent to a polarized relay, and yet free from the latter's characteristic shortcomings. Various techniques are available for the construction of noncontact relays using electronic, gas discharge, and semiconductor devices, as well as magnetic elements. Semiconductor relays are the most promising of the lot.

A survey of solid-state relays is given in [4], where it is shown that they can be designed using two different circuits: d.c. circuits and circuits with d.c. — a.c. and a.c. — d.c. conversions. The latter option is more advantageous for a reversible output relay equivalent to a polarized relay. Most publications on noncontact solid-state relays, however, give preference to d.c. circuits, which constitute d.c. amplifiers with positive feedback that have a relay characteristic.

In what follows we briefly consider a relay of the second kind, outline some deficiencies of the existing design, and describe a new, improved relay currently used in practice.

The functional principle of a noncontact reversible-output relay is illustrated in Figure 44a. The on and off states of any triode in this circuit are equivalent to the armature making or breaking one of the contacts in an electromagnetic relay. The triodes are the switches which are controlled by the voltages U_2' and U_2'' applied to their base. When the relay functions, i. e., one of the triodes is on and the other is off, a voltage $2U_B$ is applied to the cutoff transistor. The solid-state triodes have a relatively low permissible collector voltage U_{sp} . If $2U_B > U_{sp}$, a twofold problem should be solved in designing the relay: first, the relay must be allowed to function for the given U_B and, second, a simple control circuit should be developed for the switching triodes.

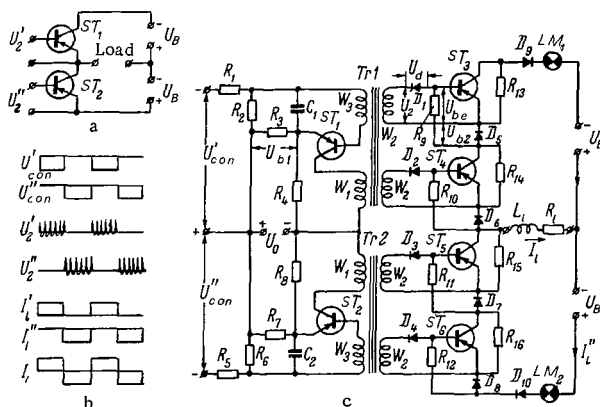


FIGURE 44.

The first problem is solved by serially connecting a number of triodes controlled through decoupling transformers. The second problem was solved until recently by converting the d. c. control signals to a c. voltage of a few kilohertz frequency. After this conversion, the signals could be transmitted through the decoupling transformers. Following detection and smoothing, these signals are delivered to the base of the switching triodes. Although this circuit ensures a high efficiency and a wide range of operating frequencies, the very low frequencies included (down to a state when one of the switches in Figure 43a remains on for an indefinitely long time), relays of this kind were in a very limited use until recently owing to the complexity of the control circuit and lack of temperature compensation, which inevitably led to unwieldiness and low reliability.

The control circuit is simplified, first, by substantially increasing the frequency of the voltage modulated by the control signals and, second, by replacing the push-pull master oscillators and modulators with two controlled oscillators. The latter are relaxation oscillators with transformer feedback, each using a single solid-state triode [15]. An oscillator of this kind is in fact a single-tube d. c. voltage converter.

The oscillator output pulses, whose frequency is close to the limiting frequency of the output switching triodes and which are modulated by the control signals, can be applied to continuously control the switching triodes without rectification and smoothing [69]. The triodes function under conditions of deep saturation, and the negative-polarity pulses of the converter oscillator (corresponding to its working cycle τ_v) are made a number of times longer than the positive-polarity pulses (the idle cycle τ_n). The output triodes are turned on by negative pulses, while positive pulses do not affect them, as they do not last long enough for the carriers to recombine. In view of the preceding the internal resistance of the on triodes remains constant and virtually equal to zero, and constant current flows in the line.

The switching triodes are cut off in the absence of control pulses by the positive bias applied to their base.

This control circuit uses only two semiconductor triodes, smaller transformers are needed, and smoothing capacitors are omitted from the base-emitter circuits of the switching triodes. A solid-state reversible-output relay can thus be made no larger than the conventional electromagnetic relay.

A functional diagram of the relay is shown in Figure 44c. Figure 44b shows the time patterns of the control voltages U'_{con} , U''_{con} , the voltages U'_2 , U''_2 applied to the base of the switching triodes ST_3 , ST_4 , ST_5 , ST_6 , and the load current I_1 .

The voltages U'_{con} and U''_{con} , having a phase shift of 180° , are delivered through a divider to the inputs of the converter oscillators (the triodes ST_1 and ST_2). When no control voltage is applied, the corresponding oscillator is reliably cut off by the bias U_{b1} , there is no voltage on the output terminals of the transformer, and the switching diodes of this arm are off. When a negative-polarity signal is delivered to the generator input, the latter is excited and the triodes are turned on. Thus, when the oscillator ST_1 functions, the triodes ST_3 , ST_4 of the upper arm are on and the triodes ST_5 , ST_6 of the lower arm are off, and vice versa.

Temperature compensation is provided by applying positive (cutoff) voltage from plane germanium diodes to the base of the switching triodes.

Triodes with a permissible negative collector voltage U_{cp} of at least 100 V at normal temperature and a collector current $I_c \leq 400$ mA in the switching mode are the most suitable for use as relay components. The limiting collector current I_{cp} of the switching triodes is determined by a small battery-supplied lamp which protects these triodes against malfunction following shortcircuiting.

Method of calculation. The following basic parameters are required for relay calculation: the switching voltage $\pm U_B$; the load current I_1 , which is virtually equal to the triode collector current I_c ; the control voltage U_{con} (or the control current I_{con}); the relay supply voltage U_0 ; the maximum ambient temperature t_m^0 .

The number Q of serially connected triodes in an arm is equal to the ratio of the maximum attainable voltage across a closed arm, $2U_B$, to the permissible collector voltage U_{sp} at the temperature t_m^0 . If U_{sp} is assumed to decrease linearly with temperature in the working temperature interval, we find

$$Q = \frac{2U_B}{U_{sp}/t_m^0 = t_m^0} = \frac{2U_B}{U_{cp} - p_0(t_m^0 - 20^0)}, \quad (117)$$

where ρ_0 is the temperature coefficient.

The power needed to ensure reliable control of the switching triodes, i. e., the power of the controlled converter oscillator, is given by

$$P_2 = QU_2 I_b, \quad (118)$$

where I_b is the base current; $U_2 = U_{be} + U_d + U_{b2}$ is the voltage on each of the secondary transformer windings w_2 (U_{be} is the base-emitter voltage, U_d is the fall of potential across the forward resistance of a point germanium diode connected to the base of the switching triode in order to delay charge-carrier recombination, U_{b2} is the bias).

Ignoring the power expended in the oscillator feedback circuit, we find the power released in the ST_1 collector:

$$P_c = \frac{P_2}{\eta} = \frac{QU_2 I_{cp}}{\eta \beta}, \quad (119)$$

where η is the transformer efficiency, β the mean current gain factor /15/.

In calculations of a controlled converter oscillator one of the fundamental problems is the determination of the duration τ_w and τ_i of the working and idle cycles. The duration τ_i should be such that the minority charge carriers accumulated in the triode base during the saturation time are not allowed to recombine. Recombination time depends on a number of factors, the main ones being the number of accumulated carriers ("saturation depth") and the resistance of the triode base circuit. The minimum carrier recombination time corresponding to the limiting gain frequency is approximately $2 \mu\text{sec}$ for Soviet-made P26B triodes.

The power P_c dissipated in the ST_1 collector should not exceed the permissible power P_{pt} for the given triode at the temperature t_m^0 . The following equation can thus be written for τ_w :

$$\tau_w = \frac{P_{pt}}{P_c - P_{pt}} \tau_i. \quad (120)$$

Making use of the relations for single-tube converters with a forward-connected diode in the secondary circuit, we obtain an expression for the pulse duty factor α of the converter oscillator:

$$\alpha = \frac{1 - f\tau_w}{f\tau_w} = \frac{f\tau_i}{1 - f\tau_i}, \quad (121)$$

where the oscillator frequency (τ_w and τ_i are in μsec) is

$$f = \frac{10^6}{\tau_w + \tau_i}. \quad (122)$$

The triode ST_1 of the converter oscillator is chosen so that U_{cp} and I_{cp} do not exceed the allowed values. These parameters are determined as follows:

$$U_{cp} = \frac{1 + \alpha}{\alpha} U_0, \quad (123)$$

$$I_{cp} = \frac{P_c}{U_0 - \Delta U - U_{b1}} (1 + \alpha), \quad (124)$$

where ΔU is the sum of voltage falls across the on triode and the ohmic resistance of the primary transformer winding.

The inductance of the primary transformer winding is

$$L = \frac{U_0}{2I_{cp}} \frac{1 + \kappa^2}{1 - \kappa^2} \tau_w. \quad (125)$$

If L is known, we can easily choose the transformer core, and from well-known relations find the number of turns, w_1 , w_2 , w_3 in the primary, secondary, and feedback windings.

A detailed example of the calculation and construction procedure for a relay of this kind is considered in /15/.

BIBLIOGRAPHY

1. AMARANTOV, V.N., K.A. BRUSILOVSKII, G.A. EMEL'YANOV, and S.Yu. EL'KIND. Analizator telegrafnykh iskazhenii (Telegraph Distortion Analyzer). — *Elektrosvyaz'*, No.10. 1961.
2. ARIPOV, M.N., Yu.I. SAVITSKII, A.G. USOL'TSEV, and L.A. SHITOVA. Ispol'zovanie gorodskikh linii dlya peredachi dannykh (Data Transmission over Local Lines). — *Trudy Uchebnykh Institutov Svyazi*, No.12. 1962.
3. ARIPOV, M.N. Statisticheskie kharakteristiki sgruppirovannykh iskazhennykh znakov v telegrafnoi svyazi (Statistics of Groups of Distorted Characters in Telegraph Communications). — *Trudy Uchebnykh Institutov Svyazi*, No.22. 1964.
4. BAZILEVICH, E.V. Beskontaknye telegrafnye rele na poluprovodnikovyykh triodakh (Solid-State Noncontact Telegraph Relays). — *Elektrosvyaz'*, No.8. 1957.
5. BALASHOV, E.P. Proektirovanie magnitnykh elementov i ustroystv elektronnykh vychislitel'nykh mashin (Design of Magnetic Elements and Digital computer Components). — Leningrad, Izdatel'stvo LETI. 1964.
6. BERKMAN, N.A., V.S. BLEIKHMAN, N.D. PASECHNIK, and A.B. PUGACH. Pribor dlya podscheta oshibok pri peredache diskretnoi informatsii na vysokikh skorostyakh (Error Counter for High-Speed Digital Data Transmission). — *Elektrosvyaz'*, No.9. 1964.
7. BERNSHTEIN, S.N. Teoriya veroyatnostei (Probability Theory). — Moskva, Gostekhizdat. 1946.
8. BLEIKHMAN, V.S. and S.L. KVVATO. Ispytatel'nye signaly dlya diskretnykh sistem svyazi (Test Signals for Digital Communication Systems). — *Sbornik nauchnykh trudov TsNIIS*, No.1. 1963.
9. BLEIKHMAN, V.S. Ob izmerenii raspredeleniya oshibok v kanalakh dlya peredachi diskretnoi informatsii (Error Distribution Measurements in Digital Data Transmission Channels). — *Sbornik nauchnykh trudov TsNIIS*, No.2. 1963.
10. BLEIKHMAN, V.S. and K.A. BRUSILOVSKII. Kodovye posledovatel'nosti dlya ispytaniya diskretnykh sistem svyazi (Code Sequences for Testing Digital Communication Systems). — *Elektrosvyaz'*, No.12. 1964.
11. BLEIKHMAN, V.S. Printsipy postroeniya ispytatel'nykh signalov dlya sistem peredachi diskretnoi informatsii (Principles of Test Signal Generation for Digital Data Transmission Systems). — Candidate dissertation, MEIS. 1964.



12. BRUSILOVSKII, K. A. and S. Yu. EL'KIND. Pribory dlya analiza iskazhenii telegrafnykh impul'sov (Telegraph Distortion Analyzers). — *Telegrafiya i Fototelegrafiya*, No. 2(8). 1958.
13. BRUSILOVSKII, K. A. and Z. I. KARAZEL. Beskontaktnyi datchik ispyatel'nykh telegrafnykh signalov (Noncontact Generator of Telegraph Test Signals). — *Elektrosvyaz'*, No. 12. 1960.
14. BRUSILOVSKII, K. A. Elektronnyi izmeritel' telegrafnykh iskazhenii diskretnogo deistviya (Electronic Digital Telegraph Distortion Meter). — *Elektrosvyaz'*, No. 3. 1962.
15. BRUSILOVSKII, K. A. and S. Yu. EL'KIND. Beskontaktnoe rele na poluprovodnikovyykh triodakh (Noncontact Solid-State Relay). — *Avtomatika i Telemekhanika*, No. 5. 1963.
16. BRUSILOVSKII, K. A. Novye elektronnye pribory dlya izmereniya i analiza telegrafnykh iskazhenii (New Electronic Instruments for Measuring and Analyzing Telegraph Distortions). — *Vestnik Svyazi*, No. 10. 1963.
17. BRUFMAN, S. S. Tsifrovye indikatory (Digital Indicators). — *Moskva-Leningrad, Energiya*. 1964.
18. BUKHVINER, V. E. Analizator statisticheskikh kharakteristik radiotelegrafnogo kanala svyazi (Statistical Analyzer of a Radiotelegraph Communication Channel). — *Elektrosvyaz'*, No. 5. 1964.
19. GAVRILIN, V. A. and I. A. LESHCHUK. Analizator maksimal'nykh iskazhenii startstopnykh signalov (Maximum Distortion Analyzer of Start-Stop Signals). — *Trudy Uchebnykh Institutov Svyazi*, No. 5. 1961.
20. GORBUNOV, A. V. Elektronnye pribor dlya izmereniya iskazhenii signalov startstopnykh telegrafnykh apparatov (Electronic Distortion Meter for Start-Stop Telegraph Instruments). — *Vestnik Svyazi*, No. 7. 1956.
21. GUROV, V. S., E. V. BAZILEVICH, N. P. ETRUKHIN, and G. A. EMEL'YANOV. Osnovy peredachi dannykh po provodnym kanalam svyazi (Fundamentals of Data Transmission Over Wire Communication Channels). — *Moskva, Svyaz'*. 1964.
22. DIVNOGORTSEV, G. P. Eksperimental'naya proverka gipotezy—kratkovremennyye prekrashcheniya v telefonnykh kanalakh kak istochnik impul'snykh pomekh (Experimental Test of the Hypothesis: Brief Interruptions in Telephone Channels are the Source of Impulse Noise). — *Elektrosvyaz'*, No. 6. 1964.
23. EMEL'YANOV, G. A. and M. B. RABINOVICH. Vliyanie drobleniya telegrafnykh posylok na ustoichivost' provodnoi telegrafnoi svyazi (The Effect of Fragmentation of Telegraph Keyings on the Stability of Wire Telegraph Communications). — *Elektrosvyaz'*, No. 8. 1959.
24. EMEL'YANOV, G. A. Nadezhnost' telegrafnoi svyazi po provodnym kanalam pri nalichii pomekh (Reliability of Telegraph Communication Over Noisy Wire Channels). — Candidate dissertation, MEIS. 1959.
25. EMEL'YANOV, G. A. K voprosu o funktsii raspredeleniya stepeni startstopnogo iskazheniya telegrafnykh impul'sov (Distribution Function of Startstop Telegraph Distortions). — *Elektrosvyaz'*, No. 3. 1960.

26. EMEL'YANOV, G.A. and L.N. KONNICHEV. Vliyanie iskazhenii kraev posylok na velichinu dostovernosti svyazi pri sinkhronnoi peredache dvoichnoi informatsii (The Effect of Edge Distortions on the Reliability of Communication in Synchronous Transmission of Binary Data). — Sbornik nauchnykh trudov TsNIIS, No. 2. 1963.
27. ZELIGER, A.N. K raschetu kodovykh sistem svyazi na osnove vtorichnykh statisticheskikh kharakteristik (Calculation of Communication Code Systems on the basis of Secondary Statistical Characteristics). — Trudy nauchno-tekhnikeskoi konferentsii LEIS, No.3. Leningrad. 1964.
28. ZELIGER, A.N. Zakon raspredeleniya smeshchenii granits kodovykh impul'sov (Distribution of Edge Displacements of Code Pulses). — Elektrosvyaz', No.3. 1963.
29. ZELIGER, A.N. Iskazhenie kraev kodovykh impul'sov pri sinkhronnoi peredachi (Edge Distortion of Code Pulses in Synchronous Transmission). — Trudy Uchebnykh Institutov Svyazi, No.14. 1963.
30. ZELIGER, N.B. Kriterii dlya otsenki kachestva telegrafnoi peredachi (Criteria for Quality Evaluation of Telegraph Transmission). — Elektrosvyaz', No.4. 1960.
31. ZELIGER, N.B. Kurs telegrafii (A Course in Telegraphy), Part 1. — Moskva, Svyaz'izdat. 1961.
32. ZYUKO, A.G. Pomekhoustoichivost' i effektivnost' sistem svyazi (Noiseproof Features and Effectiveness of Communication Systems). — Moskva, Svyaz'izdat. 1963.
33. KOTEL'NIKOV, V.A. Teoriya potentsial'noi pomekhoustoichivosti (The Theory of Potential Noiseproof Features). — Moskva, Gosenergoizdat. 1956.
34. KORDOBOVSKII, A.I. Analizatory iskazhenii telegrafnykh signalov (Telegraph Distortion Analyzers). — Trudy Uchebnykh Institutov Svyazi, No.1. 1960.
35. KOTOV, P.A. Pribory dlya issledovaniya telegrafnykh kanalov (Telegraph Channel Testers). — Elektrosvyaz', No.5. 1960.
36. KOTOV, P.A. Sposob statisticheskogo analiza binarnykh kanalov svyazi (A Method of Statistical Analysis of Binary Communication Channels). — Soviet patent No.141180. Byulleten' Izobretenii, No.18. 1961.
37. CRAMÉR, H. Mathematical Methods of Statistics. — Princeton Univ. Press. 1946.
38. LANIN, M.I., S.M. MANDEL'SHTAM, and V.V. SIDEL'NIKOV. Kolichestvennye informatsionnye kharakteristiki tekhnicheskikh izmerenii (Quantitative Information-Theoretical Characteristics of Technical Measurements). — In: "Avtomatika, telemekhanika i priborostroenie". Moskva-Leningrad, Nauka. 1964.
39. LISHAI, K.P. Metodika izmereniya startstopnykh iskazhenii (Startstop Distortion Measurements). — Vestnik Svyazi, No.3. 1962.
40. MANDEL'SHTAM, S.M. Issledovanie metodami teorii informatsii kvantovaniya pri izmereniya (Information-Theoretical Approach to Quantization in Measurements). — Candidate dissertation, LIAN. 1964.
41. MIRSKII, G. Ya. Izmereniya vremennykh intervalov (Time Measurements). — Moskva-Leningrad, Energiya. 1964.



42. MOREV, V.L. and P.A. YUNAKOV. *Sposob dlya statisticheskogo analiza oshibok, vznikayushchikh pri peredache informatsii* (A Method of Statistical Analysis of Errors in Information Transmission). — Soviet patent No.167526. *Byulleten' Izobretenii i Tovarnykh Znakov*, No.2. 1965
43. NAUMOV, P.A. and S.D. CHANTSOV. *Kurs telegrafii* (A Course in Telegraphy), Part Two. — Moskva, Svyaz'izdat. 1961.
44. NEMIROVSKII, A.S. *Veroyatnostnye metody v izmeritel'noi tekhnike* (Probability Methods in Measurement). — Moskva, Izdatel'stvo Standartov. 1964.
45. SAMOILENKO, S.I., ed. *Peredacha tsifrovoi informatsii* (Digital Data Transmission). — A collection of Russian translations, IL. 1963.
46. PETERSON, W. *Error-Correcting Codes*. — Cambridge, Mass., MIT Press. 1961.
47. PUGACH, A.B., K.A. BRUSILOVSKII, N.A. BERKMAN, V.S. BLEIKHMAN, and S.Yu. EL'KIND. *Ustroystvo dlya izmereniya iskazhenii telegrafnykh posylok* (An Instrument for Measuring Telegraph Distortions). — Soviet patent No.147227. *Byulleten' izobretenii*, No.10. 1962.
48. PUGACH, A.B. *Novye opredeleniya izokhronnogo iskazheniya i primeneniye fazovoi avtopodstroiki v izmeritel'noi telegrafnoi apparature* (New Determinations of Isochronous Distortion and Application of Phase Automatic Frequency Correction to Telegraph Measurements). — *Sbornik nauchnykh trudov TsNIIS*, No.2. 1963.
49. RADCHENKO, A.N. *Metody sinteza kodovykh kolets* (Design of Code Rings). — *Radiotekhnika i Elektronika*, No.11. 1959.
50. RADCHENKO, A.N. and V.I. FILIPPOV. *Sdvigayushchie registry s logicheskoi obratnoi svyaz'yu i ikh ispol'zovanie v kachestve schetnykh i kodiruyushchikh ustroystv* (Shift Registers with Logical Feedback and Their Use as Counting and Coding Devices). — *Avtomatika i Telemekhanika*, No.11. 1957.
51. CCITT recommendations. — Russian edition. 1959.
52. ROMANOVSKII, V.I. *Matematicheskaya statistika* (Mathematical Statistics), Part 1. — Tashkent, Izdatel'stvo AN Uzbek SSR. 1961.
53. SAVITSKII, Yu.I. and V.M. TIMOFEEV. *Analiz pyatiznachnykh kodov dlya bukvopechatayushchikh telegrafnykh apparatov* (Analysis of Five-Unit Codes For Printing Telegraph Instruments). — *Elektrosvyaz'*, No.7. 1957.
54. SERGIEVSKII, B.R. *Opredeleniye faznykh otklonenii v sistemakh peredachi diskretnoi informatsii* (Determination of Phase Deviations in Digital Data Transmission Systems). — Doctorate Dissertation, LIIZhT. 1962.
55. SMIRNOV, K.A. *Zavisimost' dostovernosti svyazi na seti s kommutiruemymi kanalami ot kraevykh iskazhenii* (Reliability of Communication over a Network of Switched Channels as a function of Edge Distortions). — *Trudy Uchebnykh Institutov Svyazi*, No.22. 1964.
56. SOLOV'EV, N.N. *Osnovy izmeritel'noi tekhniki provodnoi svyazi* (Fundamental Measuring Techniques in Wire Communications), Part 3. — Moskva-Leningrad, Gosenergoizdat. 1959.

57. KOTOV, P.A., ed. *Telegrafnye ustroystva na beskontaktnykh pereklyuchatelyakh* (Telegraph Equipment Using Noncontact Switches). — Moskva, Svyaz'. 1964
58. TEPLOV, N. L. *Pomekhoustoichivost' sistem peredachi diskretnoi informatsii* (Noiseproof Features of Digital Data Transmission Systems). — Moskva, Svyaz'. 1964.
59. UDALOV, A. P. and B. A. SUPRUN. *Izbytochnoe kodirovanie pri peredache informatsii dvoichnymi kodami* (Redundant Coding in Transmission of Binary-Coded Data). — Moskva, Svyaz'. 1964.
60. USOL'TSEV, A. G. and V. Ya. TURIN. *Issledovanie zakonov raspredeleniya oshibok v kanalakh tonal'nogo telegrafirovaniya s chastotnoi modulyatsiei* (Error Distribution in Frequency-Modulation Voice-Frequency Telegraph Channels). — *Elektrosvyaz'*, No. 7. 1963.
61. FELLER, W. *An Introduction to Probability Theory and Its Applications*. — N. Y., Wiley. 1959.
62. FINK, L. M. *Teoriya peredachi diskretnykh soobshchenii* (Theory of Transmission of Digital Messages). — Moskva, Sovetskoe Radio. 1963.
63. KHARKEVICH, A. A. *Bor'ba s pomekhami* (Combatting Noise). Moskva-Leningrad. 1963.
64. HALFMAN, D. *Design of linear multicycle coding circuits*. — Russian translation in "Teoriya peredachi soobshchenii", V. I. Siforov ed. IL. 1957.
65. SHANNON, C. E. *A Mathematical Theory of Communication*. — Bell. Sys. Tech. J., 27:379—423, 623—656. July and Oct. 1948.
66. SHLYAPOBERSKII, V. I. *Elementy diskretnykh sistem svyazi* (Components of Digital Communication Systems). — Moskva, Voenizdat. 1965.
67. ELSPAS, B. *Theory of Autonomous Linear Sequential Networks*. — Russian translation in "Kiberneticheskii Sbornik", No. 7. IL. 1963.
68. EL'KIN, Sh. S. *Modernizovannyi pribor dlya izmereniya iskazhenii telegrafnykh posylok i ispytaniya rele (II-57)* (An Improved Telegraph Distortion Meter and Relay Tester (for the II-57 relay)). — *Vestnik Svyazi*, No. 7. 1960.
69. EL'KIND, S. Yu. and V. S. BLEIKHMAN. *Elektronnoe vykhodnoe rele* (An Electronic Output Relay). — Soviet patent No. 136766. *Byulleten' Izobretenii* No. 6. 1961.
70. ALEXANDER, A., R. GRYB, and D. NAST. *Capabilities of the Telephone Network of Data Transmission*. — Bell. Sys. Tech. J., 39, No. 3:431. 1960.
71. BASSOLE, P. *Aspects Statistiques de la Notion de Distorsion Rythmique*. — *Ann. télécommuns*, 6, Nos. 8—9. 1951.
72. BASSOLE, P. *Aspects Statistiques de la Notion de Distorsion Arythmique*. — *Ann. télécommuns*, 8, Nos. 7—8. 1953.
73. BENNETT, W. R. and F. E. FROELICH. *Some Results on the Effectiveness of Error-Control Procedures in Digital Data Transmission*. — *IRE Trans. Communs systems*, CS-9, No. 1:58. 1961.
74. BERGER, J. M. and B. A. MANDELBROT. *A New Model for Error Clustering in Telephone Circuits*. — *IBM J. of Research and Dev.*, 7, No. 3:224. 1963.

75. BODONYI, A. B. Effects of Impulse Noise on Digital Data Transmission. — IRE Trans. Communs Systems, CS-9, No. 4:355. 1961.
76. CHITTENDEN, R. A. Notes on the Transmission of Data at 750 Bauds Over Practical Circuits. — IRE Trans. Communs Systems, CS-9, No. 1:7. 1961.
77. CROISDALE, A. C. Error Rates and Error Detection on Telegraph Circuits. — IRE Trans. Communs Systems, CS-9, No. 1:28. 1961.
78. DESBLACHE, A. New Equipment for Experiments on Data Transmission and Error Analysis. — IRE Trans. Communs Systems, CS-9, No. 3:244. 1961.
79. ENTICKNAP, R. G. Errors in Data Transmission Systems. — IRE Trans. Communs Systems, CS-9, No. 1:15. 1961.
80. ELLIOTT, E. O. Estimates of Error Rates for Codes on Burst-Noise Channels. — Bell System Techn. J., 42, No. 5:1977. 1963.
81. ERICKSON, G. L. A Telegraph Signal Analyser. — Electr. Engng. 67, March. 1948.
82. FIJALKOWSKI, W. Historique des Notions de Distorsion Telegraphique. — Journal UIT, 10. 1958.
83. FONTAINE, A. B. and R. G. GALLAGER. Error Statistics and Coding for Binary Transmission Over Telephone Circuits. — Proc. IRE, 49, June. 1961.
84. FUNK, G. Ein Fernschreib-Verzerrungsspektrometer. — Nachrichtentechn. Z., 3. 1960.
85. GILBERT, E. N. Capacity of a Burst-Noise Channel. — Bell System Techn. J., 39, No. 5:1253. 1960.
86. HOFMANN, E. I. Automatic Digital-Data Error Recorder. — IRE Trans. Instrument. I-10(1):27. 1961.
87. KELLER, G., and D. SANDEN. Neue Messgeräte der Fernschreibtechnik. — Nachrichtentechn. Z., 8. 1958.
88. LUTZ, R. Der Fernschreib-Verzerrungsschreiber. — Nachrichtentechn. Z., I. 1959.
89. MELAS, C. M. and E. HOPHER. Error Recording and Analysis for Data Transmission. — Proc. Nat. Electronics Conf., 16. 1960.
90. MERTZ, P. Model of Error Burst Structure in Data Transmission. — Proc. Nat. Electronics Conf., 16. 1960.
91. MERTZ, P. Statistics of Hyperbolic Error Distributions in Data Transmission. — IRE Trans. Communs Systems, CS-9, No. 4:377. 1961.
92. MERTZ, P. Error Burst Chains in Data Transmission. — IRE Internat. Convent. Rec., Pt., 8. 1962.
93. MORRIS, R. Further Analysis of Errors Reported in "Capabilities of the Telephone Network for Data Transmission". — Bell System Techn. J., 42, No. 4. 1962.
94. SHANCK, R. B., F. A. COWAN, and S. I. CORY. Recent Developments in the Measurement of Telegraph Transmission. — Bell System Techn. J., 18, No. I. 1939.
95. SUSSMAN, S. M. Analysis of the Pareto Model for Error Statistics on Telephone Circuits. — IEEE Trans. Communs Systems, CS-11, No. 2:213. 1963.
96. WHEELER, L. K. and A. C. FROST. A Telegraph Distortion Analyser. — Post Office Electr. Engng. J., 47, April. 1954.
97. YUDKIN, H. L. Some Results in the Measurement of Impulse Noise on Several Telephone Circuits. — Proc. Nat. Electronics Conf., 16. 1960.

SUBJECT INDEX

- Analyzer, channel statistics 68 ff
 - distortion 61, 62, 65 ff
 - error distribution 5, 9, 62 ff
 - error-free interval 73-74
 - for measurement of error stream parameters 64, 65
- Bias distortion 6, 33
 - constant 14
 - distribution 14
 - variable 14
- Binomial distribution 13, 23
- Burst, error 8
 - independence 28
 - length 8
- Channel, communications 3
 - a. c. 3
 - d. c. 3
 - digital 3
 - frequency response 16
 - margin 4
 - narrow-band (telegraph) 3
 - rating criteria 3 ff
 - stability margin 4, 6
 - statistics analyzer 68 ff
 - transient response 6, 16
 - wide-band (telephone) 3
- Character, frequency of a 12
- Characteristic distortions 6, 18
 - distribution 16 ff
- Circuits, linear sequential 44 ff
- Classification of pulse distortions and errors 5 ff
- Cluster, error 8
- Code, combinations 12, 39
 - probability 13
 - rings 35 ff
 - test signals based on 35 ff
 - sequence, regular 34, 35
 - start-stop 7
- Communication channel see Channel
- Correlated noise 23 ff
 - model 24
- Correspondence criterion, Pearson 15
- Counting assembly for statistical reduction
 - of data on magnetic tape 72-73
- Delay circuit 78, 79
- Delay function, Paretian 30
- Digital tester 56
- Displacement of pulse edge 10, 14, 19
- Distortion 4, 5, 6
 - analyzer 61, 62
 - electronic 65 ff
 - bias 6, 33
 - constant 14
 - variable 14
 - characteristic 6, 18, 19
 - relative 18
 - classification 5 ff
 - distribution 6
 - bias 14
 - characteristic 16 ff
 - fortuitous 14
 - isochronous 10, 14
 - fortuitous 6, 14, 19
 - instrumental 4
 - meter 5
 - digital 58 ff
 - electronic 52-58
 - permissible overall 4, 6
 - "spectrometer", telegraph 62
- Distortions, variance 6
- Distribution analyzer, error 5, 9, 62 ff
 - binomial 13, 23
 - distortions 6
 - bias 14
 - characteristic 16 ff
 - fortuitous 14
 - isochronous 10, 14
 - errors 22 ff
 - function 14, 15
 - log-normal 15
 - mutilations 15
 - normal 13
 - Pareto 30
 - density function 30
 - probability 21, 22
 - density 7
 - truncated 30
- Distributor inputs, total number of 39
- Edge displacement 10, 14, 19
 - distribution 10, 14, 19
- "End-to-end" test 10
- Error(s) burst 8, 26
 - average length 27

- Error(s) (Cont.)
 - burst independence 28
 - classification 7
 - cluster 8, 26
 - distribution analyzer 5, 9, 62 ff
 - hyperbolic 32
 - free intervals, analyzer of 73-74
 - length of 31
 - transmission, average length of 27
 - instrumental, evaluation 50, 51
 - sources 50, 51
 - models, statistical 26-32
 - multiple 9
 - persistent 8
 - probability 5, 6, 7, 15, 16
 - single 8
 - stream, discrete 8
 - model 26, 28
 - parameters 26
- Faulty reception, probability of 22
- Feedback 36, 37, 47, 48
 - register 47
- Fluctuation noise 3
- Fortuitous distortions, distribution of 14
- Frequency of a character 12
 - relative 13
- Generator, quasirandom sequences 49
 - test signals 33, 38
 - design 44 ff
 - output unit 42
 - program matrix 42
 - programmed 38
 - Q9S 40, 41
- Impulse noise 3
- Independence of error bursts 28
- Indicator control circuits 76 ff
 - digital readout 75 ff
 - elements, choice of 75-76
 - for start-stop measurement 77
- Intermediate switching elements 77
 - equivalent circuit 77
 - voltage 77, 78
- Lamps, filament 75
 - neon 76, 77
- Linear sequential circuits 44 ff
- Log-normal distribution 15
- "Loop" test 10
- Margin 4, 6
 - receiver 7
 - transmission stability 4
- Markov chain 23
 - stationary 27
- Matrix, characteristic (transition) 45
 - identity 45
 - program 42
 - test signal generator 42, 43
- Measurements, distortion and error, principles of 9 ff
- Message statistics 13
- Meter, distortion 5, 50-60
 - digital 58 ff
 - electronic 52-58
- Model, correlated noise 24
 - statistical, noise 19 ff
 - error 26-36
- Mutilation 6, 15
 - distribution 15
- Neon lamp indicator 76, 77
- Noise, additive 3, 5
 - burst 24
 - correlated 23 ff
 - external 4
 - fluctuation (smooth) 3, 5-8
 - impulsive 3, 5, 7, 8
 - model 19 ff
 - correlated 24
 - equivalent discrete 22
 - multiplicative 3
 - probability density distribution 22, 23
 - random 6
 - sinusoidal 3
 - uncorrelated 22, 23, 26
- Output unit of test signal generator 42
- Pareto distribution 30, 31, 32
 - modified 32
 - parameter 74
 - model 32
- Pearson correspondence criterion 15
 - interpolation curves 19, 29
- Probabilities, transition 27
 - unconditional 13
- Probability density 6
 - distribution 7
 - function 29
 - distribution 21, 22
 - of noise values 23
 - of a single error, average 27
 - combination 13
 - error 5-7, 15-16, 20
 - faulty reception 22
 - start-stop distortion 15
- Program matrix, test signal generators 42
- Pulse distortions, classification 5 ff
- Random noise 6
- Readout indicator, digital 75 ff
- Redundancy 5, 7

- Register 37
 - feedback 47
 - shift 39, 49
 - transistor-magnetic 38
- Relay, calculation 81 ff
 - noncontact reversible output 80
 - transistor 79 ff
- Reliability, loss of 11
 - transmission 4, 15
- Response, frequency 16
 - transient 6, 16, 18
 - threshold 16
- Rings, code 35 ff
- Sequences, regular code 34, 35
- Sequential circuits, linear 44 ff
- Signal, correction 4
 - distortion 4
 - error-correcting 7
 - error-detecting 7
 - errors, distribution 22 ff
 - statistics 12, 13
 - test, generation of 33-49
 - to-noise ratio 4
- Single error, average probability of a 27
- "Spectrometer", telegraph distortions 62
- Stability margin of transmission 4
- Start-stop code 7
 - distortion probability 15
 - phase correction 4
 - system 4
- Statistical error models 26-32
 - noise model 19 ff
- Statistics, channel 26
 - signal 12, 13
- Stream, discrete error 8
- Synchronous correction 4
 - system 4
 - transmission 14
- System, start-stop 4
 - synchronous 4
- Telegraph channel 3
 - voice-frequency 33
 - distortion "spectrometer" 62
- Telephone channel 3
- Test, "loop" 10
 - pulse generator, digital tester 57, 58
 - signal generation 33-49
 - generator 38
 - design 44 ff
 - output unit 42
 - programmed 38 ff
 - signals 33-49
 - based on code rings 35 ff
 - "end-to-end" 10
- Tester, circuit 52, 55
 - digital 56
 - noncontact 75-83
 - Threshold device 16
 - response 16
- Time delay circuit 78, 79
- Transient response of channel 6, 16
 - filter 18
- Transistor relay with reversible output signal 79 ff
- Transition probabilities 27
- Transmission, high-speed 3
 - low-speed 3
 - reliability 4
 - start-stop 9
 - distortions 15
 - statistics 22 ff
 - synchronous 9, 14
- Transposition, multiple 9
- Uncorrelated noise 22, 23, 26
- Variance of distortions 6
 - distribution 13, 14

National Aeronautics and Space Administration

WASHINGTON, D. C. 20546

OFFICIAL BUSINESS

POSTAGE AND FEES PAID
NATIONAL AERONAUTICS AND
SPACE ADMINISTRATION

030 001 32 51 3DS 68044 00903
AIR FORCE WEAPONS LABORATORY/AFWL/
KIRTLAND AIR FORCE BASE, NEW MEXICO 87117

ATTN MISS MADELINE F. CANOVA, CHIEF TECHNICAL
LIBRARY /WLIL/